

PDX-1 IS REQUIRED FOR POSTERIOR FOREGUT PATTERNING AND  
DIFFERENTIATION OF THE PANCREAS AND DUODENUM

By

MARTIN F. OFFIELD

Dissertation

Submitted to the Faculty of the  
Graduate School of Vanderbilt University  
for the degree of

DOCTOR OF PHILOSOPHY

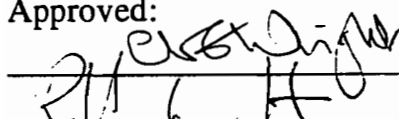
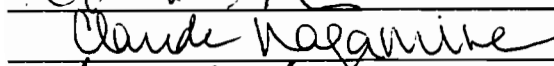
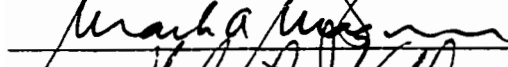
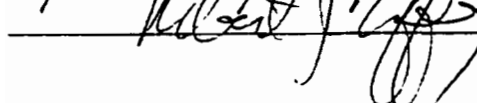
in

Cell Biology

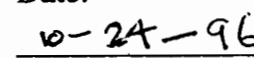
December, 1996

Nashville, Tennessee

Approved:

  
\_\_\_\_\_  
  
\_\_\_\_\_  
  
\_\_\_\_\_  
  
\_\_\_\_\_

Date:

  
\_\_\_\_\_  
10/10/96  
\_\_\_\_\_  
10/25/96  
\_\_\_\_\_  
10/25/96  
\_\_\_\_\_  
11/1/96  
\_\_\_\_\_

To Donna and my parents  
who always believed in me

## ACKNOWLEDGEMENTS

The financial support for the research of this dissertation was provided by the National Institutes of Health (grant #HD28062 to C.V.E.W. and #DK42502 to C.V.E.W. and Mark Magnuson) and by the Howard Hughes Medical Institute (funding to Brigid L. M. Hogan). The research described in this dissertation was done in collaboration with the labs of Mark Magnuson and Brigid Hogan. Specifically, the electroporation of *pdx-1* targeting constructs and subsequent production of chimeric animals was carried out by Patricia (Trish) Labosky of Brigid Hogan's lab. It was Trish's expertise in this area that allowed us to move very quickly with these experiments. Linda Hargett was also involved in this process and helped in the breeding and maintenance of the mouse lines. Tom Jetton of Mark Magnuson's lab was responsible for much of the immunostaining necessary for the analysis of the *pdx-1* mutants. Tom was not only the supplier of many of the antibodies used in these analyses, but he has been an encyclopedic source of information on pancreatic gene expression and function. Tom has been more than helpful in our attempts to analyze and describe the defects seen in *pdx-1* null animals. Mike Ray of Chris Wright's lab aided in the cloning of *pdx-1* and also in the genotyping many of the animals derived from the *pdx-1* mutant lines.

I would like to express my gratitude to the members of my committee. Claude Nagamine was a great resource during my first few years when I was attempting to clone the XIHbox-8 homolog by PCR approaches. Claude has also been very helpful in my academic process; when my mentor, Chris Wright, was unavailable, I have frequently gone to Claude with questions regarding the various meetings, forms, etc. that are all part of one's graduate training. Bob

Coffey provided key insights that helped to shape my understanding of the alimentary tract. Advice from Bob was critical in our analysis of the gut defects which we encountered in the homozygous null mutants generated by this research. Mark Magnuson and members of his lab (especially Tom Jetton) were key co-laborers in this research. Their expertise in endocrinology and pancreatic function were very important in the analysis of the pancreatic and duodenal abnormalities which result from the loss of PDX-1 function. Roland Stein and the members of his lab played a pivotal role in the initial identification of the insulin and somatostatin transcription factor (STF-1) as the rat homolog of XlHbox-8. This ultimately led to our cloning of the mouse homolog. Our continued interactions with the Stein lab are playing an important part in the characterization of the mechanisms of *pdx-1* transcriptional regulation.

I am very grateful to my mentor, Chris Wright, who has been the most significant component of my graduate training. I knew little of the techniques of molecular biology when I first joined the lab, and I attribute my current level of expertise in this area to Chris. I have also gained from Chris a greater ability to critically evaluate my own scientific work and the work of others. Chris has an innate drive for excellence in all that he does which has provided much of the impetus to make all that I do not just good, but great. Although this has many times caused conflicts between us, Chris has been patient with my stubbornness and, at times, short temper. Through it all, my skills as a scientist have been sharpened. I have the highest regard for both Chris and his wife, Jane, who have been more than my colleagues; they have been friends to me in many ways during my graduate career.

I would also like to express appreciation to my fellow graduate students in

the Department of Cell Biology. Al Candia and Laura Gamer were senior graduate students in Chris's lab during my first few years at Vanderbilt. They both taught me most on the experimental techniques that I learned in my first two years. Laura's research, which is discussed in this dissertation, was foundational to my own. My early discussions with Laura were formative in my understanding of the function of the homeobox gene, *XlHox-8*. To the current members of the Wright lab, Mandy Frisch, Abby Cheng, Caroline Erter, Maureen Gannon, Karuna Sampath and Mike Ray, I will miss you all. Thanks for your friendship and "comic relief". I am also grateful for my friends and fellow classmates, Brenda McAdory, Scott Eblen, Jean Witty and Don Pierce. They were my companions through the early trials of Biochemistry and Cell Biology. I truly enjoyed the time which we were able to spend together both academically and socially. To the members of the Greenstein, Miller and Hogan labs I would like to say thank you for your friendship and encouragement. To everyone else in the department, I appreciate all the "little things" that you all did over the past six years. These years have been very enjoyable, in part, because you were part of my life. I will miss you all!

On a personal note, I would not have gotten through my graduate career without the love, prayer and support of my wife Donna. She has been a constant encouragement to me and has put up with my moodiness, exhaustion, and just not being at home. There has not been a day that she did not in some way encourage me and motivate me to keep going.

When I was born, I had the most severe form of lumbar Spina Bifida. The spinal cord from the 3rd lumbar vertebra down was outside of the vertebra and completely disorganized. On top of this region was a large fatty tumor which had

dissolved much of the vertebrae. My doctors at the time told my parents I would never walk, I would be mentally retarded and likely would not live more than a few years. Thankfully my parents did not heed the doctor's advice to place me in an institution and forget they had had me. Because of their faith in God and His ability to produce good even from the worst circumstances, they sought out other doctors, whose outlook was less pessimistic, to give me the treatment I needed. Over the next ten years various doctors continued to make predictions of my emanate demise. In spite of this, my parents kept these things from me and instilled in me the drive to always do my best no matter what my circumstances are. All that I am is due to the courage and values that I have learned from my parents and my own faith in God who promised that, "They that depend upon the Lord shall renew their strength. They shall mount-up with wings as eagles. They shall run and not be weary. They shall walk and not faint." (Isaiah 40:31). I am living proof!

## TABLE OF CONTENTS

	Page
ACKNOWLEDGEMENTS .....	v
LIST OF FIGURES .....	x
LIST OF ABBREVIATIONS .....	xi
 Chapter	
I. GENERAL INTRODUCTION	
Establishment of the Embryonic Axes .....	2
Establishment of the Three Germ Layers .....	4
Homeobox Genes in Patterning During Development .....	9
Specification of the Primitive Endoderm .....	14
Morphological Development of the Posterior Foregut .....	18
XIHbox-8/PDX-1 in Pancreatic & Duodenal Development .....	21
 II. CLONING OF THE MURINE XIHbox-8 HOMOLOG	
Introduction .....	27
Methods and Materials .....	27
Results .....	30
Discussion .....	35
 III. ANALYSIS OF PDX-1 FUNCTION BY GENE TARGETING	
Introduction .....	37
Methods and Materials .....	38
Results .....	44
Discussion .....	64
 IV. GENERAL DISCUSSION	
Insights into Endodermal Patterning .....	71
Molecular Data Concerning Pancreatic and Hepatic Induction .....	73
Potential Ramifications for Diabetes .....	79
Future Directions .....	80
Summary .....	83
REFERENCES .....	84

## LIST OF FIGURES

Figure	Page
1. Organization of the Mouse Hox and Drosophila Hom-C Homeobox Clusters .....	12
2. Hox Gene Patterning in the Hindbrain .....	13
3. Patterning of the Primitive Endoderm .....	14
4. Cloning Attempts Using X1Hbox-8 Probes .....	31
5. Restriction Mapping of #2λ Clone of <i>pdx-1</i> .....	34
6. Targeted Mutagenesis of <i>pdx-1</i> .....	39
7. Gross Analysis of <i>pdx<sup>XBko</sup></i> Animals .....	46
8. Time Course of PDX-1/βgal Fusion Expression .....	48
9. Tracking of Pdx-1 Expression Tissues in <i>pdx<sup>lcko</sup></i> Embryos .....	50
10. Aberrant Pancreatic Duct Structures in <i>pdx-1</i> Embryos .....	52
11. Pancreatic Marker Expression in <i>pdx<sup>XBko</sup></i> and <i>pdx<sup>lacZko</sup></i> Embryos .....	55
12. GLUT2 Expression in the Dorsal Ductule .....	56
13. Analysis of the Stomach/Duodenal Region .....	57
14. Absence of Brunner's Gland's in <i>pdx-1</i> <i>-/-</i> Mutants .....	60
15. Reduction in Neuroendocrine Cells in <i>pdx-1</i> Embryos .....	62
16. Quantitation of Enteroendocrine Cells in <i>pdx<sup>XBko</sup> -/-</i> Embryos .....	63
17. Regionalization of the Early Posterior Foregut .....	72
18. Patterning of the Developmental Fates of the Posterior Foregut .....	77



## LIST OF ABBREVIATIONS

AIP	anterior intestinal portal
AP	anteroposterior
Antp	Antennapedia
bFGF	basic FGF
$\beta$ gal	$\beta$ galactosidase
BMP	bone morphogenetic protein
cDNA	complementary DNA
dATP	2'-deoxyadenosine-5'-triphosphate
DNA	deoxyribonucleic acid
dpc	days post-coitum
dpp	days post-partum
DV	dorsoventral
EDTA	disodium ethylenediamine tetra-acetate
FGF	fibroblast growth factor
GLUT2	glucose transporter 2
I-FABP	intestinal fatty acid binding protein
IDX-1	islet and duodenal homeobox gene 1
IPF-1	insulin promoter factor 1
kb	kilobase(s)
L-FABP	liver fatty acid binding protein
ml	milliliter
mM	millimolar
mRNA	messenger ribonucleic acid
PAS	periodic acid-Schiff's reagent
PBS	phosphate buffered saline
PCR	polymerase chain reaction
RT-PCR	reverse transcriptase-mediated PCR
SDS	sodium dodecyl sulfate
Shh	Sonic hedgehog
SSC	standard saline citrate
SSPE	saline, sodium phosphate EDTA
STF-1	somatostatin transactivating factor 1
TGF $\beta$	transforming growth factor $\beta$
Ubx	ultrabithorax
UV	ultraviolet light

## CHAPTER I

### GENERAL INTRODUCTION

Probably the fundamental question which is faced by all who study the processes of development is how a one dimensional DNA code is translated into a three-dimensional structure--the developing embryo (Gehring, 1987). Because of the difficulty in experimentally manipulating mouse embryos at early stages, it has been difficult to address the questions of early patterning events in this system. Due to the size and resiliency of their embryos, as well as the ability to maintain them in simple salt solutions, amphibians were the choice of many early embryologists who were trying to identify the cues responsible for setting-up the basic embryo pattern. Early morphological analysis of amphibians revealed that the establishment of the embryonic axes was the first step in this process. The first component of axis formation is determined maternally through the vegetal deposition of yolk and other factors. Fertilization leads to second messenger cascades and cortical rotation leading to the positioning of the dorsoanterior region opposite the site of sperm entry. These regional inequalities lead to the specification of the early axes and to the establishment of the three germ layers through the interaction of the animal and vegetal hemispheres. The patterning due to the mutual interactions of the three germ layers ultimately leads to the development of the various organ systems and supporting tissues. Though all of this has been known among embryologists for many years, the biochemical mechanisms of these processes have been more elusive. Much progress, however, has been made recently in identifying the factors which are involved in axis

formation, early tissue inductions, and patterning of the three germ layers in *Xenopus*. Comparative work indicates that similar molecular mechanisms are utilized not only in mice, but also in other vertebrates.

## **Establishment of the Embryonic Axes**

### **Axis Formation in *Xenopus***

Many of the initial studies designed to elucidate the mechanism of early axis formation were carried out in amphibians due to the ease of manipulating the embryos at these very early stages. In *Xenopus* prior to fertilization, the earliest components which lead to the establishment of the embryonic axes are the disproportionate stores of yolk plates and other factors vegetally, and conversely the animal hemisphere possesses the nucleus, as well as higher concentrations of both ribosomes and glycogen granules. All of the neural and mesodermal tissues arise from the animal hemisphere, whereas the vegetal hemisphere contributes to the endodermal structures of the alimentary tract. A potential signaling molecule which is vegetally localized is Vg1, a Transforming Growth Factor  $\beta$  (TGF $\beta$ ) family member, whose mRNA is tethered to the vegetal cortex of mature eggs (Melton, 1987). The potential role of Vg1 protein will be discussed below. XCAT-2 mRNA, which is structurally related to *Drosophila* nanos--a posterior determinant, is also localized to the vegetal hemisphere (Mosquera et al. 1993). Its role in amphibian development, however, is not yet determined.

The point of sperm entry provides the second half of the information necessary for setting up the anteroposterior (AP) and dorsoventral (DV) axes. The cortical rotation, which follows this event, results in a region of reduced

pigmentation, known as the gray crescent, on the opposite side of the embryo. From this region will arise the dorsoanterior structures of the head and notochord while the region of sperm entry will give rise to ventral structures such as the blood islands. In *Xenopus*, fertilization together with the maternally derived animal-vegetal axis determines the embryonic orientation with the mediolateral and right-left axes being inferred from the apposition of these two primary axes. Though the morphological aspects of these events are fairly well understood, the biochemical pathways which confer polarity have not been fully deduced. Several studies, however, have indicated that sperm fusion with the egg membrane results in activation of the Phospholipase C second messenger pathway (Busa et al. 1985) leading to production of inositol-1,4,5-triphosphate, subsequent  $\text{Ca}^{++}$  release, and activation of Protein kinase C leading to other downstream effectors. It is currently not known how this second messenger system might act in specifying the dorsoanterior regions. However, the recent information concerning the interactions between the *Xenopus* wingless related genes (Xwnt family members) and  $\beta$ -catenin provides some important clues. This will be further considered below in light of mesoderm induction.

### **Murine Axis Formation**

Axis formation in mice is not as well defined as in amphibians. No apparent asymmetries are known to be present in the rodent egg prior to fertilization, and likewise sperm entry does not appear to affect the embryonic axes. Rather, much of the information necessary for axis formation appears to be derived from the maternal uterine axes (Smith 1985; Brown et al. 1992). The DV axis appears to correspond to the mesometrial-antimesometrial axis of the uterus

with the dorsal embryonic side being towards the mesometrial side of the uterus. The AP and left-right embryonic axes are aligned with the right-left and oviduct to cervix maternal axes, respectively. The two possible orientations of these two embryonic axes appears to be randomly determined by the position of the primitive streak which forms towards either the right or left uterine wall. Again, the molecular cues that are responsible for orienting the zygote are not yet known.

### **Establishment of the Three Germ Layers**

#### **Mesoderm Induction in *Xenopus laevis***

Due to the localized deposition of presently unknown factors (although some candidates have been identified) to the vegetal and animal hemispheres, the default state of the animal half as ectoderm and the vegetal half as endoderm is predetermined maternally. Therefore, the next major event following axis specification is mesoderm induction. The current thinking on mesoderm induction has been heavily influenced by the work of Nieuwkoop (1969, 1973, and 1977) in which the upper animal cap and the lower vegetal half was separated from the equatorial blastomeres. He found that if these are kept separate, neither produces mesoderm. However, if they are combined all types of mesoderm are produced as a result of a signal from the vegetal hemisphere to the animal hemisphere. He further showed that the type of mesoderm-induced depended on the DV location of the vegetal explant. The dorsal vegetal blastomeres could induce dorsal mesoderm while the ventral vegetal blastomeres induced primarily ventral mesoderm. These results led Nieuwkoop to postulate

that there was a gradient of a mesoderm-inducing factor which emanated from the dorsal vegetal region, designated the Nieuwkoop Center. Similar experiments by Dale and Slack (1987) led them to believe that there were two separate signals provided by the vegetal blastomeres. Based on recombinations of single non-dorsal vegetal blastomeres with animal caps, they inferred that the signal from the Nieuwkoop Center specifies dorsal mesoderm while another signal specifies primarily ventral mesoderm. According to this model, intermediate types of mesoderm would subsequently be specified within the marginal zone by a third signal emanating from the newly induced dorsal mesoderm. The source of this third signal is called Spemann's organizer based on the work of Spemann and Mangold (1924). Their work demonstrated that, when implanted on the ventral side, this region could not only induce other types of mesoderm, but could recruit host cells into forming a secondary axis in which the grafted tissue contributed primarily to the notochord. This "Three Signal Model" was subsequently elaborated in a review by Smith, et al. (1985). This has more recently been modified to a "Four Signal Model" (see for review Sive 1993; Christian and Moon 1992) to include the ventralizing molecules that will be discussed below.

Since these studies were carried out, much effort has been given to identifying and characterizing potential mesoderm inducers. Early attempts focused on conditioned media from transformed cell lines while later efforts have utilized various molecular cloning approaches (see Smith 1993 for review). Because there have been numerous reviews devoted to this particular subject (Sive, 1993; Hogan, 1995; Kimelman et al., 1992; Melton, 1991 to name a few), I will attempt to provide a consensus view of the molecular mechanism of mesoderm induction and patterning. As mentioned above, the first step in this

process occurs at the time of fertilization as the resulting cortical rotation specifies the Nieuwkoop Center. The experimental characteristics of the Nieuwkoop Center are as follows: 1) it is localized to the vegetal hemisphere on the side opposite sperm entry, 2) is capable of inducing naive ectoderm to form a functional organizer, and 3) becomes incorporated into the gut endoderm following gastrulation. Xwnt-8, noggin and Vg1 were early candidates that were shown to meet these criteria to some degree. Both Xwnt-8 and noggin fulfill the 2nd and 3rd qualifications; however, Xwnt-8 is made too late and on the ventral, not dorsal, side. Likewise, noggin mRNA is not correctly localized. In UV-ventralized embryos (which blocks cortical rotation and establishment of the Nieuwkoop center; reviewed by Gerhart, et al., 1989), both Xwnt-8 and noggin are capable of rescuing complete axes. Therefore it is thought that Xwnt-8 is mimicking another Xwnt family member's activity, and/or noggin translation or processing is, in fact, correctly localized. In the case of Vg1, the mRNA is localized vegetally but the protein appears to be under some type of post-translational regulation, because unprocessed protein is abundant throughout cells of the vegetal hemisphere (Melton, 1987). However, when this regulation is by-passed by fusing the pro-region from BMP-2 to the mature-region of Vg1, the resulting protein is processed and induces dorsal mesoderm in animal cap explants (Thomsen and Melton, 1993; Dale et al., 1993). When mRNA from this construct is injected into UV-treated embryos, the resulting BMP-2/Vg1 protein can mimic the Nieuwkoop center signal and rescue a complete axis. Recently, the chick Vg1 homolog also has been shown to be capable of inducing a secondary axis when expressing cells are implanted next to pre-gastrulation embryos (unpublished observations of Jonathan Cooke, NIMR London, and Jane Dodd,

Columbia, NY). The fact that Vg1 is tethered in *Xenopus* to the vegetal cortex prior to fertilization but then released soon afterwards implies that its localization is required for a very early inductive signal emanating from within the vegetal region.

The potential candidates within the Xwnt family that are capable of inducing a secondary axis are Xwnt-1, 3A, 8, and Xwnt-8b (Torres et al., 1996). These are also capable of rescuing UV-ventralized *Xenopus* embryos. However, based on its spatiotemporal expression pattern, Xwnt-8b is possibly the best candidate at this time is. Xwnt-8b is maternally expressed and localized to the animal hemisphere during early cleavage stages and is also capable of rescuing complete axes (Cui et al., 1995). As alluded to earlier, Xwnt involvement in axis determination appears to be mediated, at least in part, through a component of the cytoskeleton,  $\beta$ -catenin (known for its role in adherens junctions; for review see Gumbiner, 1995).  $\beta$ -catenin's role in this pathway appears to be independent of its involvement in cell adhesion, because expression of truncated forms lacking the domains necessary for binding to cytoskeletal components are still capable of inducing a secondary axis in *Xenopus* embryos (Funayama et al., 1995). Rather, it appears that Xwnt signals result in an increase in nuclear localized  $\beta$ -catenin, and this then is involved in transactivating downstream targets (Yost et al., 1996). This is apparently a very early step in determining the dorsalizing center since detection of nuclear  $\beta$ -catenin on the dorsal side precedes other dorsal markers (Schneider et al., 1996). Recently, it was shown that free  $\beta$ -catenin and the transcription factor LEF-1 (lymphoid enhancer-binding factor-1) form a complex which is translocated to the nucleus and together these two molecules bind to DNA (Behrens et al., 1996). Though it is not yet known what the target genes of



this complex might be, this does suggest that  $\beta$ -catenin might directly function in regulating the transcription of genes required for axis specification.

It appears that both Xwns and noggin require a third factor, which is a TGF $\beta$  family member, in order to induce dorsal mesoderm. When animal caps from Xwnt-8 injected embryos are cultured alone no mesoderm is formed. However, in the presence of activin, dorsal mesoderm is induced. Because both Xwnt-8 and noggin can induce a secondary axis when injected into ventral vegetal blastomeres, this other factor must be vegetally localized and possibly in a latent state. The candidates for this factor include activin, which is expressed in the marginal zone, or Vg1. Since Xwnt, noggin, and Vg1 are all capable of generating a secondary Nieuwkoop Center, they could be part of an regulatory mechanism which is initiated by cortical rotation leading to a local production of a wnt family member and local production of functional noggin and Vg1, all of which might positively feed back on each other.

The identity of the ventral mesoderm inducing signal (which also emanates from the vegetal blastomeres) has received less attention. Basic fibroblast growth factor (bFGF) which is expressed at the high levels in the marginal zone has been suggested as possible candidate (see Kimelman et al. 1992). The fact that bFGF levels are highest in the responding cells, however, may imply that its production is in response to the actual ventral mesoderm inducing signal. If this is the case, then the nature and identity of this other signal is not yet apparent. The final component of the Four Signal Model is the ventralizing signal within the marginal zone which opposes the dorsalizing effects of the Organizer. Two factors have been shown to be more highly expressed ventrally and show this effect, BMP-4 (Jones et al. 1992; Dale et al. 1992) and Xwnt-8 (when delivered after the mid-

blastula transition; Sokol and Melton 1991). Both of these, when delivered after the mid-blastula transition, have been shown to inhibit the effects of activin on mesoderm induction in cultured explants.

### **Murine Germ Layer Specification**

It is unknown whether the types of pre-gastrulation inductive events seen above also occur in mouse development. Because *Xenopus*, chick, and mouse fate maps are roughly equivalent and the molecular players seen during gastrulation are very similar (see Hogan et al., 1994), it is likely that similar mechanisms for axis specification and mesoderm induction are also utilized. The differences will likely be attributable to the differences in the topological arrangements of the pre-gastrulation tissues which give rise to the embryo proper.

Prior to gastrulation in mouse, the embryonic tissues are contained within the epithelial epiblast layer (Snow, 1977). The events of gastrulation (from Hogan et al., 1994) begin around 6.5 days post-coitum (dpc) as cells at the future posterior side of the egg cylinder begin to detach from the epithelium and take up positions between the epiblast and the extraembryonic endoderm. The mesoderm of the head process, notochord, and gut endoderm are the first cells to egress followed by intermediate, lateral and extraembryonic mesoderm. Through the migration and proliferation which occurs during gastrulation, the overt embryonic axes are established and the proper juxtapositioning of the three germ layers is accomplished leading to subsequent steps of patterning along the AP axis.

## **Homeobox Genes in Patterning During Development**

Some of the key players involved in embryonic patterning and subsequent differentiation are the members of homeobox class of transcription factors. From flies to man the positional specification provided by the homeobox genes has been implicated as providing the molecular superstructure upon which the developing embryo is built. Though it is not yet clear what the mechanisms are which establish the correct patterns of expression of these genes, it is clear that the loss of function in these genes results in regional deletions and/or changes in pattern.

### **Homeobox Genes in *Drosophila melanogaster***

The first homeotic mutations were reported by Bridges and Morgan (1923) in the fruit fly, *Drosophila*. The early observations involved mutagenizing through chemicals or radiation and noting how certain mutations which resulted from these treatments caused large scale changes in the fates of body structures (antennae becoming legs, halteres becoming wings, or shifts in segment identity anteriorly or posteriorly). Subsequent molecular genetic analysis of these mutated genes led to the discovery of a large family of genes termed homeotic genes. Comparison sequence of the antennapedia (Antp) and ultrabithorax (Ubx) homeotic genes resulted in the identification of the homeobox (McGinnis, et al., 1984a & b; Scott & Weiner, 1984), a DNA binding motif, consisting of 60 amino acids that form four  $\alpha$  helices, that has become the hallmark of this gene family. The study of the role that the *Drosophila* homeobox genes play in development indicates that they function primarily in specifying segment identities (Lewis, 1978; Gehring, 1986; Akam, 1987; Scott et al., ; Kaufman et al.,

1990). Even more intriguing was the finding that many of the homeotic genes in *Drosophila* were located in two clusters, the Bithorax and Antennapedia Complexes, collectively called the HOM-C complex, which are tandemly arrayed on *Drosophila* chromosome 3. Each of the genes in these clusters is oriented in the same 5' to 3' direction. Further, this precise chromosomal arrangement also appears to have some link to each gene's expression and area of primary influence along the anterior to posterior axis, as was first noted by Lewis (1978). Those genes at the 3' end of the cluster are expressed and influence development at more anterior regions relative to the other members of the cluster--a phenomenon termed colinearity. Homeobox genes which are similar to the members of the *Drosophila* HOM-C complex have been identified in other insects as well as in members of other phyla including amphioxus (Garcia-Fernandez and Holland, 1994), flatworms (Bartels et al., 1993), sea urchin (Mao et al., 1996), mollusks (Wray et al., 1995), annelids (Aisemberg et al., 1993; Dick and Buss, 1994), nematodes (Salser and Kenyon, 1992), hydra (Schummer et al., 1992), and sponges (Degnan et al., 1995). At this time, the presence of a HOM-C related cluster has only been demonstrated for the flour beetle (*Tribolium castaneum*, Beeman et al., 1989) and nematode (*Caenorhabditis elegans*, Wang et al., 1993) among these other organisms.

### **Homeobox Genes in Vertebrates**

Even more surprising was the discovery that not only do insects and lower organisms have such homeobox genes, but that from *Drosophila* to man complex, multicellular organisms have similar homeobox genes that play key roles in the areas of regionalization and tissue specification (Akam, 1989). Using the

sequence encoding the homeodomain, the DNA binding domain, from *Drosophila* Antp, low stringency homology screens resulted in the initial cloning of a small group of *Xenopus* homeobox homologues (Carrasco, et al., 1984; Muller, et al., 1984). The numbers of vertebrate homeobox genes has greatly increased since the isolation of these

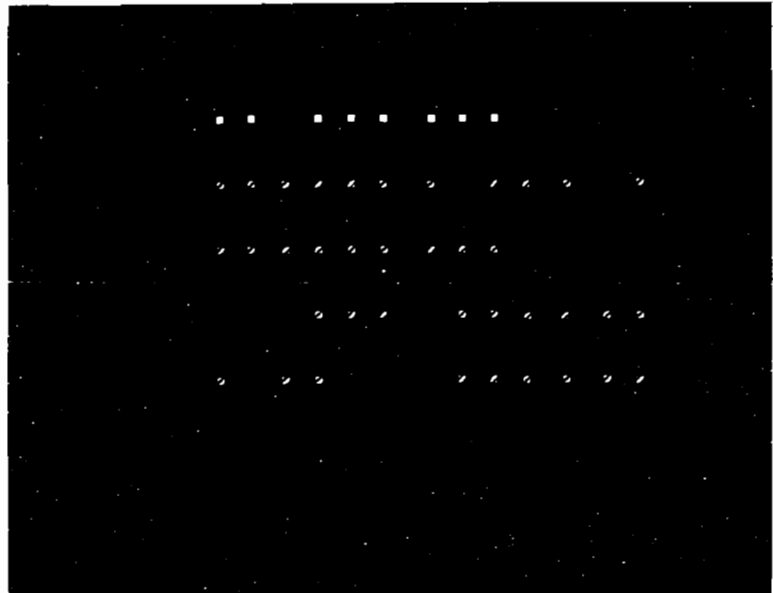


**Figure 1. Organization of the Mouse Hox and Drosophila HOM-C Homeobox Clusters.** There are four separate vertebrate clusters designated A, B, C, and D while in *Drosophila* there is only one cluster which is split into the Antennapedia and Bithorax complexes. In vertebrates, as in *Drosophila*, the order of the genes within each cluster 3' to 5' indicates its region of influence along the anterior-to-posterior axis. This figure was taken from a review by Krumlauf, et al. (1993).

early clones. As the chromosomal loci of these homeobox genes were mapped in mouse and man, it was found that many were tightly clustered in the same collinear relationship observed in *Drosophila* (Akam, 1989). Though *Drosophila* has only the HOM-C cluster (which is split into the Antennapedia and Bithorax complexes), most vertebrate species have four such clusters designated as Hox clusters A, B, C, and D (see Fig. 1; reviewed by Krumlauf, 1992). The expression data of many of these genes in the region of the hindbrain (see Fig. 2, review by Krumlauf, et al., 1993) implies that, as was seen in *Drosophila*, these genes are also involved in regionalization and patterning along the body axis and in metamerism of the vertebrate hindbrain.

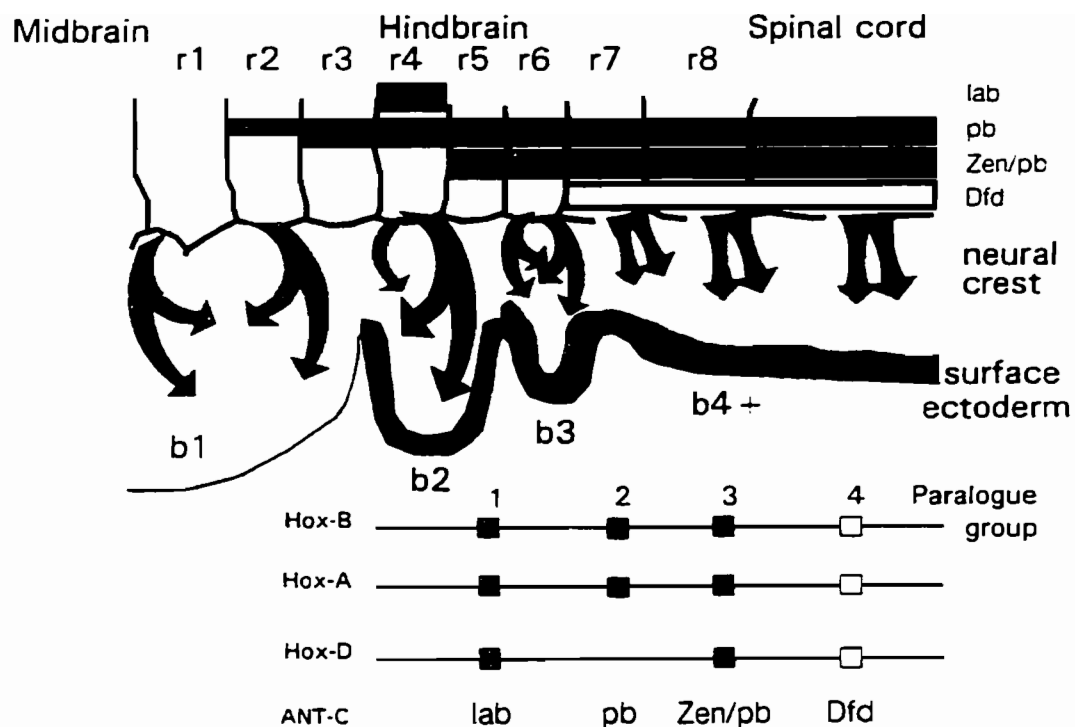


**Figure 2. Hox Gene Patterning in the Hindbrain.** A summary of the expression patterns of several hox genes in the region of the hindbrain and the branchial arches. The arrows extending from the rhombomeres indicate neural crest cells which arise from these regions. The shading patterns indicate different genes as indicated in the diagram of the Hox clusters below. The expression of these genes has been shown to be important in the processes of regionalization and tissue specification for several of the genes shown. This figure is modified from Krumlauf, 1993.

Null mutations of several murine Hox genes have shown that there are several similarities in the roles which these vertebrate homologues play in development. The HoxC8 (Le Mouellic, et al., 1990; Le Mouellic, et al., 1992), HoxA3(Chisaka & Capecchi, 1991), and HoxA1 (Lufkin, et al., 1991; Chisaka, et al., 1992; Carpenter, et al., 1993) induced mutations all indicate that the anterior most boundary of expression designates the region of the embryo where a homeobox gene has its influence. For each of these, the homozygous mutant animals showed the absence or malformation of tissues and structures from within the region corresponding to the gene's anterior expression domain. The HoxA1 null versus the HoxA3 null indicates that where there are expression patterns

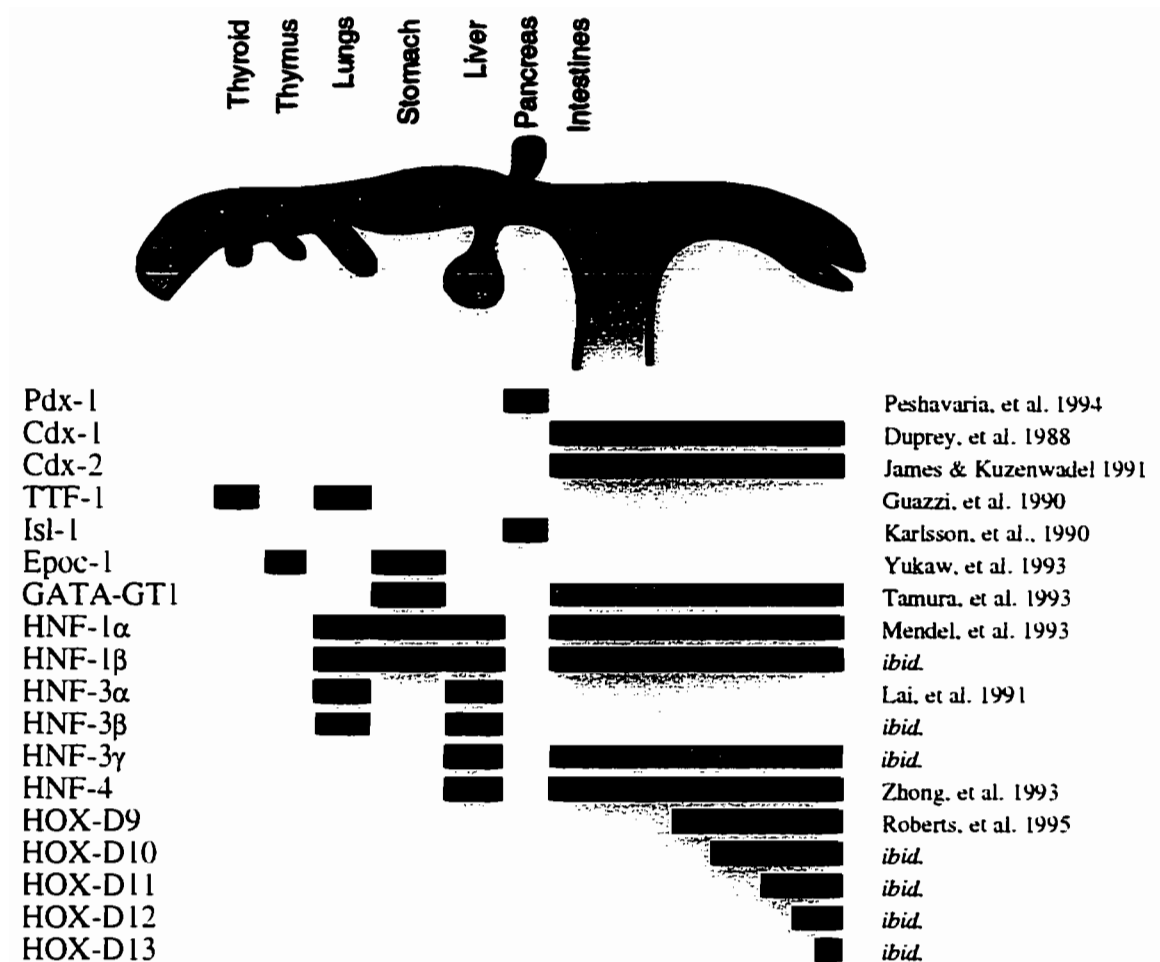


**Figure 3. Patterning Of the Primitive Endoderm.** The above figure depicts how that, just as has been shown in the neurectoderm and mesoderm, there are also tissue specific transcription factors which appear to be important in the processes of tissue specification and differentiation. This is not meant to represent a complete listing, nor does this figure properly show each individual gene's pattern of expression. It is likely the combinations of developmentally regulated transcription factors which is important in determining tissue specificity and cellular fate. This listing contains Antp-like homeobox genes (Pdx-1, Cdx-1, Cdx-2, TTF-1, and HOX D 9 to 13), LIM domain genes (Isl-1), zinc-finger motif genes (GATA-GT1), POU domain genes (Epoc-1), and forkhead-like homeodomain genes (HNF-1a, HNF-1b, HNF-3a, HNF-3b, HNF-3g, HNF-4) to illustrate how that multiple gene families interact in regionalizing the gut as has been shown in the hindbrain (see review, Krumlauf, et al., 1993).

which overlap or fall within the same region of the embryo, each gene can contribute to the differentiation of a subpopulation of cells within the region. Specifically, HoxA1 appears to act on the neurogenic neural crest lineage within

its most anterior region of expression while HoxA3 appears to specify the mesenchymal neural crest from this same region. It is also apparent from the HoxA1 (Lufkin, et al., 1991; Chisaka, et al., 1992; Carpenter, et al., 1993) and HoxA2 (Rijli, et al., 1993; Gendron-Maguire, et al., 1993) null mutant mice that these genes' sphere of influence can extend beyond those regions where their expression is seen. Cells or tissues which apparently never express a particular homeobox gene can be influenced by its expression in other cells or tissues because of a growth factor or hormone, which is released by the expressing cells, or by direct inductive events through cell-to-cell interactions between the two populations. The types of large scale respecification or homeotic transformations as seen in *Drosophila* (e.g. antennae to legs), however, have not yet been reported for vertebrate loss of function or gain of function mutants. The types of respecifications seen in mutant mice are more subtle: duplications in ear ossicles in HoxA2 null mice (Rijli, et al., 1993; Gendron-Maguire, et al., 1993); shifts in axial skeletal elements to more anterior morphology as seen in HoxC8 (Le Mouellic, et al., 1990; Le Mouellic, et al., 1992) and HoxB4 (Ramirez-Solis, et al., 1993) null mutants; and posterior shifts in axial skeletal elements as seen in HoxD4 gain of function mutants (Lufkin, et al., 1992). In general, vertebrate homeobox genes like their *Drosophila* homologs appear to function in determining the broad fates of cells within a defined region along the AP axis.

### **Specification of the Primitive Endoderm**

Within the gut, there are other homeobox genes as well as transcription factors from other gene families that have been reported and appear to play a role in patterning and/or differentiation of endodermal derivatives of the primitive gut



(see Fig. 3). Figure 3 illustrates how different transcription factors have been shown to have regional expression patterns rather than merely organ specific patterns of expression. Much data has accumulated concerning the members of the Hepatocyte Nuclear Factor (HNF) transcription factor family and the role they appear to play in liver-specific gene expression. HNF-1 $\alpha$  and  $\beta$  are both expressed as early as 8 dpc in mouse lateral plate mesoderm and primitive endoderm and in the lung, stomach, liver, and intestine of adult tissues (Mendel, et al., 1991). Mendel, et al. further show that, while HNF-1 $\alpha$  is capable of directing transcription from liver specific promoter sequences, this appears to be a tissue-specific phenomenon as these same liver-specific genes are not expressed in the lung or stomach where HNF-1 $\alpha$  is also expressed. This would imply that liver-specific coactivators are required for transactivation by HNF-1 $\alpha$ . HNF-3 $\alpha$  and  $\beta$  have been shown to be expressed in the gut endoderm at very early stages of mouse development (Ang, et al., 1993). Gualdi, et al. (1996) have recently demonstrated the early expression of HNF family members within the endoderm is involved in hepatic specification. The *Drosophila* homologue of the mouse HNF-4 gene, a member of the steroid receptor super family, is expressed in the liver and intestine and has been cloned and characterized in *Drosophila* development (Zhong, et al., 1993). Zhong, et al. have shown that the *Drosophila* HNF-4 protein is expressed in the developing mid-gut and fat-bodies. Further, null mutants for the *Drosophila* HNF-4 gene lose these gut structures indicating that the *Drosophila* gene, and likely the mouse homolog, are necessary for the development of these structures where they are expressed.

Recently, Sonic hedgehog (*Shh*), a diffusible signaling molecule implicated in limb and axial patterning (see for review, Johnson et al., 1994), has been shown

to be expressed in the endoderm of the caudal intestinal portal and to be involved in patterning the hindgut in chick (Roberts et al., 1995). Specifically, they showed that the abdominal B-related members of the Hox A and D clusters are expressed in a nested pattern within the hindgut. These boundaries of expression correspond to later anatomical boundaries within the gut. Through misexpression of *Shh*, they showed that it was capable of inducing these genes within competent endoderm, thus providing another example of hedgehog family members providing a signal that is involved in embryonic patterning.

Members of the caudal gene family also appears to play a role in endodermal differentiation. Both Cdx-1 and 2 are expressed in the duodenum, small intestine, and colon (James & Kazenwadel, 1991). The chicken homolog, CHox-cad, has been shown to be expressed in the lung, liver, pancreas, and the epithelial lining of the intestine (Doll & Niessing, 1993). Cdx-2/Cdx-3 has been shown to be expressed in rat islets and to weakly drive transcription from elements of the insulin promoter (German, et al., 1992). The Isl-1 transcription factor has been reported to be expressed only in cells derived from pancreatic islet cells, as shown by northern blot analysis (Karlsson, et al., 1990). The Isl-1 protein has a LIM domain and a highly diverged homeodomain which shows only 25-30% identity to other homeodomain proteins (Karlsson et al., 1990). They report that Isl-1 is able to bind to a region of the insulin promoter by electrophoretic mobility shift assay. Other transcription factors in the gut derivatives have also been reported: the Epoc-1 POU domain gene in the thymus and stomach (Yukaw, et al., 1993); GATA-GT1, 2, and 3 zinc-finger proteins of the stomach and intestine (Tamura, et al., 1993); and the TTF-1 homeodomain protein of the thyroid and lung (Guazzi, et al., 1990).

### **Morphological Development of the Posterior Foregut**

The vertebrate gut derivatives (i.e. lung, liver, pancreas, etc.) all begin as simple evaginations of the gut epithelium into the surrounding mesenchyme. These outgrowths are due to epithelial-mesenchymal interactions which vary between organs. The signals which are exchanged between these two tissues result in both proliferation and differentiation as the initial outgrowth expands, branches and lobulates. Studies of lung epithelial-mesenchymal interactions have shown that gut-associated mesenchyme from different regions provides region specific signals which are necessary for the development of each organ (Deucher, 1975). This study showed that lung epithelium could be redirected in its differentiation by mesenchyme from other regions such that it would adopt gastric, intestinal, or hepatic fates. The signals mediating these interactions and the target genes which lie downstream are unknown in most cases, although some of the players are now being identified.

### **Hepatic and Pancreatic Development**

The hepatic and pancreatic outgrowths are the first structures to develop from the primitive gut and the early tissue interactions have been well studied for both of these. At 8.5 dpc, the foregut pouch endoderm extends rostrally into the headfold, with its anteroventral surface in contact with pre-cardiac mesoderm and the posterodorsal surface continuous with notochordal mesoderm (Wessells and Cohen, 1967). Starting at ~9.0 dpc, the pancreas and liver arise from bidirectional endodermal outgrowths of the posterior foregut. While most of the ventral outgrowth acquires a hepatic fate, the caudal-most portion forms the ventral

pancreatic bud; the dorsal outgrowth produces the dorsal pancreatic bud. Previously, tissue recombination studies showed that pre-cardiac mesoderm induces hepatic endoderm (see for review LeDouarin, 1975), while axial mesoderm induces pancreatic endoderm (Wessells and Cohen, 1967). The liver and pancreas primordia are also, at least superficially, similar in their mechanism of induction and epithelial-mesenchymal interaction. Unlike the situation described above for the lung endoderm, both the liver and pancreatic precursors receive an early instructive signal which imparts the information necessary for the proper differentiation of the endoderm. Although both of these tissues require the presence of mesenchyme, this is a non-instructive influence (i.e. mesenchyme from other organs can be substituted) which consists, at least in part, of a diffusible peptide signal (Golosow and Grobstein, 1962)--consistent with it being some type of secreted factor. Gualdi et al. (1996), using tissue recombinations between pre-cardiac mesoderm and various regions of the primitive gut, have also provided evidence that the inductive influence of the pre-cardiac mesoderm is dominant over the programs of non-hepatic endoderm, including that which gives rise to the dorsal pancreas. Collectively, these data suggest that the posterior foregut patterning and subsequent differentiation could be the result of an interplay between the opposing hepatic and pancreatic influences, with the endoderm producing either hepatic or pancreatic cell types according to the relative strengths and/or proximity of these signals.

### **Duodenal Development**

The duodenum, which is derived, at least in part, from the "non-induced" endoderm of this same region, is not simply a conduit in which to combine the

exocrine products of the liver and pancreas with gastric contents. Rather, the duodenal epithelium is a complex mixture of cell types, each with a unique and necessary task to carry out in digestion (Walsh and Dockray, 1994).

Differentiated cell types are not apparent within the duodenum until after the transition from a pseudostratified to columnar epithelium which occurs at around 16 dpc (Roth et al., 1991). The current inability to detect differentiated cell types at earlier time points could merely be a reflection of a lack of markers for these cells at early stages of differentiation. Most of the differentiated cell types are apparent post-natally and the remainder can be detected soon afterwards (Walsh and Dockray, 1994).

Beginning at the neck of the duodenum, the first anatomical feature of note is the Brunner's glands. These are epithelial evaginations into the submucosa, which form just before birth. The secretion of a bicarbonate and mucin mixture by these glands contributes to the acidic to basic pH shift that occurs as gastric contents move into the intestines. Moving caudally, the duodenum is lined with villi which are covered primarily by columnar epithelium with interspersed goblet cells and enteroendocrine cell types. The latter of these is a family of cell types, each of which is distinguished by the peptide factor it produces (reviewed by Solcia et al, 1987). These cell types monitor components of the luminal milieu and feedback on the digestive system to regulate gastric and intestinal contractions, control pancreatic and hepatic secretions, potentiate the response to blood glucose levels by pancreatic  $\beta$ -cells, as well as other functions (Walsh and Dockray, 1994). Since each of these cell types play unique roles in digestion, one might expect that their location within the gut might be somehow influenced by their function, and this is the case. For example, the CCK cells,

which sense fatty acid levels and release cholecystokinin (CCK) to regulate hepatic bile secretions (necessary to emulsify lipids), are present in high numbers within the proximal duodenum. This provides a rapid, pliant response to newly released gastric contents. The profiles of these various cell types along the gut suggests that the duodenum and the rest of the gut display complex patterning at both the macroscopic and microscopic levels

### **XlHbox-8/PDX-1 in Pancreatic & Duodenal Development**

#### **XlHbox-8 in *Xenopus* Development**

The XlHbox-8 Antp-like homeobox gene, which lies outside the four homeobox gene clusters, has been shown to be involved in endodermal development during *Xenopus* embryogenesis. Immunolocalization using affinity purified antibodies to the C-terminal end of the XlHbox-8 protein has shown that the XlHbox-8 protein was expressed in a narrow band within the endoderm of the posterior foregut (Wright, et al., 1988). However, no expression is seen in the surrounding mesoderm, heart, or in any neural structures at any stage examined, a feature which is unique to XlHbox-8 among vertebrate Antp-class homeodomain proteins. More recently, work by Laura Gamer (Gamer & Wright, 1995) has detected XlHbox-8 mRNA as early as stage 12.5 neurula embryos. This work has further shown that XlHbox-8 is expressed autonomously within the dorsal region of vegetal explants taken prior gastrulation (stage 8-9). However, UV ventralization eliminates XlHbox-8 expression in these cells. Because UV treatment blocks the formation of the Nieuwkoop center, this implies (at least in amphibians) that the initial signal(s) that leads to XlHbox-8 expression does not come from

adjacent mesodermal tissue after gastrulation; rather, the early dorsalizing signals are likely responsible for XlHbox-8 induction, either directly or indirectly.

During organogenesis, XlHbox-8 expressing cells within the future duodenum begin to proliferate at opposing dorsal and ventral sites growing out to form the dorsal and ventral pancreatic buds by st. 38 (Wright, et al., 1988). As the pancreas differentiates giving rise to the various endocrine and exocrine cell populations, XlHbox-8 expression is seen throughout the pancreas and in the endodermally derived epithelium of the duodenum (Gamer & Wright, 1995). In the adult pancreas, expression is seen in the exocrine duct cells and a proportion of the acinar cells. In the islets, 91% of insulin producing  $\beta$ -cells also express XlHbox-8, 47% of somatostatin producing  $\delta$ -cells, and only 6% in glucagon expressing  $\alpha$ -cells co-express XlHbox-8. Based on these expression data, it appears that XlHbox-8 plays a key role in specifying the fate of the region of the endoderm which gives rise to the pancreas and may play a role in the differentiation of the  $\beta$ -cell lineage.

### **XlHbox-8 Homologues in Rat and Mouse**

XlHbox-8 homologs were cloned by three independent groups in mouse and rat, and these are also expressed exclusively within the pancreas and duodenum during development. Islet and duodenal homeobox gene-1 (IDX-1; Miller, et al., 1994) and somatostatin transactivating factor 1 (STF-1; Leonard, et al., 1993) were cloned by PCR from rat cDNA libraries of immortalized cell lines derived from pancreatic islet cells. Insulin promoter factor 1 (IPF-1; Ohlsson, et al., 1993) likewise was cloned by PCR from a mouse immortalized insulin producing cell line. These three genes all share 100% identity in the homeodomain with

XIHbox-8 and are 67% similar N-terminal of the homeodomain (Peshavaria, et al., 1994). The XIHbox-8 N-terminal antibody also cross reacts with the STF-1 protein isolated from the  $\beta$  TC-3  $\beta$ -like cell line (Peshavaria, et al., 1994). Immunolocalization studies of adult mouse pancreas with the XIHbox-8 N-terminal antibody have shown remarkable similarity with those in *Xenopus*. Expression in mouse is seen in the duct cells and primarily within the  $\beta$ -cells of the islets (91% of insulin expressing cells co-express STF-1; Peshavaria, et al., 1994) as seen for *Xenopus*. Miller, et al. (1994) used degenerate PCR primers to the highly conserved third helix of the homeobox with rat islet cDNA as the template and isolated eleven different DNA sequences. Only the sequences corresponding to IDX-1/STF-1 had deduced amino acid sequences which were 100% identical to XIHbox-8. Cdx-4 was the next most similar at 70% identity (over the region amplified). This would seem to indicate that there are no other XIHbox-8-like genes that are expressed in this tissue. Based on this and the concordance of the expression data, IDX-1/STF-1 and IPF-1 appear to be the rat and mouse homologues of XIHbox-8. In order to consolidate the nomenclature for this gene, the name PDX-1 (Pancreatic/ Duodenal homeoboX gene 1) has recently been approved by the International Committee for Mouse Nomenclature to replace the previous names, IPF-1, IDX-1, and STF-1.

### **Transactivation by PDX-1**

Several groups have studied the ability of PDX-1 to transactivate putative downstream target genes (i.e. insulin and somatostatin). Based on electromobility shift assays using rat Insulin-II regulatory elements, PDX-1 is capable of binding to both the Flat-E and the IPF elements (Peshavaria, et al., 1994). This has been



corroborated by Peers, et al. (1994) by similar techniques and DNase footprinting. *In vitro* assays in insulin-producing cell lines indicate that the F1at-E element is primarily responsible for driving expression in these cells (Peshavaria et al., 1994), based on mutational analysis of the two elements. Studies of the involvement of PDX-1 in somatostatin expression have demonstrated that PDX-1 also binds specifically to both the TSE-I and TSE-II elements and wild type PDX-1 is capable of driving reporter gene expression from these elements (Miller et al., 1994; Leonard et al., 1993).

The transactivation domain of PDX-1 has been mapped by two separate techniques. Using GAL4/PDX-1 fusions to drive GAL4 reporter constructs, it was determined that the first 84 amino acids possess a transactivation domain while the region C-terminal to the homeodomain appears to inhibit this activity (Peers et al., 1994). Similar activities were detected using N-terminal and C-terminal deletions of PDX-1 (utilizing the DNA binding domain of PDX-1) to drive reporter expression from somatostatin regulatory elements (Lu et al., 1996). For both insulin and somatostatin transactivation, PDX-1 has been shown to act synergistically with a cofactor. In the case of insulin, the helix-loop-helix transcription factor, Pan1/E47, has been shown to bind the Far and Nir elements of the insulin gene and interact with PDX-1 to drive reporter gene expression from insulin regulatory elements (Peers et al., 1994). Peer, et al. report that this interaction does not affect PDX-1 binding, rather the effects are only seen at the level of transactivation. The somatostatin gene, however, utilizes the mammalian extradenticle homolog, Pbx (Peers et al. 1995). This study indicates that the PDX-1/ Pbx interaction requires the conserved homeopeptide, located N-terminal to the homeodomain, as well as the N-terminal portion of the homeodomain. In

contrast to the report by Peers, et al. for insulin transactivation, this study demonstrated that this interaction stabilized PDX-1 binding resulting in an increase in reporter expression.

Based on the above *in vitro* studies and the coincidence of PDX-1 and insulin expression, PDX-1 appears to play a role in endogenous insulin expression. This contention is further supported by the observation that chronic hyperglycemic conditions that lead to loss of insulin expression also result in a loss of PDX-1 expression (Peshavaria et al., 1995). It is uncertain what role PDX-1 plays in endogenous somatostatin expression since PDX-1 is only made by a small fraction of mature somatostatin-expressing cells of the pancreas (Peshavaria et al., 1994). PDX-1 may be required for certain earlier stages of development or for a subpopulation of somatostatin expressing cells.

XIHbox-8 and PDX-1 are unique in that based on all known expression data their only function appears to be within the pancreas and duodenum. An increased understanding of how PDX-1 functions in pancreatic and duodenal development could be important in gaining a better understanding of diseases like diabetes. The study of PDX-1 in pancreatic/duodenal development promises not only to provide information regarding the steps in pancreatic and duodenal differentiation, but also to help elucidate how Antp-like homeobox genes function in regionalization, specification, and differentiation in the vertebrate embryo. The PDX-1 expression profile and the data which show that it is capable of regulating pancreatic gene expression indicate that PDX-1 could play a vital role in specifying the pancreatic fate as well as directing pancreatic differentiation.

This dissertation describes my initial attempts at cloning the mouse

XIHbox-8 homolog, *pdx-1*; as well as the actual cloning and mapping of the locus using the rat STF-1 cDNA sequence. Also described are the details of a genetic test of the function of PDX-1 using the techniques of gene targeting to generate two null alleles in mouse. This work attempts to provide some answers to the question of what role PDX-1 plays in pancreatic and/or duodenal patterning and differentiation. Utilizing a targeting strategy which results in a  $\beta$ -galactosidase ( $\beta$ gal) fusion to PDX-1 this study was able to address the question of whether PDX-1 is required to maintain its own expression or the survival of the cells which normally express it. Analysis of these animals also provides three-dimensional information concerning PDX-1's spatiotemporal expression patterns which was not previously apparent from standard *in situ* hybridization and immunohistochemistry techniques.

## CHAPTER II

### CLONING OF THE MURINE XlHbox-8 HOMOLOG

#### Introduction

Following the characterization of XlHbox-8 in *Xenopus* by Wright, et al. (1988) and based on the patterning roles that other homeobox genes seemed to play in vertebrates it seemed likely that XlHbox-8 played a pivotal role in the development and differentiation of the pancreas and duodenum. In order to test this hypothesis it was necessary to transition to the mouse system in order to take advantage of the genetic approaches for gene targeting and production of transgenic animals. The first step towards this end was the cloning of the mouse homolog of XlHbox-8. Several approaches were used to accomplish this including genomic and cDNA library screening, PCR with degenerate primers, and RT-PCR from pancreatic/duodenal RNA with degenerate primers.

#### Methods and Materials

##### Southern Blotting

Potential probe regions from the *Xenopus* XlHbox-8 cDNA (see Fig. 4) were tested by Southern blot prior to library screening. Wild-type mouse ICR strain DNA was digested with *Bam*HI, *Pst*II, and *Eco*RI and electrophoresed on 0.8% agarose gels. The DNA was transferred to supported nitrocellulose (Schleicher and Schuell) by capillary action with 20X SSC (see Sambrook et al., 1989), and subsequently baked for 1-1.5 hr at 80°C under vacuum. The filters

were blocked for 3-6 hrs in a solution consisting of 40% formamide, 0.5% SDS, 5X SSPE, 5X Denhardt's solution, 0.02% sodium pyrophosphate, 6-7% dextran sulfate, and 125 units/ml heparin sulfate. Hybridization were carried out in the same solution at temperatures ranging from 30 to 45°C to determine which probes seemed to cross react at single copy levels and to ascertain which conditions provided the best signal to noise ratio. Random primed <sup>32</sup>P-dATP labeled DNA probes were generated as previously described (Fienber and Volgelstein, 1983). Following overnight hybridization, the filters were washed once in 2X SSC at room temperature and twice in 2X SSC at the empirically determined temperature. The filters were exposed to X-ray film from overnight to several days, according to the level of signal.

Following the cloning of *pdx-1*, high stringency conditions were employed for same species hybridizations used in mapping the locus. A hybridization temperature of 42-45°C was used with 40% formamide, as above.

### **Library Screening**

The libraries used were as follows: a 8.5dpc mouse cDNA library, a λZap 10.5 dpc mouse cDNA library, a λ2001 mouse genomic library, and λFixII 129/Sv mouse genomic library. Four different *Xenopus* cDNA probes derived from XlHbox-8 sequences were utilized on separate screens, as illustrated in Fig. 4. Ultimately, a 900 bp portion of the rat XlHbox-8 homolog was obtained as a gift from Mark Montminy, and it was cut in half at a *MluI* site 5' of the homeodomain; each half was used on two separate screens of the 129/Sv genomic library. For each screen, 4-6 plates were plated for cDNA libraries and 6-8 plates for genomic libraries with 2.5 to 3x10<sup>5</sup> pfu/plate. Following overnight incubation, plaques

were lifted onto supported nitrocellulose using standard procedures and baked as above. The filters were hybridized using the empirically determined conditions (hybridization with the rat STF-1 probes were done at 50°C) with <sup>32</sup>P-dATP labeled DNA probes, generated as above. Positive clones were plaque purified and subcloned into the Bluescript vector for sequencing and further analysis.

### PCR Techniques

Standard conditions were used, as recommended by Perkin-Elmer Co., consisting of the following: buffer containing 50 mM KCl, 10 mM Tris HCl (pH 8.6), 1-6 mM MgCl<sub>2</sub>, 200 ng/ml gelatin, 10-200 mM dNTP's, 2.5 units Taq polymerase, plus the appropriate primers. Three separate degenerate primers were utilized for these experiments, one sense strand primer made to the first homeodomain of XIHbox-8 α helix whose sequence was AAYAARMGNACN-MGNACNGC (designated XIH85', ambiguities indicated by Sanger ambiguity codes), one antisense primer made to the third helix and specific for the XIHbox8 specific histidine whose sequence was TTYTGRAACCADATYTTDATR (designated XIH83'), and a second antisense primer was made to a region of the third helix which is common to Antp-class homeodomain proteins (designated BB21, personal communication from Bruce Blumberg). The reaction conditions for these primers were determined using *Xenopus* genomic DNA as template and mouse template with single copy amounts of XIHbox8 plasmid clones. The MgCl<sub>2</sub>, dNTP concentrations, and annealing temperature for each primer set were empirically determined.

For RT-PCR reactions, RNA was isolated from 1 dpp (day post-partum) by

removing the pancreas and proximal duodenum and freezing them in liquid nitrogen. The tissue was homogenized in guanidium isothiocyanate and purified on a CsCl gradient. First strand synthesis was done using Avian Reverse Transcriptase with random hexamer primers and 10 ug of RNA template. This was then used in PCR reactions with both primer sets at the conditions determined.

## **Results**

### **Initial Library Screens**

A 8.5 dpc mouse cDNA library was screened using a probe extending from the 3' end of the homeobox to a downstream *PstI* site (Fig. 4). Low stringency conditions (30°C hybridization and washes) were used and over 100 clones were isolated. These were subsequently subcloned into Bluescript and analyzed by standard Sanger dideoxy sequencing from each end, using vector specific T3 and T7 primers, and using the BB21 homeobox specific primer (see Methods and Materials). Though several novel homeobox genes were cloned, none appeared to be homologous to XIHbox-8 (there was less than 85% homology within the homeodomain sequences and none had the XIHbox-8 specific, histidine residue within the third helix).

A λZap 10.5 dpc mouse cDNA library was also screened with the entire coding region of XIHbox-8. Reduced stringency was used, 35% formamide, 40°C annealing temperature, and 47°C for the final wash (see Methods and Materials). Several clones were purified from this screen which were subsequently sequenced using the degenerate homeobox primer, as above, but none of these clones contained a homeobox of any type.

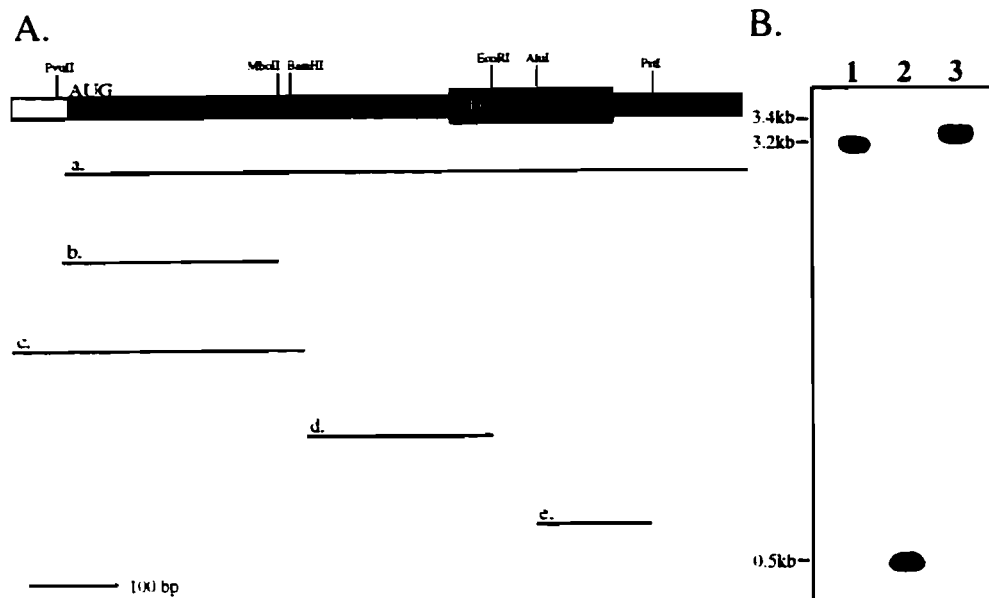


**Figure 4. Cloning Attempts Using XIHbox-8 Probes.** The above figure illustrates some of the preliminary library screens to clone the XIHbox-8 homolog. (A) Panel A shows a diagram of the near full length cDNA of XIHbox-8 which was used for producing the probe fragments. Fragment a extends from the AUG to the stop codon and was used to probe the  $\lambda$ Zap 10.5 dpc mouse cDNA library. Fragment b includes from just upstream of the initiator AUG down to a *MboII* site just upstream of a repetitive DNA region which encodes a His repeat within the protein. This was used on one attempt at screening a  $\lambda$ 2001 mouse genomic library. Fragment c extends from the 5' end of the cDNA to a *BamHI* site just downstream of the His repeat and was used twice for screening the  $\lambda$ 2001 mouse genomic library. Fragment d extends from the same *BamHI* site downstream to an *EcoRI* site in the 5' end of the homeodomain. This was also used twice in screening the  $\lambda$ 2001 mouse genomic library. Fragment e is the same fragment which was used for producing the C-terminal antibodies to XIHbox-8. This was used on the initial screen of a mouse 8.5 dpc cDNA library. Panel B shows a scanned autoradiograph of a Southern of *BamHI* (1), *EcoRI* (2), and *PstI* (3) digested mouse genomic DNA probed with fragment c.

Several different fragments of the XIHbox-8 cDNA were tested at low stringency on ICR mouse genomic Southern to determine the optimum probe and conditions. Three fragments from the N-terminal end of the protein were identified which gave good signal-to-noise ratios on genomic Southern (see Fig. 4). Because the pancreatic contribution of mRNA isolated from whole embryos



would be expected to be small and due to the possible presence of pancreatic RNases, it is possible that mRNA's from the pancreas could be under-represented in a cDNA library. To account for this possibility, these probes were used several times to screen a  $\lambda$ 2001 mouse genomic library. Multiple clones were isolated, but none of the clones was related to XlHbox-8 by sequence analysis.

### PCR Cloning Attempts

Degenerate PCR primers were made based on the XlHbox-8 homeobox sequence. A 5' sense primer was made to the amino acid sequence NKRTRTA from the 5' end of the homeobox. A 3' anti-sense primer was made to the amino acid sequence HIKIWFQ, which should be specific for XlHbox-8 since the histidine at this position is glutamine in all other Antp-like homeobox genes which have been described in vertebrates (Gehring, et al., 1994). The degenerate, homeobox specific primer described above was also used. The reaction conditions were optimized using plasmid clones of XlHbox-8 and *Xenopus* genomic DNA as templates. Fragments of the expected size were cloned from *Xenopus* DNA reactions to confirm that XlHbox-8 was being amplified. The optimized conditions were used with mouse genomic DNA and modified further. The conditions included 2-3 mM MgCl<sub>2</sub>, 100-150 mM dNTP (in addition to other components which were not optimized, see Method and Materials), and 46°C annealing temperature for 35-40 cycles with both primer sets. The band of the expected size was cloned from several separate reactions. Over a hundred clones were analyzed by dideoxy sequencing. Although clones containing sequences corresponding to several known homeobox genes (several were members of the HOX clusters) and two novel genes were isolated, none of these appeared to be

homologous to XlHbox-8, based on the degree of homology within the homeodomain.

Due to the possibility that an intron could fall within the homeodomain of the XlHbox-8 homolog, RT-PCR was utilized in an attempt to amplify the XlHbox-8 homolog directly from pancreatic mRNA. After first strand synthesis from random hexamers with reverse transcriptase, this was used as the template for PCR reactions. The reaction was gel purified and the expected band size was purified and subcloned. These were analyzed by dideoxy sequencing. Although some contained homeobox sequences from previously cloned genes, none showed any similarity to XlHbox-8.

### **Homology Screen Using rat STF-1 XlHbox-8 Homolog**

After the initial attempts to clone the mouse homolog of XlHbox-8 using *Xenopus* sequences, a portion of the cDNA of the rat STF-1 gene containing the entire coding region (obtained by PCR and subcloned into pBluescript as a *BamHI* fragment) was acquired in 1993 from Mark Montminy (Salk Institute). STF-1, as described in Chapter I, is 100% identical in the homeodomain and 67% identical N-terminal of the homeodomain, as compared with the XlHbox-8 sequence. Both the 5' region (400 bp *BamHI-MluI* fragment not including the homeodomain) and the 3' region (500 bp *MluI-BamHI* fragment) of this sequence were used as probes to screen a mouse 129/Sv strain genomic library. These two screens were carried out by C.V.E.W. and Michael Ray. The 5' probe gave high background (i.e. thousands of hybridizing plaques) using moderate stringency (35% formamide and washing at 50°C in 0.1X SSC), and therefore the 3' homeodomain containing portion was used with slightly higher stringency (40%

formamide and washes at 50°C in 0.1X SSC). Four independent positive clones were obtained and plaque purified. Southern analysis of DNA samples from these clones using STF-1 cDNA probes revealed that the #2 clone contained both 5' and 3' cDNA regions and appeared to contain the largest amount sequence 5' of the putative transcriptional start site. This clone was chosen for detailed mapping and sequence analysis.

### Characterization of #2λ Clone

The #2 clone was subcloned into Bluescript as a single *Sall* fragment (*Sall* sites are from the λFixII vector and flank the *XhoI/Sau3A* insertion site), as five independent *XbaI* subclones, and as two *Sall/BamHI* subclones. These were restriction mapped and individual maps were compared and combined to generate the complete map of the locus (see Fig. 5). To define the intron/exon boundaries, the BB21 homeodomain specific primer (which reads in an antisense direction) and a primer made to the 5' cDNA sequence were used to sequence the 3kb and

### Map of #2λ Clone of *pdx-1*:

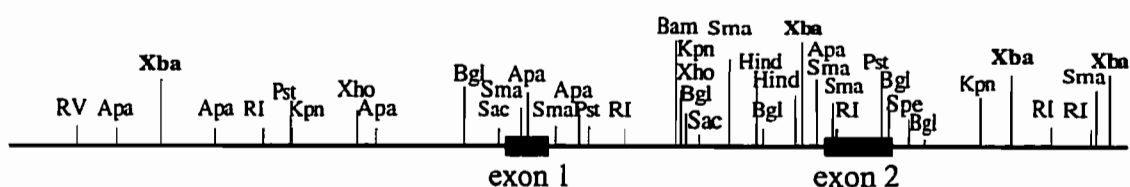


**Figure 5. Restriction Mapping of #2λ Clone of *pdx-1*.** Of the four *pdx-1* clones which were isolated from the 129Sv genomic library, the #2 clone appeared to contain all of the coding regions as well as ~6 kb of upstream sequences, based on the initial Southern blotting results. The entire insert from this clone, as well as the *XbaI* and *BamHI* fragments from this clone, were subcloned into Bluescript and extensively restriction mapped. The above map represents the entire region contained within the #2 clone, based on the compilation of these results.

9kb *XbaI* subclones, respectively. This revealed an intron/exon boundary lying just upstream of the homeodomain sequence in a position almost identical to that in *XlHbox-8*. The initiation start site was mapped by RNase protection by C.V.E.W. (data not shown) and found to be quite complex, consisting of at least 3 start sites lying near the *SacI* site just 5' of the 1st exon (Fig. 5). This has also been reported to be the case for the rat homolog (using a combination of primer extension and RNase protection; Sharma et al., 1995). These initiation sites lie just 5' of the longest *pdx-1* cDNA obtained from a screen of a cDNA library from the  $\beta$ TC3 cell line (data not shown).

### Discussion

Both the rat and mouse homologs show a high level of sequence homology in the N-terminal and homeodomains, as was previously noted. It is unclear, therefore, why the initial homology screens failed to recover any *pdx-1* clones. At 8.5 dpc, only very low levels of PDX-1 expression are detectable in the primitive gut endoderm (Guz et al., 1995, and Chapter III), but by 10.5 dpc PDX-1 is expressed at much higher levels in both pancreatic buds (see Chapter III), and would be expected to be well represented within the 10.5 dpc library which was screened in the initial attempts at cloning *pdx-1*. Likewise, *pdx-1* should have been equally represented within the genomic libraries. It appears that at least part of this failure can be attributed to the N-terminal regions of *pdx-1* and *XlHbox-8* cDNA which gave false positives and high background (with both the *Xenopus* and rat probes) on genomic Southern and when used for library screens. The PCR cloning strategy from pancreatic cell lines which resulted in the cloning of the rat STF-1/IDX-1 (Leonard et al., 1994; Miller et al., 1994,

respectively) and mouse IPF-1 (Ohlsson et al., 1993) was able to circumvent these problems by essentially screening for any homeodomain containing gene(s) within these lines.

The #2 clone obtained from the genomic screen with the STF-1 3' cDNA sequences contains all of the coding region of *pdx-1* and ~6 kb of 5' sequences and ~4 kb of 3' sequences. Transgenic analysis of these sequences in collaboration with Laura Gamer indicates that the enhancer elements necessary for pancreatic and duodenal expression are contained within the 5' sequences (data not shown). The sequences from this clone have been used exclusively for the gene targeting experiments detailed in Chapter 3, for subsequent targeting and transgenic experiments which are in progress, and will not be covered in this dissertation.

## CHAPTER III

### ANALYSIS OF PDX-1 FUNCTION BY GENE TARGETING

#### Introduction

As described in Chapter I, the Hox cluster homeobox genes play critical roles in pattern formation along the main body and limb axes during early embryogenesis (for review see Krumlauf, 1994; McGinnis, 1994). In addition, several homeobox genes located outside the Hox clusters are essential for the development of specific organs. Mutations in *pit-1*, which is expressed in the developing pituitary, lead either to reduction in pituitary function or to loss of the pituitary gland (Camper et al., 1990; Li et al., 1990). Similarly, inactivation of the *Hox11* gene, which is expressed, among other places, in the mesodermal precursors of the spleen, leads to asplenia in homozygous mutant mice (Roberts et al., 1994).

This chapter details the use of gene targeting to study the role of *pdx-1* in endodermal development, with special reference to the development of the pancreas. Two separate targeting strategies were used, both of which are expected to generate null mutations. The second approach, in which a  $\beta$ gal reporter cassette was inserted into the *pdx-1* locus, allows the easy detection of the endodermal cells normally expressing *pdx-1* in the presence and absence of functional PDX-1 protein.

Using a similar strategy, Jonsson et al. (1994), reported that *pdx-1*  $-/-$  pups are apancreatic and die postnatally with a highly elevated urine glucose level. Both of the targeted mutations reported here also result in a failure to generate

the pancreas. However, the pancreatic buds form and undergo some ductal outgrowth and branching, but pancreatic endocrine and exocrine differentiation is blocked. The *pdx-1*<sup>-/-</sup> animals also suffer malformations of the rostral duodenum, often resulting in a block to gastric emptying, and the abundance of enteroendocrine cells is greatly reduced in the rostral duodenum. These findings offer important additional information regarding the role of *pdx-1* in the determination and differentiation of the posterior foregut, specifically regarding the proliferation and differentiation of the endodermal precursors of the pancreas.

## Methods and Materials

### *Pdx-1* Gene Targeting Constructs

As described in Chapter II, a 500 bp *MluI*-*BamHI* fragment of the rat STF-1 cDNA (a gift of Mark Montminy) was used to isolate murine genomic clones from a 129/Sv library under high stringency. The #2 $\lambda$  clone contains the entire *pdx-1* locus as shown in Fig. 6A. All fragments for constructs and probes described in this chapter derive from this clone. Gene targeting constructs were produced in a pUC-based vector (pKO-I; a gift of Manfred Blessing) that contains PGK-II and MC1 thymidine kinase cassettes flanking an MC1neo<sup>r</sup> cassette. Unique *XhoI* and *BamHI* sites are present on the PGK-II<sub>tk</sub> and MC1<sub>tk</sub> sides of the neo<sup>r</sup> cassette, respectively. The same 3' arm of homology was used in both XBko and XSlacZ constructs, and was made by inserting a blunt-ended 1.5 kb *PstII*/*XbaI* fragment from the 3' end of the locus into the filled-in *BamHI* site in pKO-I. Orientation was determined by restriction mapping and sequencing. For XBko, the 5' arm of the targeting construct was made by inserting a blunt-ended 7 kb *XbaI*/*BamHI*

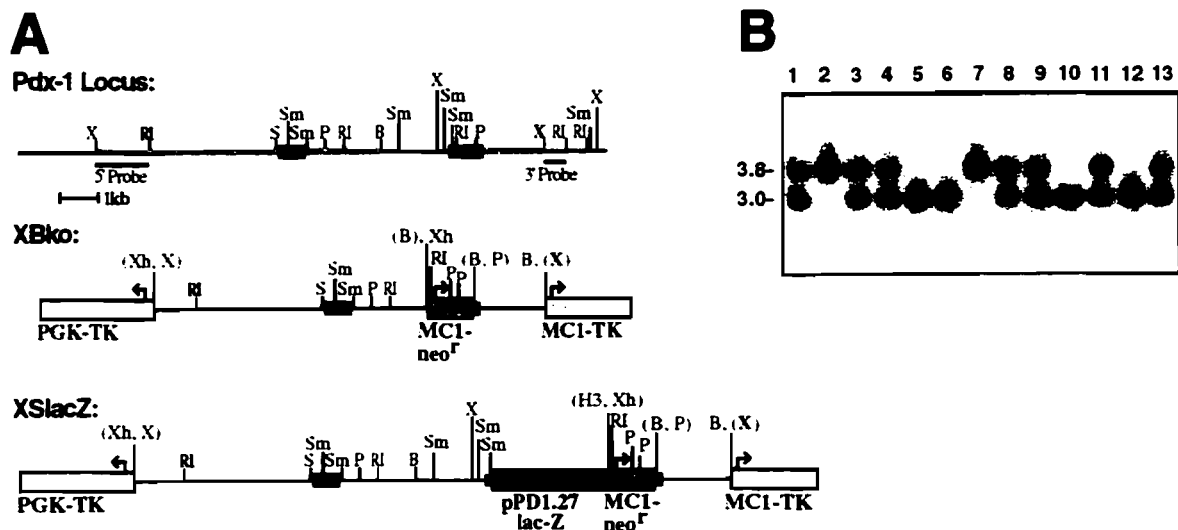


**Figure 6. Targeted Mutagenesis of *pdx-1*.** (A) *pdx-1* contains two exons; the second exon contains the homeobox coding sequence (lighter box). Targeted deletions of homeobox sequences were produced with the XBko construct, which replaces intron and protein coding sequences of the second exon with a MC1neo<sup>r</sup> cassette, and the XSlacZ construct, which fuses a nuclear targeted  $\beta$ -galactosidase cassette (with its own 3' SV-40 poly-A signals followed by the MC1neo<sup>r</sup> cassette driven by its own promoter) in frame with PDX-1. The XBko construct contains 7 kb of 5' homology and 1.5 kb of 3' homology (thickened lines on the *pdx-1* locus map). The XSlacZ construct contains 9 kb of 5' homology, from the 5' *XbaI* site to the *SmaI* site in the homeobox, and the same 3' region of homology as XBko. Both constructs contain 5' PGK-II thymidine kinase and 3' MC1-thymidine kinase cassettes (transcription direction for tk and neo<sup>r</sup> cassettes is indicated by arrows). Homologous recombinants were detected using the 3' probe (500 bp *XbaI-EcoRI* fragment) on Southern blots of *EcoRI* digested DNA by an 800 bp shift from 3 kb (endogenous locus) to 3.8 kb (targeted locus). Further Southern blot analysis of targeted lines used *EcoRI*, *PstI*, and *XbaI* digested DNA probed with both the 3' probe and 5' probe (2 kb *XbaI-EcoRI*, internal probe). (B) Southern analysis of DNA samples from a complete litter of *pdx*<sup>XBko</sup> pups (derived from +/- mating) digested with *EcoRI* and probed with the 3' probe. **Abbreviations:** Xh, *XhoI*; H3, *HindIII*; X, *XbaI*; R, *EcoRI*; S, *SacI*; Sm, *SmaI*; P, *PstI*; B, *BamHI*.

fragment, containing the first exon, into the filled-in *XhoI* site. The structure of the XBko construct was confirmed by extensive restriction mapping, and sequencing from primers derived from the 5' end of the 7 kb *XbaI/BamHI* fragment, the 3' end of the neo<sup>r</sup> cassette, and 3' end of the 1.5 kb *Pst-Xba* fragment.



For the XSlacZko PDX-1/ $\beta$ gal fusion protein gene targeting construct, the 5' arm of homology extends from an *XbaI* site (upstream of exon 1), to a *SmaI* site in the second exon. Because of the additional *SmaI* site in the intron, this region was assembled in several steps. First, a 450 bp *XbaI/SmaI* fragment, upstream of the second exon, was inserted into the *XbaI* and *SmaI* sites of the pPD1.27 lacZ expression vector (which encodes a nuclearly targeted  $\beta$ gal, followed by SV40 polyadenylation signals; a gift from Andrew Fire; Fire et al., 1990). Second, the 90 bp *SmaI* fragment including the 5' end of exon 2 was inserted into the *SmaI* site to fuse PDX-1 N-terminal sequences in frame with the  $\beta$ gal coding region. The structure was confirmed by sequencing with an antisense primer located at the 5' end of the lacZ cassette. Third, the 9 kb *XbaI* fragment containing exon 1 was inserted into the *XbaI* site. Orientation was confirmed by sequencing with a primer reading out from the 5' end of the *XbaI* fragment. Finally, the fused PDX-1/ $\beta$ gal sequences were excised with *Sall* and *NotI*, blunt-ended and inserted into the filled-in *XhoI* site of the pKO intermediate above (contain the 1.5kb 3' homology inserted into the *BamHI* site). Orientation was confirmed by sequencing with the primer at the 5' end of the *XbaI* fragment.

Constructs were released from the vector by *NotI* digestion prior to electroporation. The alleles resulting from homologous recombination of XBko and XSlacZ are designated  $\text{pdx}^{\text{tm1CVW}}$  and  $\text{pdx}^{\text{tm2CVW}}$ , respectively, according to the guidelines of the International Committee on Standardized Genetic Nomenclature for Mice (Jackson Labs). For clarity, these alleles are referred to as  $\text{pdx}^{\text{XBko}}$  (derived from XBko construct) and  $\text{pdx}^{\text{lacZko}}$  (from XSlacZ construct).

### **Electroporation and Selection of ES Cell Clones.**

For each targeting construct,  $4 \times 10^7$  ES cells (129 strain-derived line R1; kind gift from Drs. Janet Rossant and Andras Nagy) were electroporated with 200  $\mu$ g of the linearized targeting construct in 0.8 ml phosphate buffered saline (PBS) with one pulse of 800 V/3  $\mu$ F from a Gene Pulser (Biorad). ES cells were then subjected to positive-negative selection with geneticin (GIBCO) and gancyclovir (Syntex) according to standard protocols (Hogan et al., 1994; Winnier et al., 1995). After 7-10 days, individual clones (700 for XBko, and 500 for XSlacZ) were isolated and DNA screened for the presence of the targeted allele.

### **DNA Analysis**

DNA from doubly resistant ES cell clones was prepared as previously described (Hogan et al., 1994), and samples were screened by *EcoRI* digestion and Southern blot hybridization with the 3' external probe (Fig. 6A). ES cell cultures from targeted lines were expanded and DNA isolated from these was analyzed by Southern blot analysis of *XbaI*, *EcoRI*, and *PstI* digests with the 3' probe, and internal 5' probe (Fig. 6A). Pups and embryos were genotyped by Southern blot analysis using *EcoRI* digestion and the 3' probe. DNA from pups was obtained from tail snips at 3 weeks of age. For 18.5 dpc embryos, the cerebellum or a piece of liver was used to make DNA. For younger embryos, the extraembryonic membranes and/or the entire brain was used, depending on the age of the embryo. DNA was prepared as described (Hogan et al., 1994), and analyzed with the 3' probe.

## **Generation of Chimeric Mice**

ES cells were injected into C57BL/6 blastocysts and transferred into pseudopregnant ICR females as described in Hogan et al. (1994). Male chimeras were bred to Black Swiss females (Taconic Farms) and agouti offspring were genotyped by Southern blot analysis. Heterozygous (Black Swiss x 129/Sv) offspring were interbred to produce homozygous animals.

## **X-gal Staining**

$Pdx^{lacZko}$  embryos and tissues were dissected in PBS and kept on ice until fixation. Embryos younger than 12 dpc were stained whole. For older embryos, the entire alimentary tract was dissected out. Fixation and staining was as previously described (Bonnerot and Nicolas, 1993). Briefly, tissues were fixed in 4% paraformaldehyde at 4°C with agitation for 30-40 minutes, permeabilized (except for 9.5 dpc embryos, which were simply rinsed in PBS), and X-gal stained overnight at room temperature. Tissues were post-fixed in 4% paraformaldehyde at 4°C and then rinsed in PBS. Some tissues were cleared for photography by two 15 minute incubations in 100% methanol followed by 2:1 benzyl benzoate:benzyl alcohol. Afterwards, these were rinsed twice with methanol before transferring to 100% ethanol prior to paraffin embedding. X-gal staining patterns are specific for *pdx-1* driven  $\beta$ gal activity, because homozygous wild-type embryos were devoid of background staining at the stages analyzed.

## **Immunohistochemistry**

Paraffin or cryostat sections (5  $\mu$ m) were hydrated to PBS and subjected to either immunoperoxidase or immunofluorescence staining. Immunoperoxidase

staining was carried out as previously described (Jetton et al., 1994). Primary antibodies to the following antigens (made in rabbit unless otherwise indicated) were used at the indicated dilutions: insulin (Zymed), prediluted; mouse monoclonal to human insulin (Zymed), prediluted; guinea pig anti-insulin (Linco), 1:1000; guinea pig anti-insulin C-peptide (Linco), 1:1000; amylase (gift of R. MacDonald and G. Swift, Dallas), 1:1000; mouse GLUT2 (gift from B. Thorens, Lausanne), 1:2000; glucagon (Linco), 1:1000; pancreatic polypeptide (PP; ICN), 1:1000; somatostatin (ICN), 1:1000; neuron-specific enolase (NSE; Zymed), prediluted; Chromagranin A (Zymed), prediluted; glucagon-like peptide-1 (GLP-1; Peninsula), 1:1000; gastric inhibitory peptide (GIP; Peninsula), 1:1000; secretin (Peninsula), 1:1000; cholecystikinin (CCK; Peninsula), 1:2000; serotonin (Zymed), prediluted. Primary antibodies were incubated overnight at room temperature or 4°C. For immunoperoxidase detection, goat anti-rabbit-horseradish peroxidase (HRP) antibody (Jackson ImmunoResearch; 1:500) or donkey anti-mouse-biotin IgG (Jackson ImmunoResearch; 1:500) followed by Z-Avidin-HRP (Zymed Laboratories; 1:500) were incubated for 1 hour at 22°C. Immunoperoxidase was detected with DAB/H<sub>2</sub>O<sub>2</sub> for 2-5 minutes. Some samples were counterstained with hematoxylin. For immunofluorescent studies the following secondary antibodies (Jackson ImmunoResearch; “ML grade”) were used: donkey anti-rabbit-FITC, 1:250; donkey anti-rabbit-Cy3 at 1:1000; donkey anti-guinea pig-FITC, 1:250; and donkey anti-guinea pig-Cy3, 1:1000. Some samples were counterstained with the nuclear dye, YO-PRO-1 (Molecular Probes; 1:10,000 dilution in PBS).

Fluorescently labeled samples were imaged on a Zeiss LSM 410 confocal microscope. Excitation wavelengths were 488 nm from an Ar-Kr laser (for

YO-PRO-1 or FITC) and 543 nm from a HeNe laser (for Cy3). Fluorescence images were ascribed green (YO-PRO-1 and FITC) or red pseudocolors (Cy3), and were digitally optimized using the Zeiss system software (v.3.56b). TIFF images (512 X 512 pixel) were transferred to either a Silicon Graphics Indigo imaging workstation or a Macintosh PowerMac 8100 for secondary optimization and formatting, and printed on a Tektronix dye sublimation printer.

### **Periodic Acid-Schiff Staining**

Sections were hydrated to tap water, oxidized in 0.5% periodic acid (w/v) for 10 minutes, washed for 5 minutes, rinsed briefly in demineralized water and stained in Schiff's reagent (Fisher) for 10 minutes. Following three rinses in 9.5% sodium metabisulfite (w/v), sections were washed, counterstained with Harris's hematoxylin (Sigma Chemical).

## **Results**

### **Targeted Mutagenesis of *pdx-1***

Two different targeting constructs were used to disrupt *pdx-1* (see Fig. 6A). In the XBko construct, the protein-coding sequences in exon 2 are deleted, including those encoding the DNA-binding homeodomain. In XSlacZ, nuclear targeted  $\beta$ gal is fused in-frame with PDX-1 at the 5' end of exon 2, deleting the homeodomain and bringing  $\beta$ gal activity under the control of *pdx-1* promoter/enhancer elements. Positive-negative selection was carried out, and doubly resistant ES cell clones were screened by Southern blot analysis, which confirmed precise targeting for both XBko and XSlacZ without rearrangement,

duplications, or additional random insertions (Fig. 6A,B; data from 5' probe not shown). The targeting frequency was 1 in 34 of doubly resistant clones for XBko (13 lines), and 1 in 43 (7 lines) for XSlacZ.

Chimeras were produced from 3 lines for  $pdx^{XBko}$  (lines BA5, CB8, and CC4), and 4 lines for  $pdx^{lacZko}$  (3D2, 3D4, 2E3, and 2G2). Germline transmission was obtained for all seven lines, and breeding to Black Swiss mice generated heterozygotes. No reduction in the viability or fertility of  $pdx-I$  heterozygous mice was detected, and male and female heterozygotes were bred to produce homozygous mutant animals for each allele. Pups of genotype  $pdx-I$   $+/+$ ,  $+/-$ , and  $-/-$  are born in the Mendelian distribution of 1:2:1 (e.g. Fig. 6B). For  $pdx^{XBko}$  the ratio (percent of total) was 23:50:27 ( $n=230$ ), and for  $pdx^{lacZko}$  it was 27:47:27 ( $n=60$ ); thus no embryo loss in utero is caused by the mutation. The homozygous null mutant phenotype is indistinguishable between animals derived from both targeted alleles, and data from a detailed analysis of CC4 and BA5 ( $pdx^{XBko}$ ), and 2E3 and 3D4 ( $pdx^{lacZko}$ ) are reported here.

The homeodomain helix-turn-helix motif provides a sequence-specific DNA recognition function (see Gehring et al., 1994). Certain *Drosophila* homeodomain proteins have some function without their homeodomains (Fitzpatrick et al., 1992), and the production of mammalian Hox gene mRNAs lacking the homeobox has been reported (e.g. Murphy and Hill, 1991). There has been no evidence that this could be the case for  $pdx-I$ ; therefore, the loss of the DNA-binding domain in both of these targeted mutations is thought to generate null alleles of  $pdx-I$ . This conclusion is supported by the following: (1) PDX-1 was not detected in 9.5 dpc  $-/-$  embryos ( $pdx^{XBko}$ ) by immunostaining with

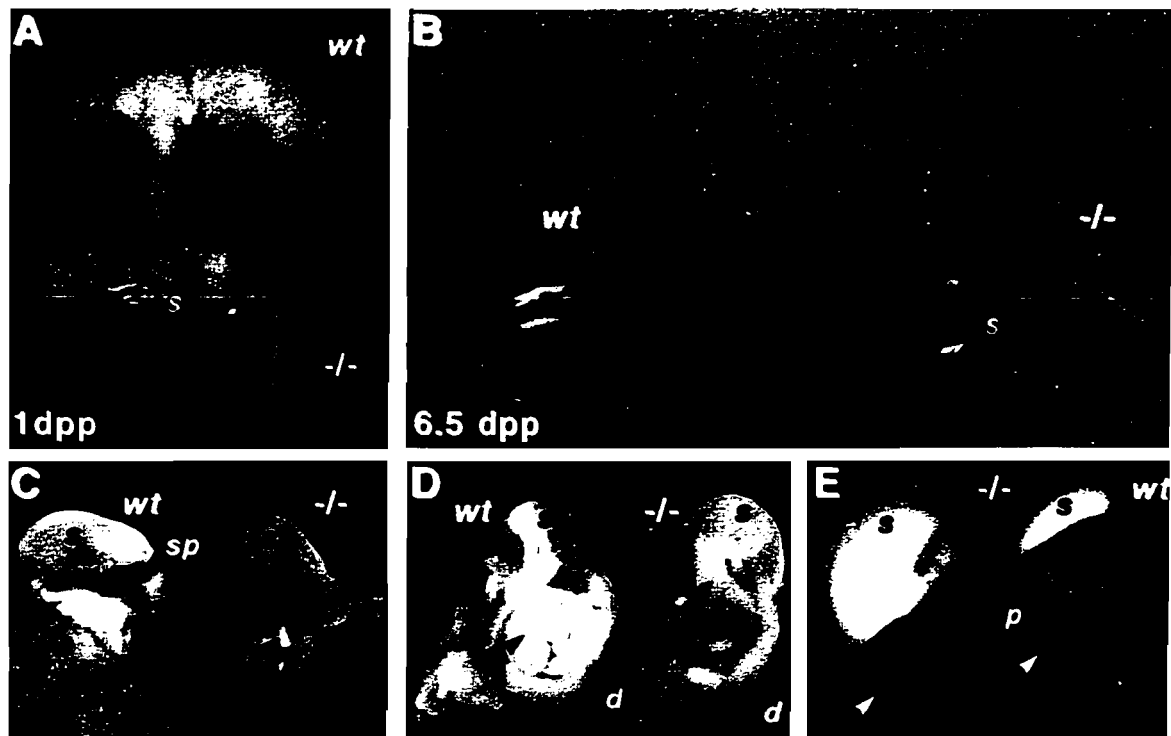


**Figure 7. Gross Analysis of *Pdx<sup>XBko</sup>* Animals.** (A) At 1 day post-partum (1 dpp), the *pdx<sup>XBko</sup> -/-* pups (bottom) begin to show signs of growth retardation and apparent dehydration, compared to wild-type littermates (upper). (B) By 6.5 dpp, *pdx-1 -/-* animals are extremely dehydrated. Though their stomachs contain milk (arrowhead), they show ~60% reduction in weight compared to wild-type littermates. (C and D) 18.5 dpc *-/-* embryos (right) show a complete absence of pancreatic tissues and malformations at the stomach/duodenal junction (see Fig 3 for these malformations). (E) In many 1 dpp *-/-* pups (left), a stomach/duodenal obstruction occurs, as evidenced by stomach distension and a lack of gastric emptying. The small intestines appear to be empty (white arrowheads; note the light-colored wild-type gut, indicating milky gut contents). **Abbreviations:** s, stomach; p, pancreas; d, duodenum; sp, spleen; c, colon.

antibodies against the N-terminus of PDX-1 (data not shown), and (2) there was no dominant negative effect in *pdx<sup>XBko</sup> +/-* or *pdx<sup>lacZko</sup> +/-* animals.

### Gross Analysis of Homozygous *pdx-1* Mutants

Immediately after birth, *pdx<sup>XBko</sup>* and *pdx<sup>lacZko</sup> -/-* null mutants are indistinguishable from *+/+* or *+/-* littermates. However, within the first day post partum (dpp), *-/-* animals show signs of growth retardation and dehydration,

although they feed because their stomachs contain milk (Fig. 7A). By 1 dpp, the stomachs of some  $-/-$  mutants are distended because of a lack of gastric emptying into the gut (Fig. 7E), which may result from malformations at the stomach-duodenum junction that are described below.  $Pdx^{XBko} -/-$  pups can survive until at least 6.5 dpp (Fig. 7B), but the animals were not maintained longer for ethical reasons. At this age,  $pdx^{XBko} -/-$  pups still have milk in their stomachs, but they are severely dehydrated, having a thin and cracking skin with very little fur, and are much smaller (up to 60% less by weight) than  $+/+$  or  $+/-$  littermates. The developmental retardation in  $-/-$  pups is likely attributable to malnutrition resulting from lack of digestion in the absence of a pancreas and functional rostral duodenum (see below), and/or diabetic consequences of the loss of pancreas (Jonsson et al., 1994). Heterozygotes are healthy and otherwise indistinguishable from  $+/+$  littermates at the level of examination described here. However, because PDX-1 may be an insulin gene transactivator (see Chapter I), physiological defects under certain feeding conditions in heterozygous  $pdx-1 +/-$  animals cannot be ruled out.

Dissection of  $pdx^{XBko} -/-$  pups at 1 dpp revealed that the liver, gall bladder, spleen, stomach, common bile duct, and other viscera are present and normal, but that the pancreas is noticeably absent in all cases (Fig. 7C,D). This observation is entirely consistent with the conclusion of Jonsson et al. (1994) that a similar null mutation of  $pdx-1$  blocked pancreatic development.



### $\beta$ gal Expression in $Pdx^{lacZko}$ Heterozygotes Detects *pdx-1* Expression

In  $pdx^{lacZko} +/-$  animals analyzed between the ages of 8.0 dpc and adult (n=35), *pdx-1* expression (as visualized by X-gal staining) marks endodermal tissues previously shown to express *pdx-1* endogenously (Guz et al., 1995,

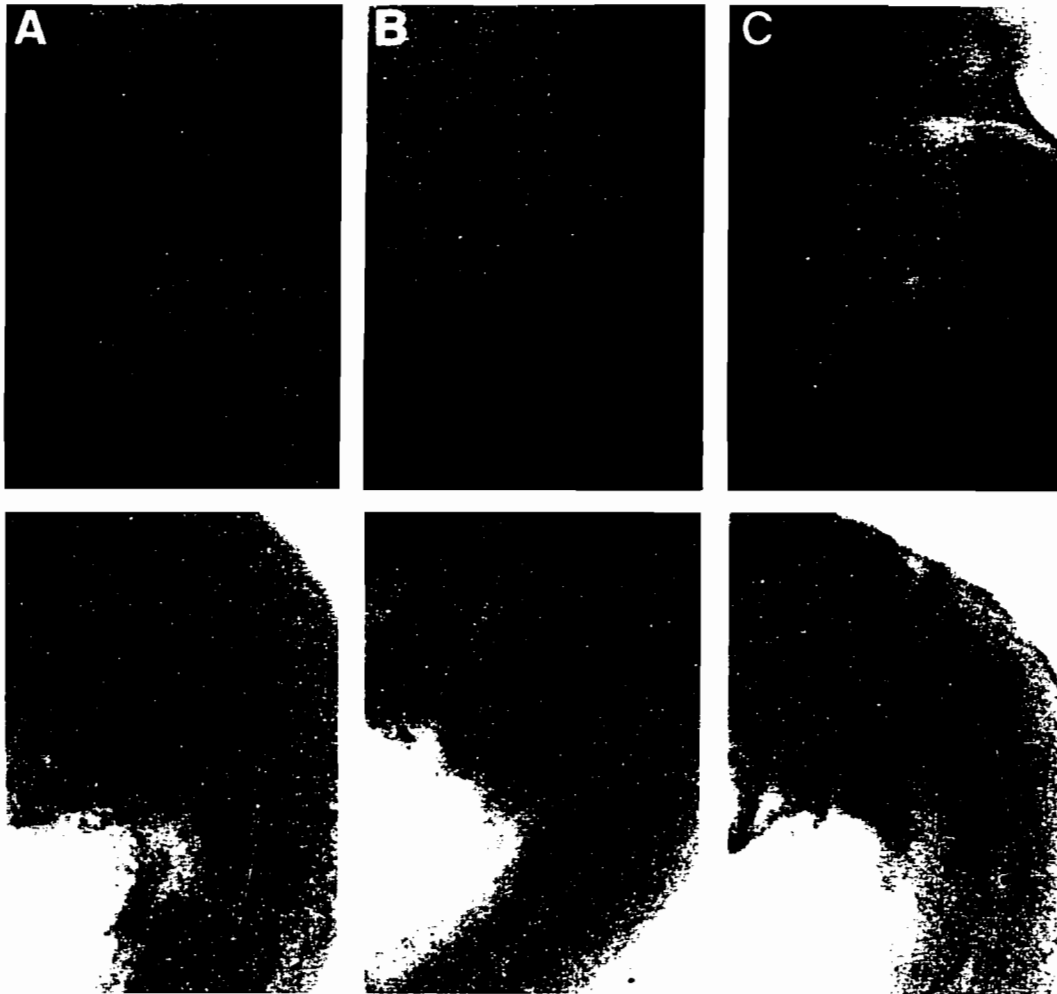


**Figure 8. Time Course of PDX-1/ $\beta$ gal fusion expression.** Embryos from 6.5-9.5 dpc, derived from heterozygous  $pdx^{lacZko}$  matings, were analyzed by X-gal staining for their expression of the PDX-1/ $\beta$ gal fusion protein. (A) The earliest expression is at ~8.0 dpc (7 somites) detected on the left side of the anterior intestinal portal (AIP). (B) By 8-9 somite stages, the left expression has spread and a small area on the right side is also staining. (C-F) Progressing towards ~9.0 dpc, the ventral staining continues to spread and intensify, as this region becomes constricted into the future common bile duct. At ~9.0, the first dorsal staining is detected marking the region of the future dorsal outgrowth. **Abbreviations:** AIP, anterior intestinal portal; v, ventral; d, dorsal.

Miller et al., 1994; Ohlsson et al., 1993), while *+/+* embryos remained completely unstained. Thus, the PDX-1/ $\beta$ gal fusion protein expression provides a sensitive way of tracing cells expressing *pdx-1*, without alterations caused by the *neo<sup>r</sup>* cassette located 3' of the lacZ reporter (Fig. 6A).

To identify the earliest time point at which *pdx-1* is expressed, 6.5-9.5 dpc embryos derived from heterozygous matings were analyzed by X-gal staining. The appearance of a few X-gal positive cells is first seen at ~8.0 dpc (7 somites) on the left side of the anterior intestinal portal (Fig. 8A). At ~8.5 dpc, the numbers of staining cells increases on the left side and a few positive cells are seen on the right side at this time point (Fig. 8B). By 9.0 dpc, the ventrally stained regions have fused and constricted to form the presumptive common bile duct (Fig. 8F). Also at this time, light staining of the dorsal gut epithelium demarcates the region of dorsal pancreatic bud outgrowth. This X-gal marked expression of *pdx-1* precedes the expression reported previously by Guz et al. (1995) using immunohistochemical detection with the XIHbox-8 N-terminal antibody, and also precedes the expression of other early pancreatic markers. This reporter gene approach provides a more complete understanding of the tissues expressing PDX-1 than previous analyses of the endogenous antigen, which is unusually sensitive to the fixation conditions (unpublished observations).

At 9.5 dpc, heterozygous embryos PDX-1/ $\beta$ gal is expressed throughout the dorsal and ventral pancreatic buds and in the intervening endoderm of the presumptive duodenum (Fig. 9A). At 11.5 dpc, expression continues in the dorsal and ventral buds, and the duodenal epithelium staining is more intense than earlier (Fig. 9B). In addition, the epithelia of the cystic duct, common bile

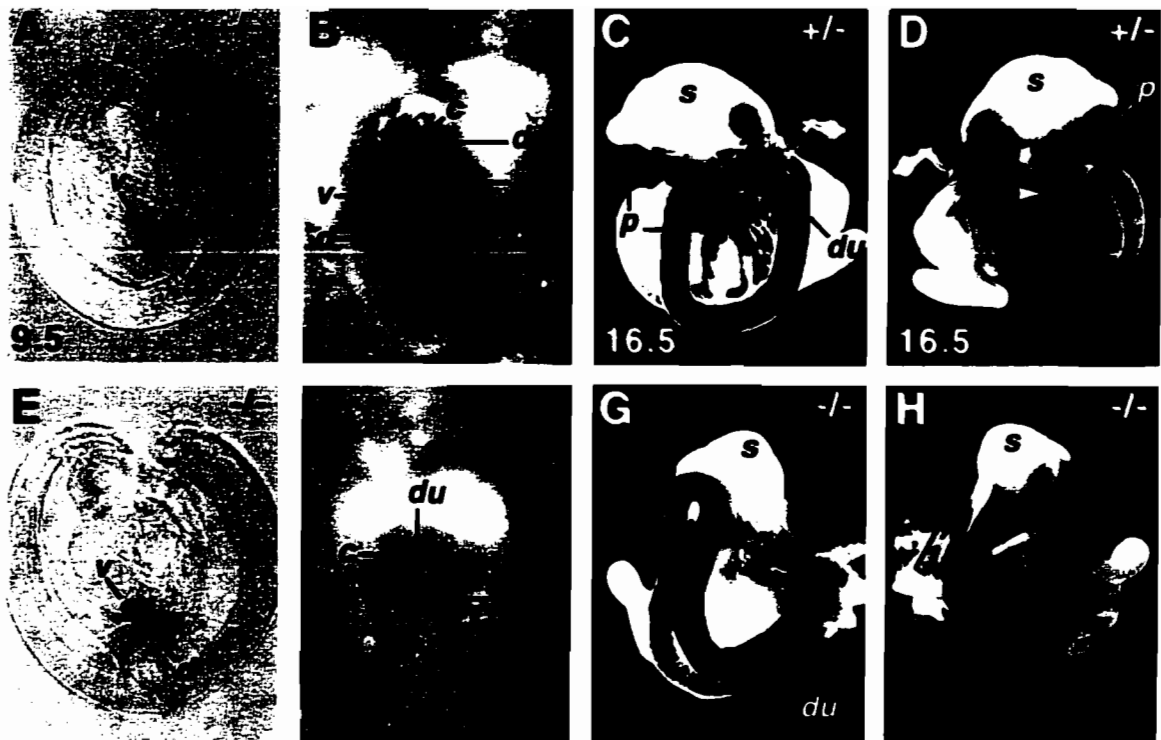


**Figure 9. Tracking of *pdx-1* Expressing Tissues in *pdxlacZko* Embryos.** (A and E) At 9.5 dpc, dorsal and ventral buds stain for  $\beta$ gal expression in both *pdxlacZko* +/- and -/- embryos. The presumptive duodenum between the buds is also stained. The heads were removed to obtain DNA for genotyping, anterior is upper right. (B and F) The ventral (v) and dorsal (d) buds are much larger by 11.5 dpc in wild-type +/- animals and stain throughout with X-gal. However, pancreatic buds are absent in -/- littermates. An extra duct structure (dd) replaces the dorsal bud. X-gal staining labels the antral stomach (a), duodenum (du), and common bile duct (c) in both +/- and -/- embryos. (C and G) At 16.5 dpc, a similar staining pattern is seen in both wild-type +/- and -/-. Pancreatic tissues are still undetected in -/- embryos. (D and H) In both +/- and -/- embryos, staining in the gut epithelium tapers off gradually from the distal duodenum to the ileum (arrowheads indicate punctate staining in the presumptive jejunum). The bracket in H indicates the region corresponding to the cuboidally lined discontinuity at the stomach/duodenal junction. **Abbreviations:** v, ventral bud; d, dorsal bud; c, common bile duct; dd, dorsal ductule; du, duodenum; a, antral stomach; s, stomach; p, pancreas.

duct, and antral stomach are stained at 11.5 dpc (Fig. 9B). The PDX-1/ $\beta$ gal expression boundaries at the liver/common bile duct and at the antral/fundic stomach boundary are relatively sharp, whereas expression in the duodenum declines caudally, becoming increasingly punctate in the more distal gut (Fig. 9B).

At 16.5 dpc, PDX-1/ $\beta$ gal expression is maintained in the antral stomach, common bile duct and cystic duct, and in duodenal enterocytes and enteroendocrine cells (Fig. 9C,D; data not shown). The biliary ducts proximal to the common bile duct also express PDX-1/ $\beta$ gal (data not shown). At this stage, the embryonic gut has changed from a pseudostratified to a columnar epithelium, the pancreatic buds have fused, and differentiation of exocrine and endocrine cell types has started. Pancreatic PDX-1/ $\beta$ gal staining begins to be extinguished in non-islet cell types at this stage (see below). Towards the caudal expression domain of *pdx-1* in the gut mucosa, X-gal-positive cells are few in number and well dispersed, and colocalization of the *pdx-1* expression with enteroendocrine peptide markers is very often encountered (data not shown). Just before birth (18.5 dpc), pancreatic PDX-1/ $\beta$ gal expression becomes restricted mostly to the developing islets. In the gut, enterocytes and enteroendocrine cells of the rostral duodenum epithelium are all labeled, and scattered epithelial cells again stain in the more distal gut (data not shown). At all stages examined, X-gal staining is absent from mesodermal tissues (see below).

### **PDX-1/ $\beta$ gal Expression is Maintained in Homozygous Null Animals**

As summarized in Fig. 9, an analysis of embryos from 9.5-16.5 dpc (n=18) shows that the intensity and anteroposterior extent of PDX-1/ $\beta$ gal expression in *pdx*<sup>lacZko</sup> homozygous null animals is similar to that in *pdx*<sup>lacZko</sup> heterozygotes. This includes conspicuous labeling of the early dorsal and ventral pancreatic buds, which are comparable to those in +/- littermates (compare Fig. 9A and E), and the endodermal lining of the prospective duodenum (Fig. 9E,F). At 11.5 and

16.5 dpc, the expression boundaries at the liver and within the stomach are the same in +/- and -/- littermates (Fig. 9F,G,H). This strongly suggests that PDX-1 is not necessary for maintaining its own expression, nor for the survival of the endodermal cells that normally express it, although at this level of analysis the loss of a relatively low number of scattered cells cannot be ruled out. Most notably, the generation of the pancreatic buds does not require *pdx-1* function.

### Loss of PDX-1 Function Blocks Pancreatic Bud Outgrowth.

At 11.5 dpc, a separate outgrowth derived from the ventral pancreatic bud is no longer visible in

*pdx<sup>lacZko</sup> -/-* embryos (Fig. 9F), possibly because the cells derived from the

ventral bud became incorporated into the biliary duct, or died. The common bile duct is greatly shortened, and the liver primordium is juxtaposed to the duodenum (Fig. 9F). The extensive dorsal pancreatic outgrowth of normal +/+ or +/- embryos (Fig. 9B,C,D) is replaced by a short ductular structure in *pdx<sup>lacZko</sup> -/-*

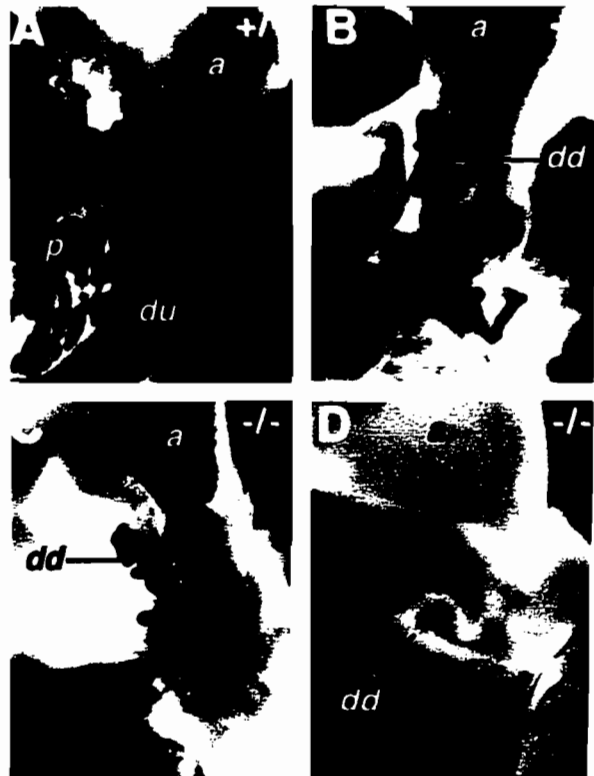


**Figure 10. Aberrant Pancreatic Duct Structures in *pdx-1*  $-/-$  Embryos.** (A) At 16.5 dpc, a regular branching pattern is seen in the pancreas of +/- embryos. (B and C) In -/- mutant littermates, the pancreatic tissues are replaced by small irregularly branched dorsal ductules (dd) lined by a PDX-1/ $\beta$ gal-expressing epithelium. These vary somewhat in size and complexity but are seen in all -/- animals (n=24). (D) Similar dorsal ductules are produced in *pdxXBko* embryos (n=61), shown here at 18.5 dpc. **Abbreviations:** du, duodenum; a, antral stomach; s, stomach; p, pancreas; dd, dorsal ductule.

animals (e.g. Fig. 9F; Fig. 10). A “duodenal” gut tube is seen in mutant embryos, and it is of similar length to that in wild-type embryos, as judged by the domain of PDX-1/ $\beta$ gal expression (e.g. Fig. 9F,G). At any stage examined, homozygous null mutant embryos for either mutant allele never displayed necrotic plaques that might indicate large areas of cell death caused by the absence of PDX-1 function. However, this level of analysis cannot rule out the possibility of increased levels of apoptosis in some regions due to the absence of PDX-1 function.

The dorsal ductule derived from the dorsal bud in  $-/-$  animals persists into perinatal stages and goes through some outgrowth and irregular branching (Fig. 10), although it is stunted greatly compared to the dorsal pancreas of  $pdx^{lacZko}$   $+/-$  embryos (e.g. compare Fig. 9C with 9G, and Fig. 10A with 10B,C,D). Similarly abrogated ductular trees were noted in all  $-/-$  mutant embryos (from 11.5-18.5 dpc) in both  $pdx^{XBko}$  (Fig. 10D) and  $pdx^{lacZko}$  (Fig. 10B,C) animals. Such ductal structures, other than the normal pancreatic and biliary ducts, are never present in  $+/+$  or  $+/-$  embryos.

### **Pancreatic Marker Expression in *pdx-1* $-/-$ Mutant Embryos**

Immunostaining was used to determine whether any cells present in or around the dorsal ductule of *pdx-1*  $-/-$  embryos express markers of specific mature pancreatic cell types. As reported previously (Pang et al., 1994; Teitelman et al., 1993), glucagon-positive cells are found in  $+/-$  9.5 dpc embryos as small clusters peripheral to, and dispersed within, the pancreatic bud (Fig. 11A). Similar populations of glucagon-positive cells are found in the pancreatic buds of  $-/-$  embryos (Fig. 11B). In both  $+/-$  and  $-/-$  pancreatic buds, the peripheral glucagon-positive cells do not express *pdx-1*, as indicated by absence of

PDX-1/ $\beta$ gal expression, but the *pdx-1* expression status of glucagon-positive cells within the bud is somewhat uncertain because of masking by intensely X-gal-positive cells.

In 11.5 dpc *pdx*<sup>lacZko</sup> heterozygotes, glucagon-positive cells are again detected within the pancreatic buds, and in clusters of X-gal negative cells at the bud periphery (Fig. 11C). In *pdx*<sup>lacZko</sup>  $-/-$  mutant embryos at the same stage, a small number of glucagon-positive cells is found at, or close to, the junction of the dorsal ductule with the gut lumen (data not shown), but glucagon-positive cells are absent from distal regions of the dorsal ductule (Fig. 11D).

At 16.5 dpc and later, *pdx*<sup>lacZko</sup> heterozygotes show large numbers of glucagon- and insulin-positive cells in the emerging islets (Fig. 11E,G), and amylase expression in the developing exocrine acini (Fig. 11F). In 16.5 dpc *pdx*<sup>lacZko</sup> homozygous null embryos (n=3), PDX-1/ $\beta$ gal negative, glucagon-positive, cells are detected within the dorsal ductule (e.g. Fig. 11I), but amylase is still not detectable (compare Fig. 11F with J). In light of the role proposed for *pdx-1* in the derivation of mature  $\beta$  cells in the pancreatic islet (Guz et al., 1995), an extensive search for insulin-expressing cells in homozygous null mutants was done, under conditions in which wild-type sibling tissues displayed numerous insulin-positive cells (Fig. 11G,H). No insulin-positive cells were detected by immunohistochemical analysis of the entire serially sectioned dorsal ductule and rostral duodenum, in a total of three embryos at 16.5 dpc (Fig. 11K), or five embryos at 18.5 dpc (Fig. 11L).

To further characterize the dorsal ductule, immunostaining was used to examine the expression of the glucose transporter-2 (GLUT2; Thorens et al.,

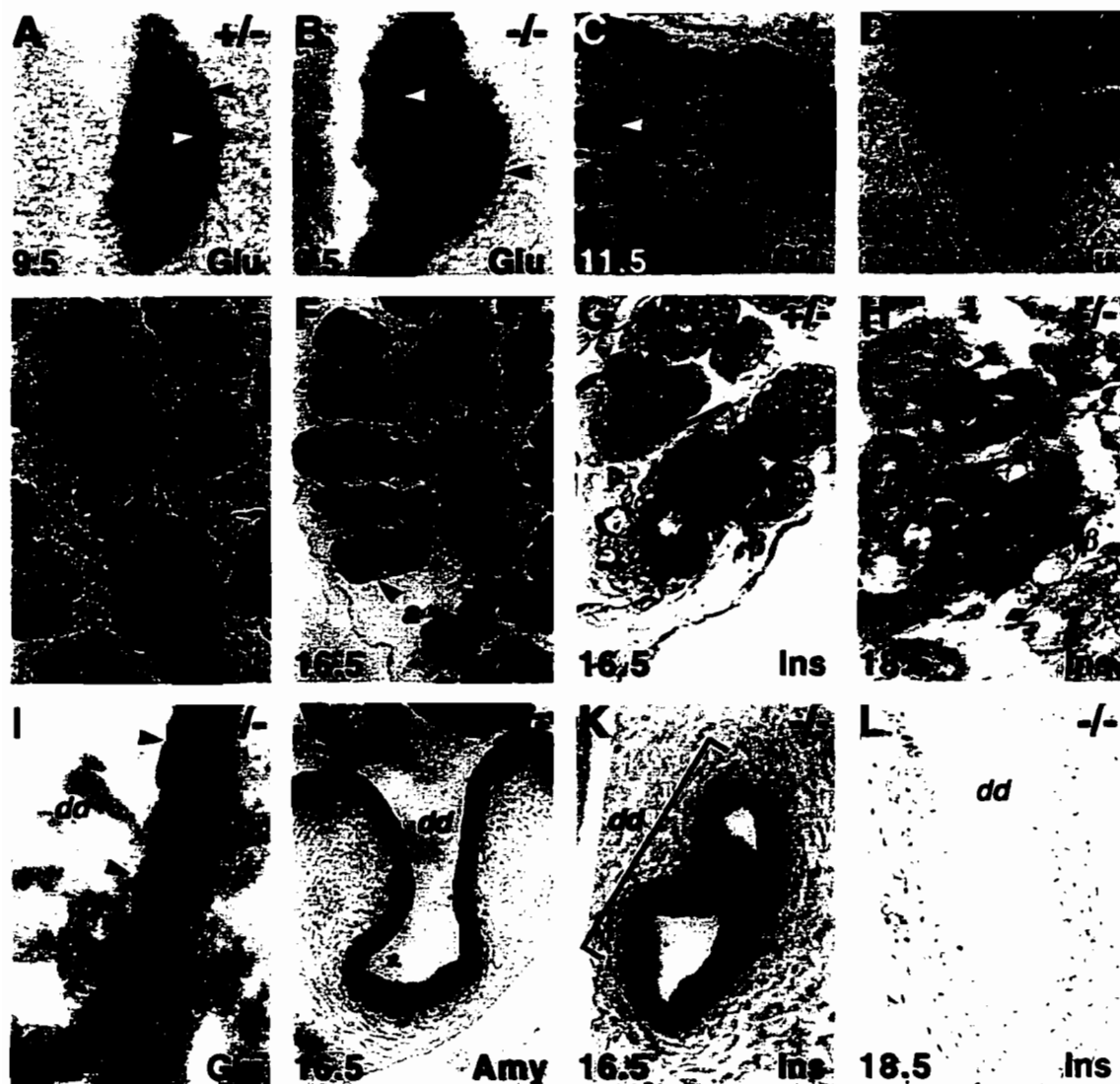


**Fig. 11. Pancreatic Marker Expression in *pdxXBko* and *pdxlacZko* Embryos.** (A and B) At 9.5 dpc in *pdxlacZko*  $-/-$  and  $+/-$  embryos, brown glucagon-positive cells are found in clusters (black arrowheads) at the endoderm/mesenchyme boundary and within the X-gal stained buds (white arrowheads). (C) At 11.5 dpc, wild-type  $+/-$  *pdxlacZko* embryos contain larger numbers of glucagon-expressing cells. (D) In 11.5 dpc  $-/-$  littermates, the dorsal pancreatic bud is replaced by the dorsal ductule (dd). Glucagon-expressing cells are not detected in distal regions of this ductule, but are found in tissue that is closer to the duodenal lumen (data not shown). (E) In 16.5 dpc  $+/-$  *pdxlacZko* embryos, glucagon-positive cells ( $\alpha$ ) are seen in the budding islets. (I) In  $-/-$  littermates, glucagon-positive cells (arrowheads) are seen within the X-gal stained epithelium of the ductules (dd). (F and J) Amylase is also detected at this stage in *pdxlacZko*  $+/-$  embryos in the acini (a), but is not seen in  $-/-$  animals. (G and H) A high level of insulin expression is seen at 16.5 and 18.5 dpc, respectively, in the developing islets of wild-type  $+/-$  *pdxlacZko* embryos, but is not detected at either time point (K,L) in the dorsal ductule or the malformed rostral duodenum in *pdxlacZko*  $-/-$  littermates. Panels H,L were hematoxylin counterstained, but not X-gal stained. **Abbreviations:** dd, dorsal ductule; i, islet;  $\beta$ , beta cell; a, acini;  $\alpha$ , alpha cell.



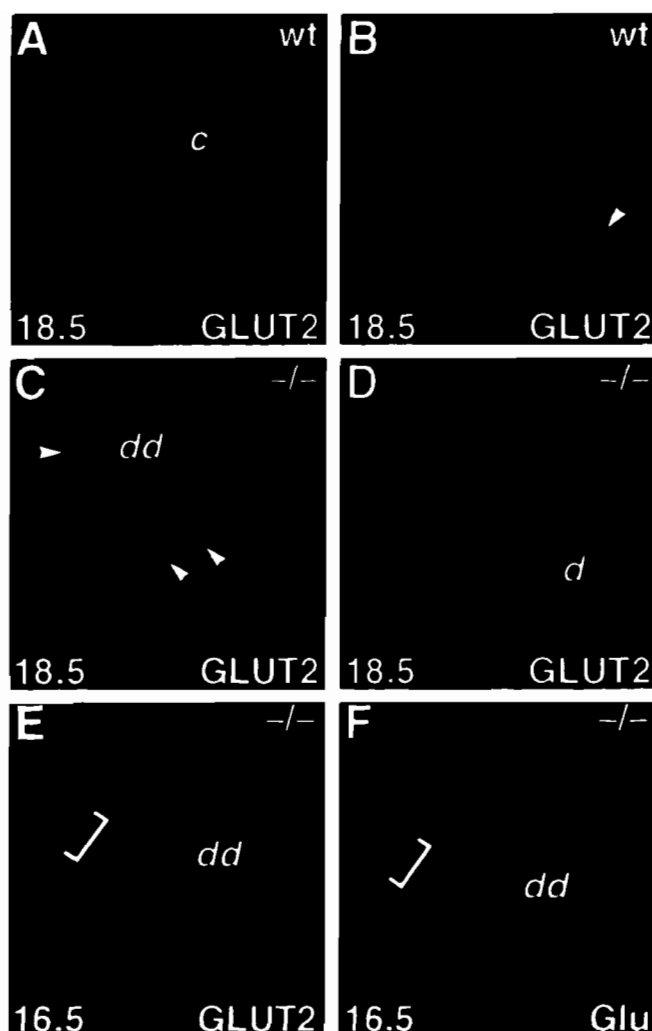
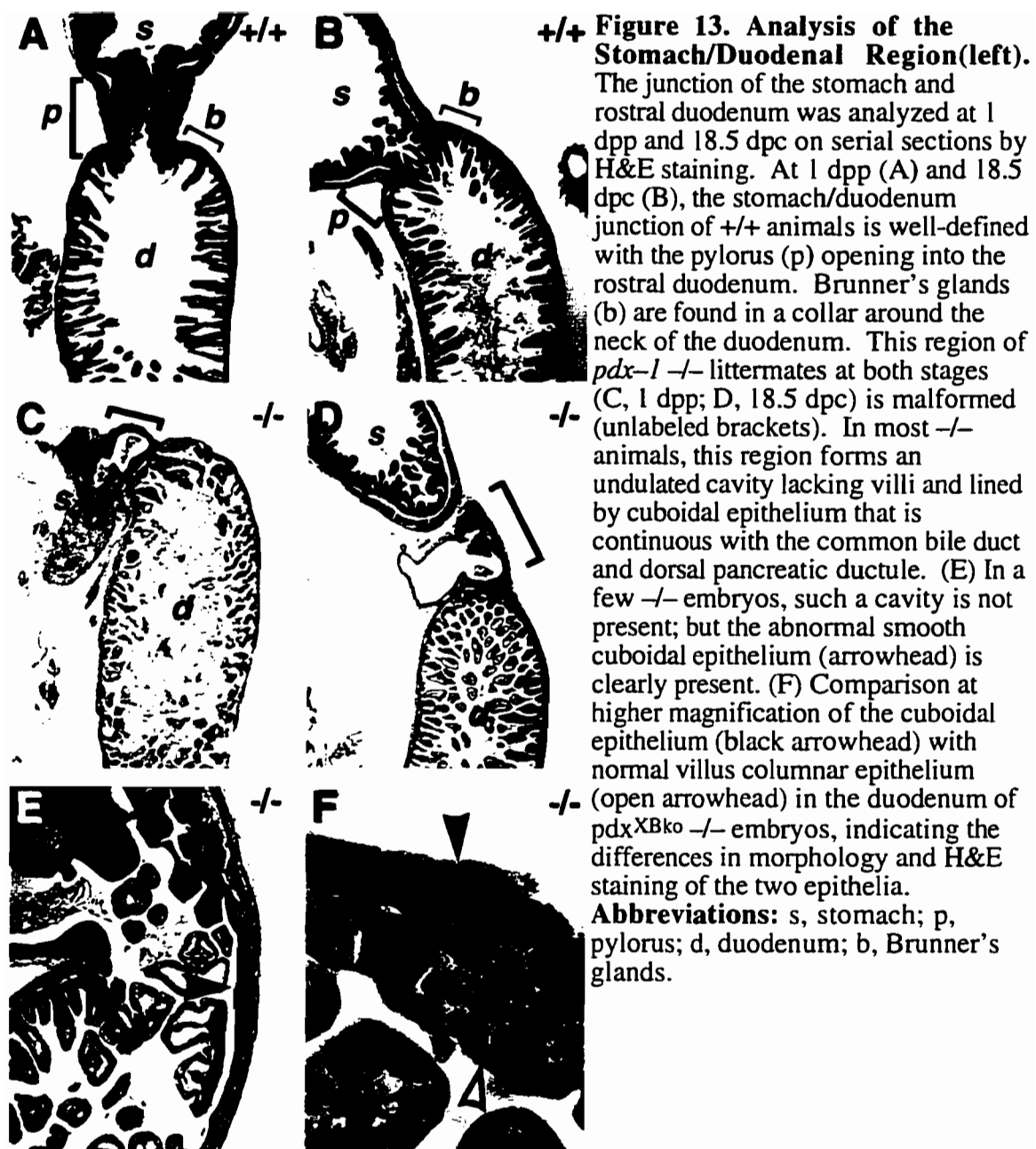


**Figure 12. GLUT2 Expression in the Dorsal Ductule (left).** The dorsal ductule and rostral duodenum were immunostained for insulin, glucagon, and GLUT2 expression at 16.5 and 18.5 dpc and imaged by confocal microscopy. All sections were stained for insulin (assigned a red pseudo-color), and double-stained for glucagon (Glu) or GLUT2 (indicated in lower right corner, assigned green pseudocolor). Note that no insulin-positive cells are present in any panel. (A) High levels of GLUT2 are detected in the epithelial lining of the cystic duct (c) of *pdx<sup>lacZ</sup>ko<sup>+/+</sup>* embryos at 18.5 dpc. (B) GLUT2 in the villi is found primarily on the basolateral surfaces (arrowhead) of the epithelium. (C) The dorsal ductule (dd) epithelium of *-/-* litter-mates has a cuboidal morphology similar to the cystic duct in A, and equally intense GLUT2 expression. (D) The GLUT2 signal in the abnormal duodenal epithelium is more intense than that in the villi (circular cross-sections within the lumen). (E and F) At both time points (16.5 dpc shown), glucagon-positive cells are found at the tips of the GLUT2-positive evaginations of the dorsal ductule epithelium (white brackets), as well as within the epithelium proper (see Fig. 11D). **Abbreviations:** c, cystic ducts; dd, dorsal ductule; d, duodenum; Glu, glucagon.

1990), while also double-staining for insulin or glucagon. In wild-type embryos, the GLUT2 signal is intense in the common bile duct epithelium (Fig. 12A) and, as in rat (Thorens et al., 1990), is expressed at lower levels in the basolateral surfaces of the columnar epithelial cells of the duodenal villi (although apical staining is apparent in some cells; see Fig. 12B,D). GLUT2 is also expressed at relatively high levels in the early pancreatic buds (Pang et al. 1994), but is then downregulated so that only very low levels exist in the pancreatic duct



epithelium of late gestation embryos (data not shown; Bob Gimlich, Genetics Institute, personal communication). In contrast, the epithelium of the dorsal ductule in *pdx-1* *-/-* mutants expresses GLUT2 intensely (Fig. 12C), with several evaginations showing somewhat decreased GLUT2 signal intensity. Many of these evaginations have small clusters of glucagon-positive cells at their distal tips (Fig. 12C,E,F), in addition to glucagon-positive cells within the dorsal ductule

epithelium itself (Fig. 11D).

Based on the morphology of the dorsal ductule and the absence of expression for specific markers, it appears that differentiation of islets, mature pancreatic  $\beta$  cells, and acinar cells is blocked in *pdx-1*<sup>-/-</sup> embryos, in agreement with the findings of Jonsson et al. (1994). Non-epithelial and epithelial glucagon-positive cells are found, but they are intimately associated with a GLUT2-positive dorsal ductule epithelium, and therefore these cells could be more related to embryonic glucagon-positive cells than mature islet cell types (see Discussion).

### **Malformations at the Stomach/Duodenal Junction of *pdx-1*<sup>-/-</sup> Null Mutants**

During the analysis of the defects in pancreatic development, structural abnormalities were noted centered around the rostral duodenum of *pdx-1*<sup>-/-</sup> embryos that might explain the lack of gastric emptying and subsequent stomach distension (Fig. 7E). These defects are illustrated in Fig. 13. In normal, late gestation embryos, the pyloric sphincter lies at the stomach/duodenum junction, and villi covered by a columnar epithelium protrude into the gut lumen throughout the rostral duodenum (Fig. 13A,B). In *pdx-1*<sup>-/-</sup> animals, the pylorus is very contorted, although at least some of its tissues are recognizable, such as the characteristic smooth muscle bands (data not shown). Because the expression of PDX-1/ $\beta$ gal extends over the antral stomach (Fig. 9,10), this could indicate a direct role for *pdx-1* in the differentiation of antral stomach tissues, although it is possible that the pylorus defects are a consequence of the adjacent gut tube malformations described below.

In *pdx-1*<sup>-/-</sup> animals, the villi of the rostral-most duodenum are replaced by an area of smooth cuboidal epithelium (Fig. 13C-F), continuous with the dorsal

ductule epithelium, resembling the cystic/biliary duct epithelium both in its morphology and in its GLUT2 expression (compare Fig. 12A with C,D). Similar structural alterations are also seen in  $\text{pdx}^{\text{lacZko}}$  homozygous null embryos, and the cells in this abnormal epithelium express PDX-1/ $\beta\text{gal}$  (data not shown). The topology of the gut lumen over this region is changed profoundly from a fairly straight tube in normal embryos to a diverticulated or spiraled tube, and parts of the lumen are tightly constricted compared to the wild-type duodenum. Of 6  $\text{pdx}^{\text{XBko}} -/-$  animals analyzed, three 18.5 dpc embryos and two 1 dpp pups showed this phenotype. The remaining 18.5 dpc  $-/-$  animal showed an almost normal connection of the pylorus and rostral duodenal lumen, but the columnar to cuboidal conversion of epithelium and absence of villi was obvious (Fig. 13E).

### **Absence of Brunner's Glands in *Pdx-1* $-/-$ Mutants**

Brunner's glands are epithelially derived, submucosal glands that secrete bicarbonate and mucin into the duodenal lumen via connecting ducts. In mouse, they are apparent just prior to birth and are located in a collar around the neck of the duodenum adjacent to the stomach (Fig. 13A,B). A small number of circular structures with a superficial similarity to Brunner's glands were observed in some  $\text{pdx}^{\text{XBko}} -/-$  gut sections (Fig. 14B,D). To characterize these structures, sections of  $\text{pdx}^{\text{XBko}} -/-$  and  $+/+$  littermates were stained with periodic acid/Schiff's reagent (PAS), which detects the basic mucins of the luminal surface and perinuclear Golgi in Brunner's gland cells (Fig. 14A,C). The structures found in  $\text{pdx}-1 -/-$  embryos differ from wild type Brunner's glands in several ways. As shown in Fig. 14D, they do not stain with PAS, either lumenally or intracellularly.

Second, they are seen only in a few mid-longitudinal sections, while the wild type Brunner's glands form a continuous ring around the neck of the pylorus. Finally, the degree of complexity in the lobulation of the normal glands is not apparent in the

*pdx-1*<sup>-/-</sup> animals. EGF has also been reported to be expressed in the Brunner's glands of rats and humans (Poulsen et al, 1986).

However, immunolocalization of EGF detected no expression in

either wild type or *pdx-1*<sup>-/-</sup> animals at perinatal stages (data not shown). This is in agreement with previous reports on studies in mouse (Beerstecher et al., 1988).

The findings reported here suggest that these structures seen in mutant animals are likely sections through the base of the duodenal crypts. A

second possibility is that these could be incompletely formed and dysfunctional Brunner's glands. It remains to be seen whether *pdx-1* is directly involved in the differentiation of these glands, or if their failed development is secondary to the

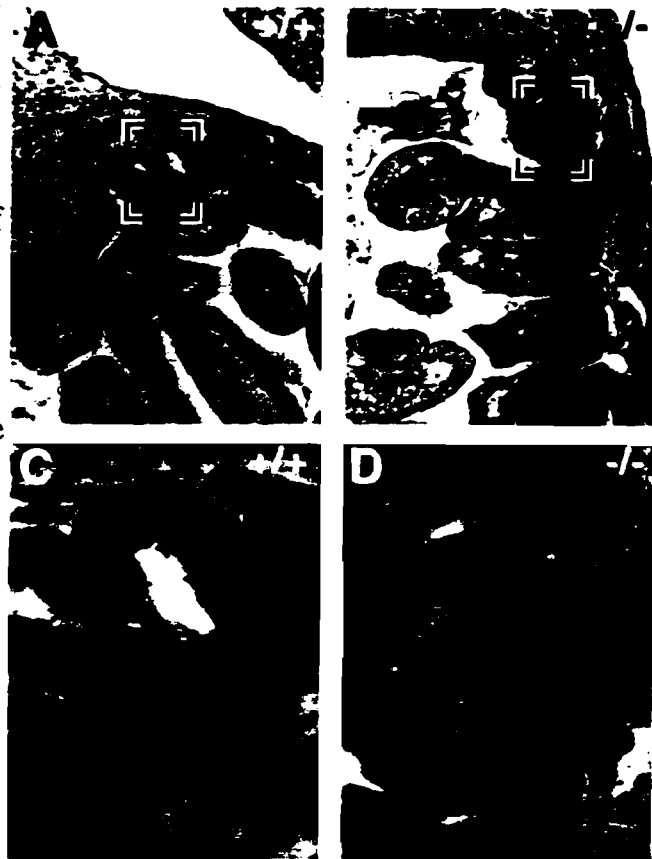


**Figure 14. Absence of Brunner's Gland's in *pdx-1*<sup>-/-</sup> Mutants.** (A) In +/+ 18.5 dpc embryos, the Brunner's glands, located just below the pylorus (Fig. 7A), stain characteristically with PAS. (B) Circular structures morphologically resembling Brunner's glands are seen in some sections of -/- embryos. (C) High magnification of bracketed region in A shows PAS staining the mucins on the luminal surface and within the perinuclear Golgi (arrowheads) of Brunner's gland cells. (D) The indicated region of *pdx-1*<sup>-/-</sup> gut shown in B has a different morphology from that of Brunner's glands, and is PAS-negative (arrowhead indicates lack of perinuclear Golgi staining).

abnormal morphogenesis of the rostral duodenum in homozygous null embryos. However, Brunner's gland development involves epithelial budding and differentiation, which is reminiscent of the processes of pancreatic outgrowth. Numerous clustered evaginations of the PDX-1/ $\beta$ gal-positive epithelium were noted in the rostral-most duodenum of  $\text{pdx}^{\text{lacZko}} -/-$  embryos at 16.5 dpc (data not shown). These evaginations were not seen in older  $-/-$  embryos, and it is possible that they represent a transient stage of abnormal Brunner's gland development. Nevertheless, the absence of mature Brunner's glands supports the hypothesis that loss of PDX-1 function affects duodenal differentiation as well as pancreatic development.

### **Enteroendocrine Cells are Decreased in *pdx-1* $-/-$ Embryos.**

Interspersed among the mucosal enterocytes, the mammalian gut epithelium contains enteroendocrine cells that are characterized by their morphology and their secretion of specific peptide hormones (see Solcia et al., 1987 for review). The relative abundance of the different cell types varies regionally along the gut; thus, they are useful markers of gut patterning. Therefore, wild-type  $+/+$  and  $-/-$  tissues were analyzed from 18.5 dpc embryos for the distribution and number of these cell types by immunohistochemistry with neuroendocrine peptide antibodies. Late gestation embryos were analyzed because enteroendocrine cells are detected properly only after the gut has changed from a pseudostratified to a columnar epithelium with villi (occurring in mice between 16 and 18 dpc) and because neuroendocrine peptide expression is upregulated after 17 dpc in preparation for feeding (Roth et al., 1991). Postnatal animals were not analyzed due to variable pathological effects on the gut

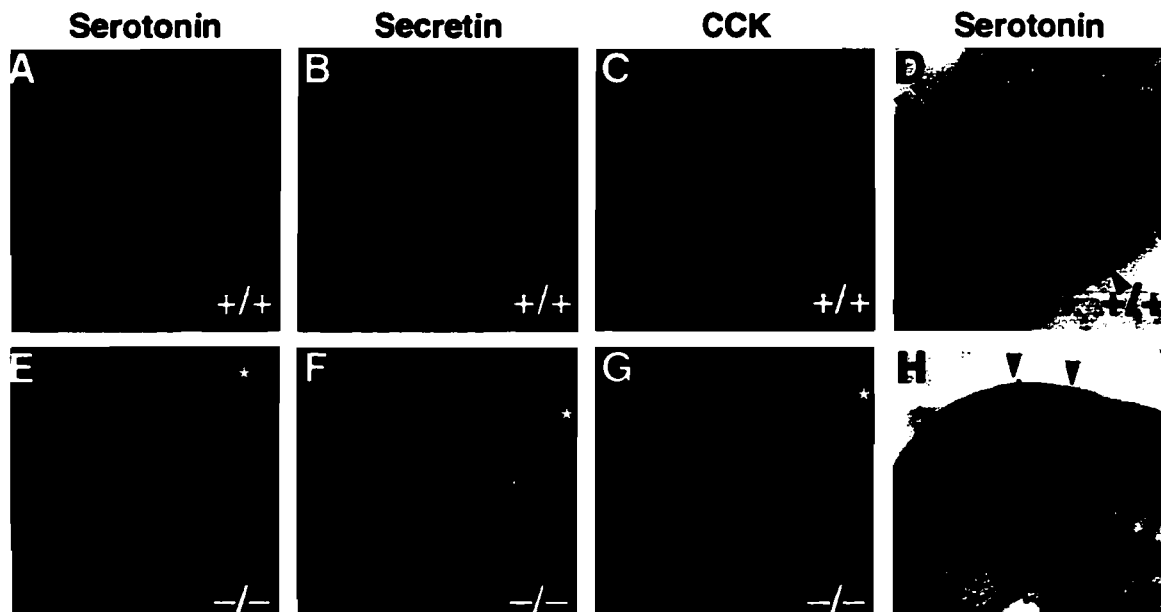


**Figure 15. Reduction in Neuroendocrine Cells in *pdx-1*<sup>-/-</sup> Embryos.** (A-C) Confocally imaged immunolocalization of enteroendocrine cells (red pseudo-color) shows abundant serotonin, secretin, and CCK-positive cells in the rostral-most duodenum of 18.5 dpc *pdx*<sup>XBko</sup> *+/+* animals. Nuclei were counterstained by YO-PRO-1 (green pseudocolor). (E-G) Similar analysis of *pdx*<sup>XBko</sup> *-/-* embryos reveals ~60% reduction in these neuroendocrine cells in the first 1 mm segment of columnar epithelium (see Fig. 10). The lumen of the aberrant cuboidal epithelium of the rostral-most duodenum is indicated (asterisks). (D and H) Immunoperoxidase detection in both *+/+* and *-/-* embryos shows the characteristic morphology of these cells interspersed among the mucosal enterocytes (arrowheads indicate serotonin-positive cells).

epithelium likely stemming from the digestive problems in these animals (Fig. 13C).

Cells positive for most gut neuroendocrine peptides (see Methods and Materials) were detected in *pdx*<sup>XBko</sup> *-/-* and *+/+* littermates, but only secretin, CCK, and serotonin-positive cells were numerous enough for statistical comparisons. In *pdx*<sup>XBko</sup> *+/+* embryos, CCK, secretin, and serotonin expressing cells are abundant in the rostral duodenum just below the pylorus, and their numbers decline sharply towards the distal duodenum (Figs. 15 and 16). A reduction of approximately 60% in the numbers of all three cell types occurs in

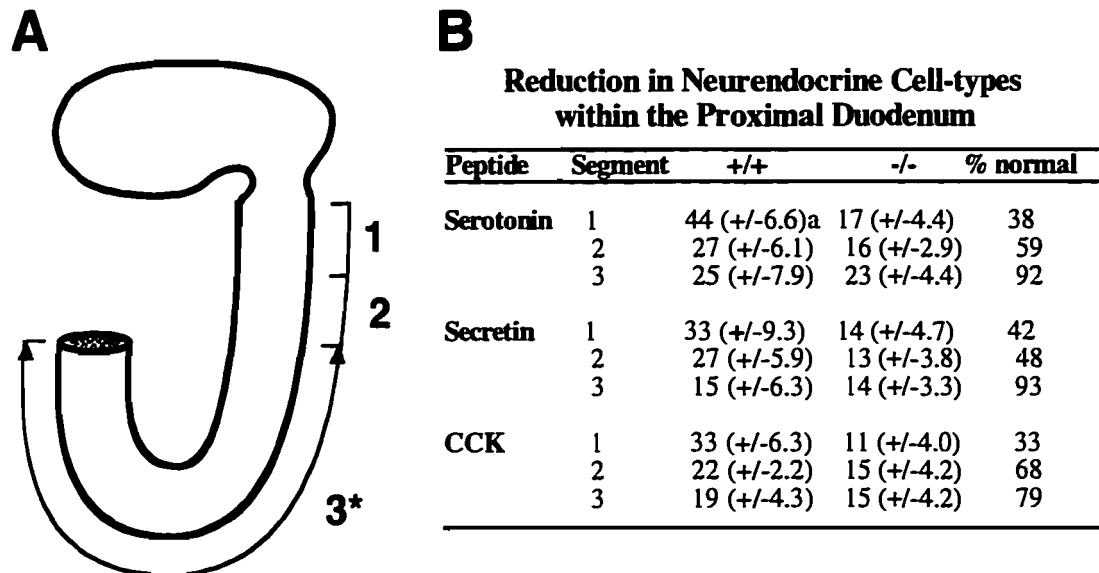


**Figure 16. Quantitation of Enteroendocrine Cells in *pdx<sup>XBko</sup> -/-* Embryos.**

(A) Neuroendocrine cells were counted over three 1 mm long segments of normal columnar epithelium in 18.5 dpc *pdx<sup>XBko</sup> +/+* and *-/-* embryos (four of each genotype). Segments 1 and 2 were adjacent, but differences in gut folding and sectional plane led to segment 3\* often being separated from segment 2, as indicated by the double-headed arrow. In *-/-* embryos, segments 1 and 2 were displaced approx. 0.3 mm from the pylorus because of the abnormal cuboidal epithelium. For each segment (1,2,3) in all 8 embryos, markers were scored on four non-adjacent longitudinal sections, thus avoiding double-scoring of cells. (B) For each embryo analyzed, the average number of positive cells within segment 1, 2, or 3 was calculated. For each segment, the table shows the mean ( $\pm$  standard error of the mean, s.e.m.) of the four animals' individual averages. All three cell types show ~60% reduction in segment 1 of 18.5 dpc *pdx<sup>XBko</sup> -/-* animals, but their levels approach that of wild-type embryos in distal segments (e.g. serotonin).

the rostral duodenum of *pdx<sup>XBko</sup> -/-* embryos, while in the more distal duodenum their numbers approach normal (Figs. 15 and 16).

The enterocyte population of the duodenum and distal gut in *pdx<sup>XBko</sup> -/-* mutants was analyzed by immunohistochemistry for L-FABP and I-FABP (liver and intestinal fatty acid binding proteins; Cohn et al., 1992; Sweetser et al., 1988). Neither marker is expressed in the abnormal cuboidal epithelium of the rostral duodenum (data not shown). Just distal of this region, where villi are present, the



expression of both enterocyte markers is indistinguishable between wild-type and mutant animals (data not shown). Furthermore, no obvious histological abnormalities or morphological defects in other regions of the gut were noted (data not shown).

## Discussion

Jonsson et al. (1994) have previously reported that null mutation of the *pdx-1* gene prevents pancreatic development and differentiation of exocrine cells and islet  $\beta$  cells, resulting in extreme hyperglycemia and perinatal death. The analysis presented here of two similar *pdx-1* mutant alleles corroborates these results, but provides additional information with important ramifications regarding the role *pdx-1* plays in posterior foregut development and organogenesis. First, the formation of the dorsal and ventral pancreatic buds apparently occurs normally in *pdx-1* homozygous null mutants. The ventral bud is not maintained as a discrete structure, while the dorsal bud undergoes limited branching outgrowth and forms a stunted, irregular epithelial tree that persists in newborn pups. Glucagon-expressing cells are detected in the mutant dorsal ductule, but immunohistochemical analysis of late gestation embryos fails to detect any insulin- or amylase-positive cells in this region. The current analyses do not preclude the transient existence of a population of insulin- or amylase-positive cells in earlier embryos; however, these data support the conclusion that loss of *pdx-1* function prevents the differentiation of mature islets, acini, and  $\beta$  cells in perinatal embryos. Second, the architecture of the rostral-most duodenum is altered in perinatal *pdx-1*  $-/-$  embryos, such that it forms a contorted tube lined by a cuboidal (rather than columnar) epithelium that is continuous with the dorsal

ductule and bile duct epithelium. Third, Brunner's glands fail to differentiate in homozygous null animals, and enteroendocrine cells are greatly reduced in number in the villus epithelium of the rostral duodenum.

### ***pdx-1* Expression in the Embryonic Gut.**

The pattern of  $\beta$ gal expression described here from the  $pdx^{lacZko}$  allele agrees well with endogenous PDX-1 expression (Guz et al., 1995; Ohlsson et al., 1993; Miller et al., 1994; Leonard et al., 1993), but the sensitivity of the X-gal staining described here is able to detect *pdx-1* expressing cells at least 12 hrs earlier than previous studies. Further these results show for the first time expression in the antral stomach, common bile duct, and in the cystic and hepatic ducts adjacent to the common bile duct. These data therefore expand the potential sphere of influence for *pdx-1* gene function in gut differentiation. This analysis of the defects in *pdx-1* homozygous null mice has focused on the pancreas and rostral duodenum, based on the previously reported *pdx-1* expression domain. However, in similar *pdx-1* homozygous null mutants generated by Thomas Edlund, the gastrin cells (a neuroendocrine cell type of the antral stomach) fails to differentiate from its somatostatin positive precursor (unpublished observations). This finding is entirely consistent with the expression data shown here within the antral stomach. If the biliary ducts were scored for more subtle differences in the expression of suitable markers, similar effects might also be seen in these regions.

By analyzing mice homozygous null for a Krox-20/ $\beta$ gal fusion protein allele, Schneider-Maunoury et al. (1993) showed that the hindbrain rhombomeres normally expressing *Krox-20* were formed but subsequently degenerated in the

absence of *Krox-20* function. Based on this paradigm, removing PDX-1 function could have caused the death of most or all endodermal cells normally expressing it. In contrast to this possibility, the persistence throughout development of PDX-1/ $\beta$ gal expressing cells in the rostral duodenum and pancreas in *pdx<sup>lacZko</sup> -/-* embryos indicates that these cells do not require *pdx-1* function for their survival, and that the establishment and maintenance of embryonic *pdx-1* expression boundaries does not require PDX-1 function. Because of the stability of the  $\beta$ gal enzyme and the non-quantitative nature of the X-gal staining procedure, this analysis cannot exclude the possibility that PDX-1 could positively or negatively regulate its own expression to some degree.

### ***pdx-1* and Pancreatic Development.**

These results strongly suggest that the endodermal expression domain of *pdx-1* is a major component of the developmental program of the pancreas. The blocked proliferation and differentiation of pancreatic exocrine and endocrine cell types in *pdx-1 -/-* animals, described here and by Jonsson et al. (1994), provides strong evidence consistent with this proposal. As outlined in Chapter I, early classical studies suggest pancreatic development results from a primary instructive induction of the endoderm by axial mesoderm, and secondary mesenchymal signals that induce outgrowth and branching morphogenesis. The latter signals are apparently non-instructive, since similar effects are produced by heterologous mesenchyme (Wessells and Cohen, 1967). Further, transfilter and protease experiments suggest that the signals are comprised of diffusible polypeptides (Golosow and Grobstein, 1962; Wessells and Cohen, 1967). The production of a dorsal pancreatic bud and its subsequent change in architecture

to a branched epithelial outgrowth in *pdx-1*  $-/-$  embryos could represent a partial response to the mesodermal signals described above. However, without the specific developmental instructions provided by *pdx-1* expression, pancreatic precursors cannot proliferate fully and do not differentiate into mature pancreatic cell types, as evidenced by the lack of amylase and insulin expression, and loss of normal tissue morphology. The analysis of the phenotype of *Hox11* homozygous null mutant mice (Roberts et al., 1994) suggests that a similar situation exists during development of the spleen, because the splenic precursors are generated normally, but then fail to differentiate and are lost through apoptosis (Dear et al., 1995).

These data are consistent with the conclusion that the dorsal ductule represents pre-pancreatic tissue arrested in an “early embryonic” state. In *pdx-1*  $-/-$  embryos, the epithelium throughout the dorsal ductule remains GLUT2-positive at 16.5 dpc and 18.5 dpc, which contrasts the change in wild-type embryos from uniform GLUT2 expression in the buds to very low level expression in the mature pancreatic ducts. Notably, glucagon-expressing cells are present in the dorsal bud, and are still found in the later ductule derived from it, in *pdx-1*  $-/-$  animals (Figs. 11 and 12). Together with the finding that many glucagon-positive cells in the 9.5 dpc bud do not express PDX-1/ $\beta$ gal (Fig. 11A), this suggests that the induction of some islet  $\alpha$ -cell precursors could be independent of *pdx-1* function (Fig. 11B). It is currently unknown, however, what relationship the early glucagon-expressing cells have to the later islet cell type and *bona fide*  $\alpha$  cells in the mature pancreas. The glucagon positive cells detected within the epithelium of the dorsal ductule of *pdx-1*  $-/-$  animals may represent scattered endocrine precursors that in the absence of PDX-1 function

are unable to differentiate into mature islet cell types. A rigorous test of this possibility will require the development of methods for determining the lineage relationship of early “pre-endocrine” cells to mature islet cells.

### ***pdx-1* and Duodenal Development.**

The *pdx-1* gene is clearly required for normal rostral duodenal patterning, although it is not involved in the production of columnar epithelium, villi, and enteroendocrine cells *per se*, as they are all present in the more distal duodenum of *pdx-1*  $-/-$  animals, and outside the *pdx-1* expression domain. As described in Chapter I, posterior foregut patterning may involve opposing hepatic and pancreatic programs. Therefore, the mutant duodenum phenotype in *pdx-1*  $-/-$  animals could be explained by an expansion of “hepatic influences” in the absence of *pdx-1* function, and resulting in the rostral-most duodenum adopting a bile duct-like fate. Consistent with this proposal, the cuboidal epithelium replacing the villi lacks enterocyte-specific marker expression, and resembles the bile duct epithelium both in morphology and GLUT2 expression. In addition, scattered GIP and secretin positive cells have also been detected within the cuboidal epithelium (data not shown). This is also true of the biliary ducts; however, these cell types are also seen within the epithelium of wild type duodenum. The examination of other well-defined regional markers, once they become available, will be useful to more clearly define what the aberrant region of the *pdx-1*  $-/-$  duodenum represent.

Although the above hypothesis is attractive in many respects, it is also possible that the cuboidal epithelium in the rostral duodenum represents tissue arrested at an early, but probably abnormal, morphogenetic state. The change in

the epithelial phenotype could be due to a failure in the transition from a pseudostratified gut epithelium to the normal columnar cell type, and the resulting epithelium is unable to proceed to a more advanced architecture, forming neither villi, enterocytes, nor enteroendocrine cells. Finally, it is possible that the absence of proper differentiation in the rostral duodenum and/or the absence of a directional pancreatic outgrowth simply results in a local disorganization, and allows the spread of cuboidal epithelium, continuous with the biliary duct and dorsal ductule, into the rostral-most duodenum.

Just distal to the deformed rostral duodenum, superficially normal villi are formed, and enterocytes and most enteroendocrine cell types are produced. Defects in patterning are apparent, however, in *pdx-1*<sup>-/-</sup> mutants, as evidenced by a substantial suppression in the numbers of enteroendocrine cells. One explanation for this phenotype is that *pdx-1* acts locally in the rostral duodenum, together with other factors, to affect directly the numbers of enterocyte versus enteroendocrine cells born from their common stem cells in the endodermal crypts. This is in contrast to the differentiation block seen in the gastrin expressing enteroendocrine cells of the stomach of *pdx-1*<sup>-/-</sup> mutants produced by Thomas Edlund (as mentioned above). Alternatively, the reduction in the numbers of enteroendocrine cells in the duodenum could be caused indirectly by interactions with the malformed, rostral-most duodenum and/or the blockage in pancreatic development.

In summary, the data presented here show that the initial generation and outgrowth of the pancreatic progenitors does not require *pdx-1* function. Their production therefore occurs via separate regulatory pathways upstream of *pdx-1*, by early endodermal programs in which *pdx-1* plays a redundant role, or they are

directly induced by the adjacent mesoderm. Nonetheless, these data strongly suggest that *pdx-1* is required for the proper differentiation program of the posterior foregut as a whole, including the duodenum, rather than affecting only pancreatic development.

## CHAPTER IV

### GENERAL DISCUSSION

#### **Insights into Endodermal Patterning**

##### **A Model of Pancreatic and Hepatic Induction**

Early classical studies of pancreatic and hepatic development, outlined in Chapter I, suggest that the endoderm of the posterior foregut is patterned by two spatially distinct sets of signals, those derived from the pre-cardiac mesoderm, which lead to a hepatic program for development, and those of the axial mesoderm, which lead to a pancreatic program (see Fig. 17). If this model is correct, then the endoderm of the posterior foregut would be expected to display a window of competence to respond to either of these two signals. Second, the specification of hepatic, biliary, duodenal, and pancreatic fates might result from an interplay of the two opposing signals. There are several anecdotal pieces of evidence that are relevant to this proposed pancreatic/hepatic dual competence. In response to specific forms of pancreatic trauma, pancreatic duct cells will proliferate and efficiently regenerate mature pancreatic cell types (Shaw and Latimer, 1926). However, after ethionine-induced destruction of pancreatic tissue, regrowth in the presence of a mutagen results in the generation of hepatocytes, in addition to normal pancreatic cell types (Scarpelli and Rao, 1981). It is also of interest that ectopic pancreas formation in humans (Branch and Gross, 1935; de Castro Barbosa et al., 1946) occurs most frequently in regions of the gut that are now known to express *pdx-1* (i.e. intestine, biliary ducts, and stomach).



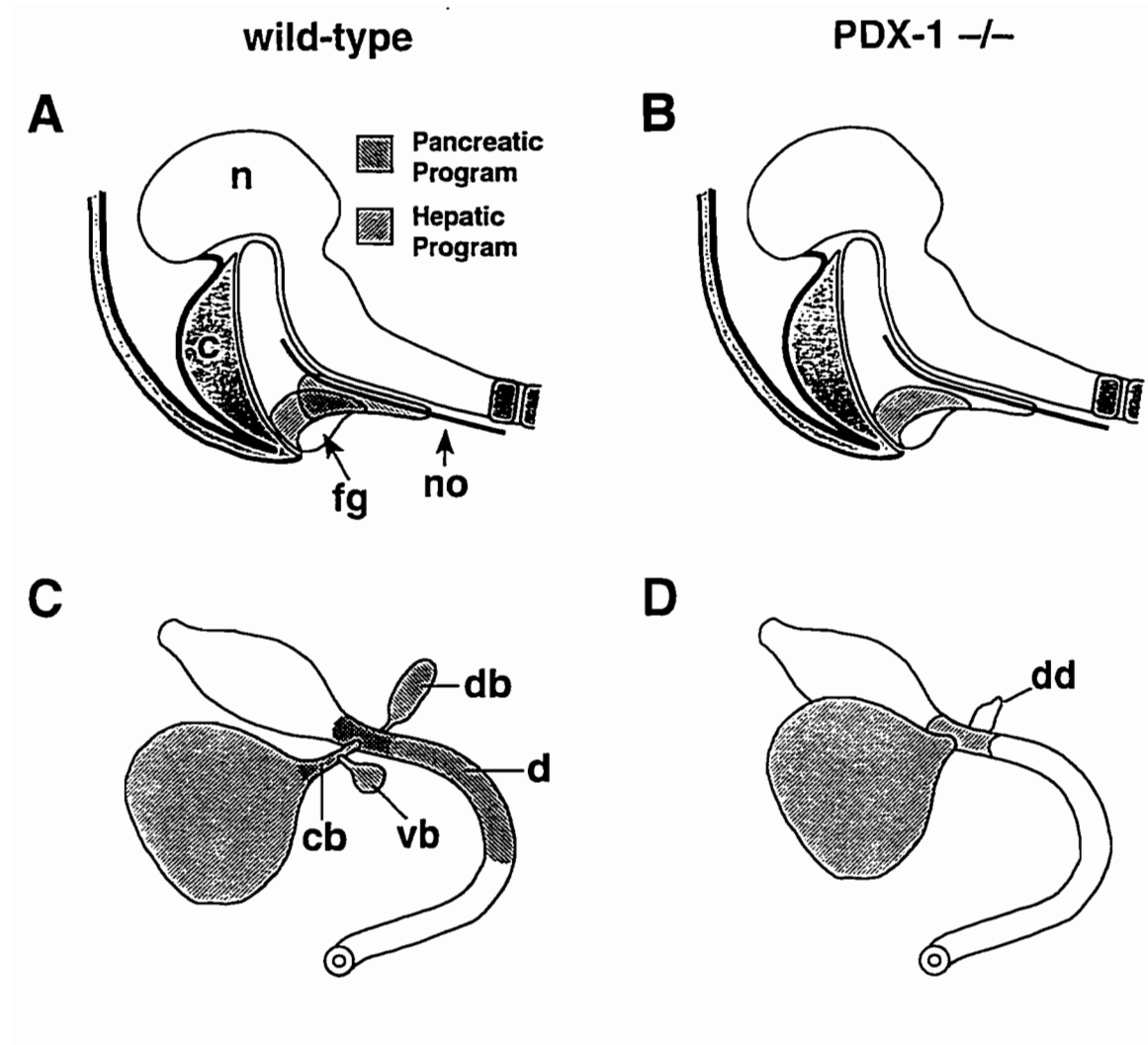


**Figure 17. Model for Early Posterior Foregut Regionalization.** The posterior foregut gives rise to the liver, duodenum, and the dorsal and ventral pancreatic buds. (A and C) The hepatic and pancreatic precursors are induced by the opposing pre-cardiac and notochordal mesoderm. These inductive influences result in the endoderm autonomous developmental program which is necessary for the development of these two tissues. (B and D) Based on the results reported here, it appears that the interaction or the combination of these two developmental programs is responsible for patterning the posterior foregut leading to the proper boundaries and specification of the hepatic, pancreatic, and duodenal derivatives. In support of this, in *pdx-1*  $-/-$  mutants, loss of the part of the pancreatic program which is mediated by *pdx-1* appears to result in a spread of hepatic influences into the region of the duodenum, and definitive pancreatic structures are completely lost. **Abbreviations:** n, neural tissue; c, cardiac mesoderm; fg, foregut pouch; no, notochord; db, dorsal bud; vb, ventral bud; cb, common bile duct; d, duodenum; dd, dorsal ductule.

### **Molecular Data Concerning Pancreatic and Hepatic Induction**

The results from the analysis of the two *pdx-1* null alleles described in Chapter III and recent reports from the lab of Ken Zaret (Gualdi et al., 1996) both appear to be consistent in many respects with the above model. The work by Gualdi et al. indicates that most, if not all, of the early, naive embryonic endoderm is competent to respond to hepatic signals emanating from the pre-cardiac mesoderm. They found that conjugating mouse endodermal explants from the dorsal midline (presumptive pancreatic and intestinal endoderm) with pre-cardiac mesoderm resulted in the induction of both albumin and  $\alpha$ -fetoprotein (as detected by RT-PCR) within the endoderm (these markers are indicative of early hepatic induction). The responsiveness of this region of endoderm to hepatic signals had been previously undetected using classical histological characterizations (LeDouarin, 1975). Gualdi, et al. further demonstrated that the axial tissues provided signals that could repress the differentiation of normal hepatic endoderm. Recombinations of presumptive hepatic endoderm and pre-cardiac mesoderm, which alone results in hepatic differentiation, when combined with non-hepatic endoderm and axial tissues (notochord, somites and neural tube), resulted in a block of albumin induction in both ventral and dorsal endoderm. These data support the idea that the posterior foregut is instructed by, at least, two sets of signals, a pre-cardiac/hepatic signal and other axial/non-hepatic signals which inhibit liver development and support other differentiation pathways (likely pancreas and duodenum). Further, the primitive endoderm appears to be responsive to both of these signals.

In the case of pancreatic induction, it has been previously shown that contact of the dorsal endoderm with axial mesoderm prior to 8.0 dpc was

necessary for later pancreatic development (Wessells and Cohen, 1967). The expression of *pdx-1* described in Chapter III is first detected at this same time but is seen on the ventral side, opposite and well separated from the axial mesoderm. This would seem to be in conflict with the expression of *pdx-1* being influenced by axial signals, since the ventral endoderm does not contact the axial mesoderm at 8.0 dpc. As mentioned in Chapter I, the study of XlHbox-8 in *Xenopus* has previously demonstrated that XlHbox-8 expression is, in fact, dependent on early dorsal signals. Wild type vegetal explants taken prior to stage 8 (preceding gastrulation) and cultured until stage 35 autonomously express XlHbox-8 protein and mRNA (Gamer and Wright, 1995). This demonstrates that XlHbox-8 expression does not require the processes of gastrulation or signals from the mesoderm. It is interesting to note that the cells that will later express XlHbox-8 are specified at a time when they are juxtaposed to the source of dorsalizing signals. However, XlHbox-8 expression is only detected after these associations have been altered by the processes of gastrulation. It is possible that similar mechanisms are at work in the context of the mouse embryo. If this is correct, *pdx-1* expression could be specified within a localized subset of the endoderm very early during murine gastrulation, or just before. The later initiation of expression would then be due to some type of embryonic clock mechanism or other non-instructive interactions with other tissues with which the *pdx-1*-specified region contacts. Alternatively, *pdx-1* expression could be specified by the axial mesoderm just prior to its initiation, before the gut tube begins to form. At 7.5 dpc, prior to head fold formation, the embryonic endoderm consists of a small, flat sheet of cells whose most posterior aspect is continuous with axial mesoderm and lies just beneath the node (see Hogan et al., 1994). At this stage, it

is possible that signals from the axial mesoderm or the node specify the later *pdx-1* expression within the adjoining endoderm. As the head fold forms, the endoderm also folds so that some of these cells would become repositioned ventrally before the initiation of *pdx-1* expression at 8.0 dpc. Further experiments, described below, are necessary to distinguish these two possibilities.

Though the above model appears to fit well with the current information concerning pancreatic induction/specification, it is likely that other local signals and tissue interactions are also necessary for normal pancreas development. One possible interaction that has not yet been considered is the potential interaction between the embryonic and extraembryonic endoderm. Fate mapping studies at ~7.5 dpc (see Hogan et al., 1994) indicate that the posterior boundary between these two tissues marks the posterior-most aspect of the foregut endoderm. Interactions at this boundary could help to specify ventral pancreatic outgrowth since at 9.5-10.0 dpc the position of the ventral bud is juxtaposed to the extraembryonic yolk sac endoderm. Other data of importance to early events in pancreatic development come from the analysis of the motor neuron marker, *Isl1*, and mice that are *-/-* for this gene (Thomas Edlund, Helena Edlund, Sam Pfaff, and Tom Jessell; unpublished observations). Prior to 9.0 dpc, *Isl1* is expressed within the dorsal-most lateral plate mesoderm (more ventral regions do not express *Isl1*) adjacent to the future dorsal pancreatic outgrowth. This mesoderm later moves medially towards the notochord and surrounds the embryonic endoderm. In *Isl1 -/-* mice, although the ventral pancreatic bud is apparently unaffected, the dorsal pancreatic bud is completely lost. This suggests the competence of the ventral and dorsal buds are under the control of separate mesenchymal induction systems. The dorsal component is clearly dependent on

*Isl1*, and the ventral component is specified by other unknown factors.

With regard to endodermal patterning, the data from this dissertation suggests that *pdx-1* is necessary for specifying some of the boundaries between the various regions arising from the posterior foregut. Careful inspection of the earliest expression of *pdx-1* from 8.0 dpc to 9.0 dpc (Fig. 8) reveals that at ~8.5 dpc the two ventral regions of expression on the left and right sides of the AIP (Fig. 8C) are closely opposed to the region of the endoderm that is committed to hepatic fates. As this hepatic region evaginates into the pre-cardiac/pre-hepatic mesoderm, the cells that express *pdx-1* are drawn towards the midline, as the *pdx-1* expressing domain of cells continues to spread and intensify. This suggests that *pdx-1* expression could be inhibited medially by the presumptive hepatic endoderm or by the overlying pre-cardiac mesoderm (similar to axial inhibition of hepatic differentiation above). Conversely, in the absence of functional PDX-1 it appears that the boundary between the pancreas and liver is not precisely specified, as evidenced by the common bile duct being greatly shortened at 11.5 dpc (Fig. 9F) and by the malformations of the rostral duodenum. These defects could be caused by a dorsal shift in the biliary domain of the endoderm, into the rostral duodenum, in the absence of PDX-1. Therefore, PDX-1 might have some inhibitory effects on the hepatic program in that it assists in defining and limiting the hepatic program's area of influence.

One question to be addressed is how could two overlapping endodermal programs specify four separate regional identities, liver, bile ducts, duodenum, and pancreas. It would seem that it would only be possible to specify three regions representing only the hepatic program, both programs, and only the pancreatic program. This could imply the existence of other components which are not yet

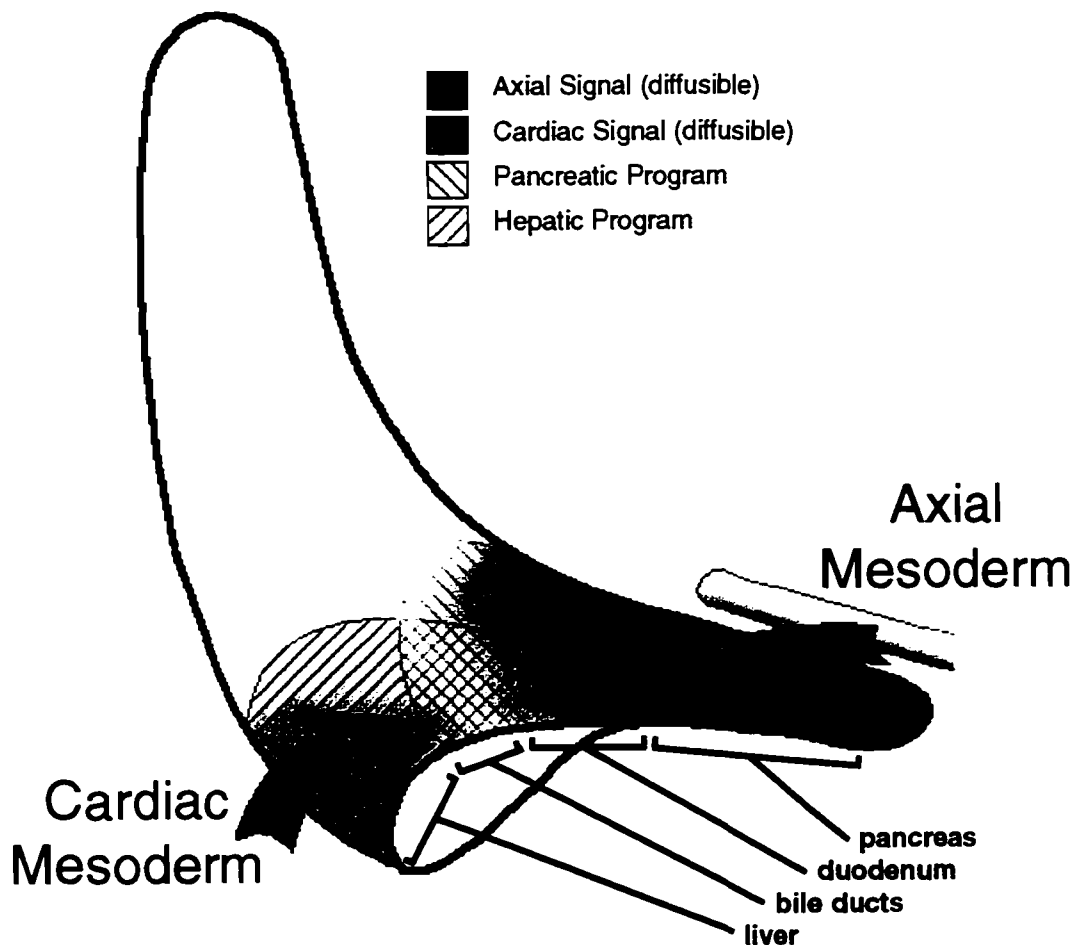


**Figure 18. Patterning of the Developmental Fates of the Posterior Foregut.** The establishment of four distinct regions can be accomplished by the overlaps of the pancreatic and hepatic programs due to the nature of the signals which specify these programs. Both the pancreatic and hepatic programs appear to be comprised of a cell autonomous component within the endoderm and a diffusible component released by the axial and pre-cardiac mesoderm. As illustrated above the strengths and overlaps of these components could provide the necessary patterning information to specify the hepatic, biliary, duodenal, and pancreatic regions of the posterior foregut.

identified which would define part of the region of overlap as bile duct and part as rostral duodenum. This is not necessary, however, in order to rationalize the proposed model. The studies of Gualdi et al. (1996) described above found that the axial tissues inhibited hepatic development. It is plausible that, in a complementary way, the pre-cardiac mesoderm also inhibits pancreatic

development (based on the earliest expression of PDX-1, as mentioned above). Based on this scenario, each of the two development programs in the proposed model would consist of a cell autonomous endodermal component (perhaps the HNF family members for liver and PDX-1 for pancreas) and a diffusible, distance dependent component emanating from the opposing mesodermal sources (see Fig. 18). The liver then would be specified by a high level of the pre-cardiac signal which induces the HNF family members. The lack of PDX-1 expression might be due to the absence of the axial signal and/or repression by the hepatic influences. The biliary region would be specified by a moderate level of the pre-cardiac signal and low levels of the axial signal resulting in the induction of both the HNF family members and PDX-1. This would be consistent with the expression data showing PDX-1/ $\beta$ gal expression in the biliary ducts, which tapers sharply towards the liver, (Fig. 9 and data not shown). The rostral duodenum would likewise be specified by moderate levels of the axial signal and low levels of the pre-cardiac signal, again leading to the induction of the HNF family members together with PDX-1. Finally, in the presence of high levels of the axial signal alone PDX-1 is induced, leading to pancreatic specification. If the malformation of the rostral-most duodenum seen in the *pdx-1*  $-/-$  animals represents a shift towards hepatic fates, then PDX-1 must somehow mediate the inhibitory influence of the axial signal within the endoderm. This is based on the observation that in the absence of functional PDX-1 the biliary region is allowed to spread into the gut to the exclusion of the rostral duodenum. However, as previously stated (see Chapter III Discussion), a transformation mechanism is not the only possible explanation of this phenotype. The malformed region of the rostral duodenum must be further evaluated in order to test this hypothesis. Better

early markers are necessary to distinguish between the bile duct, pancreatic and duodenal epithelia. Once these are available, then the abnormal regions can be further analyzed and compared with the wild type structures. Also some techniques are needed for rigorous lineage tracing of the early endodermal components to their later differentiated structures. The mouse explant culture system described by Gualdi et al. should be very useful in evaluating potential tissue interactions which might be involved in posterior foregut patterning and/or differentiation. Markers specific for each of the four regions (liver, bile duct, duodenum, and pancreas) at early stages of differentiation would be necessary for these studies. Using combinations of competent endoderm with potential signaling regions and analyzing for the expression the region specific markers, the components of the proposed model could be thoroughly tested.

### **Potential Ramifications for Diabetes**

These observations of the function of PDX-1 in normal pancreatic development may someday lead to genetic treatments for diseases such diabetes. In disease states such as insulin-dependent diabetes mellitus (IDDM) in which the islets are lost (due to a poorly defined autoimmune response), one might envisage various forms of intervention designed to replace or regrow islets from the existing pancreatic tissues. However, adult islets are known to have a poor regenerative capacity (Lazarow, 1952). Although there are a couple of examples of islet regeneration from ductal precursors (the embryological source of islet stem cells, Higuchi et al., 1992; Gu and Sarvetnick, 1993), this has been seen only in transgenic model systems, and this regeneration was also accompanied by other adverse affects of the transgene. Because the expression of *pdx-1* becomes



restricted during pancreatic development, it is possible that *pdx-1* expression in non- $\beta$ -cells is indicative of an undifferentiated state. Transient over-expression of *pdx-1* in adult pancreatic ducts might then allow the regeneration of islet cell types. In support of notion, during  $\beta$ -cell regrowth following streptozotocin treatment, all of the newly proliferating cells express *pdx-1* (Gladys Teitelman, unpublished observations). Currently, however, it is unknown exactly what role PDX-1 plays in these events as well as other aspects of pancreatic differentiation. Further studies, described below, are necessary to ascertain whether PDX-1 is necessary for normal islet production and  $\beta$ -cell differentiation and whether reinitiation of PDX-1 expression in the ducts would be sufficient to support islet regeneration.

## **Future Directions**

### **Defining *pdx-1*'s Mechanisms of Transcriptional Regulation**

The study of the positive and negative transcriptional regulatory elements within the *pdx-1* locus will provide important information concerning upstream events that lead to the normal pattern of *pdx-1* expression. These analyses are already underway using both *in vivo* and *in vitro* approaches. The mapping of *pdx-1* regulatory elements in transgenic mice has been partially accomplished in collaboration with Laura Garner, formerly of C.V.E.W.'s lab, and the lab of Mark Magnuson. These experiments have used regions of the 14.5 kb #2 $\lambda$  clone, described in Chapter II, to drive the expression of lacZ reporter constructs. The initial results indicate that the cis-acting sequences necessary for driving *pdx-1* expression in the duodenum and pancreas appears to be contained within a ~4

kb *XbaI* - *SacI* region upstream of the first exon (see Fig. 5). There also appears to be at least two regulatory regions, one that directs islet specific expression and one that drives the expression throughout the pancreas and duodenum. The most rigorous test of the putative regulatory regions would be the rescue of normal pancreas and duodenum development in *pdx-1*  $-/-$  animals by transgenic copys of the *pdx-1* coding regions together with the apparent regulatory regions. This experiment has been initiated by myself, Laura Gamer, and Maureen Gannon in collaboration with Mark Magnuson. These experiments are being continued by Maureen Gannon in the lab of C.V.E.W.

Similar studies are also being done in immortalized cell lines, representing  $\alpha$ ,  $\beta$ , and non-pancreatic cell-types, in collaboration with the lab of Roland Stein. Transient transfection of reporter constructs driven by regions of the *pdx-1* locus has defined a ~1 kb region that drives expression in insulin-producing cell lines. It is compelling that, these sequences correspond to the islet specific region defined in transgenic mice. *DNaseI* hypersensitivity studies in insulin-producing,  $\beta$ TC3 cell lines have revealed three sites, two of which correspond closely with the regions mapped in transgenic animals and one which would correspond to the *pdx-1* promoter. A higher resolution mutational analysis of the ~1 kb region is ongoing, but should soon result in identifying the specific element(s) in this region that are necessary for *pdx-1* expression specifically in  $\beta$ -cells. The identification of these elements ultimately will lead to the upstream transcription factor(s) that control *pdx-1* transcription, which is an important long term goal of the C.V.E.W. lab.

### **Analysis of *pdx-1*'s Role in Later Stages of Pancreas Development**

Because null mutations of PDX-1 block pancreatic differentiation completely, the analyses described in this dissertation have been unable to demonstrate what role, if any, PDX-1 might play in later stages of pancreas development. To address this problem, a third strategy has been designed using the CRE/lox system (Sauer and Henderson, 1989; Sauer, 1993). The loxP recombination sites to be placed flanking exon 2, at positions which should not affect normal PDX-1 function (Gu et al., 1993). Mice carrying this allele will then be bred to transgenic mice which express CRE from cell-specific (e.g. using the insulin enhancer) or later stage specific enhancer/promoters. This should allow the function of PDX-1 to be analyzed in certain cell types and/or after the initial stages of development.

### **Pancreatic Specification and *pdx-1* Induction**

Although the general features of pancreatic induction and development are well established in the classical literature, there are still many questions regarding the early inductive mechanisms in mouse. The  $pdx^{lacZko}$  allele described in this dissertation should be very useful in detecting and analyzing the initial steps in pancreatic induction. These data demonstrate that *pdx-1* expression (detected by the PDX-1/ $\beta$ gal fusion) precedes all other pancreatic markers currently available. Because the X-gal staining technique allows the detection of a single expressing cell, competent endoderm from  $pdx^{lacZko}$  embryos should provide the basis for very sensitive assays of potential inducing tissues or factors. With tools such as the  $pdx^{lacZko}$  allele, RT-PCR, as well as a much more

extensive selection of antibodies to key developmental players, it will soon be possible to address some of the questions regarding pancreatic induction using cultured explant recombinations. Specifically, the following questions need to be addressed: 1) What is the earliest stage when the pancreas and/or *pdx-1* expression is specified? 2) What tissue(s) is capable of such specification? and 3) What is/are the factor(s) which mediate this induction?

### **Summary**

The study of PDX-1 both in the *Xenopus* system and mouse has provided important information as to how the primitive endoderm is patterned and what types of interactions might be involved in pancreatic specification. The data contained within this dissertation, together with the recent reports concerning hepatic induction, support the following conclusions regarding posterior foregut patterning and tissue inductions: 1) This region of the endoderm is acted on by two opposing signals from the pre-cardiac and axial mesoderm, 2) The endoderm of this region is competent to respond to either of these signals, and 3) Both of these signals, and the developmental programs they establish, work in opposition to each other in order to establish the proper boundaries between liver, biliary ducts, pancreas, and duodenum. It is expected that this system will continue to be fruitful in providing an improved understanding of the processes of endodermal patterning, tissue inductions, and organogenesis. These mechanisms will then allow genetic interventions to be designed to treat not only pancreatic dysfunctions such as diabetes, but likely the paradigms generated here may be generally applicable to and help in designing similar schemes for treating other diseases.

## REFERENCES

- Aisemberg, G. O., Wysocka-Diller, J., Wong, V. Y. and Macagno, E. R.** (1993). Antennapedia-class homeobox genes define diverse neuronal sets in the embryonic CNS of the leech. *Journal of Neurobiology* **24**:1423-1432.
- Akam, M.** (1989). Hox and HOM: homologous gene clusters in insects and vertebrate. *Cell* **57**:347-49.
- Akam, M.** (1987). The molecular basis for metameric pattern in the *Drosophila* embryo. *Development* **101**:1-22.
- Ang, S. L., Wierda, A., Wong, D., Stevens, A., Cascio, S., Rossant, J. and Karet, K. S.** (1993). The formation and maintenance of the definitive endoderm lineage in the mouse: involvement of the HNG-3/forkhead proteins. *Development* **119**:1301-15.
- Bartels, J. L., Murtha, M. T. and Ruddle, F. H.** (1993). Multiple Hox/HOM-class homeoboxes in Platyhelminthes. *Molecular Phylogenics and Evolution* **2**:143-151.
- Beeman, R. W., Stuart, J. J., Haas, M. S. and Denell, R. E.** (1989). Genetic analysis of the homeotic gene complex (HOM-C) in the beetle *Tribolium castaneum*. *Dev. Biol.* **133**:196-209.
- Beerstecher, H. J., Huiskens-van der Meij, C. Warnaar, S. O.** (1988). An immunohistochemical study performed with monoclonal and polyclonal antibodies to mouse epidermal growth factor. *J Histochem. Cytochem.* **36**:1153-1160.
- Behrens, J., von Kries, J. P., Kühl, M., Bruhn, L., Wedlich, D., Grosschedl, R. and Birchmeier, W.** (1996). Function interaction of  $\beta$ -catenin with the transcription factor LEF-1. *Nature* **382**:638-642.
- Bonnerot, C. And Nicolas, J.** (1993). Application of LacZ gene fusions to postimplantation development. *Meth. Enz.* **225**, 451-469
- Branch, C. D. and Gross, R. E.** (1935). Aberrant pancreatic tissue in the gastrointestinal tract. *Arch. Surg.* **31**, 200-224.
- Bridges, W. and Morgan, T.** (1923). Carnegie Inst. Washington Publ. 327:137.
- Brown, N. A., McCarthy, A. and Seo, J.** (1992). Development of the left-right axes. *CIBA Found. Symp.* **165**:144-154.
- Busa, W. B., Ferguson, J. E., Joseph, S. K., Williamson, J. R. and Nuccitelli, R.** (1985). Activation of frog (*Xenopus laevis*) eggs by inositol triphosphate. I.

Characterization of Ca<sup>2+</sup> release from intracellular stores. *J. Cell Biol.* **100**:677-682.

**Camper, S. A., Saunders, T. L., Katz, R. W. and Reeves, R. H.** (1990). The Pit-1 transcription factor gene is a candidate for the murine Snell dwarf mutation. *Genomics* **8**: 586-590.

**Carpenter, E. M., Goddard, J. M., Chisak, O., Manley, N. R. and Capecchi, M. R.** (1993). Loss of HoxA1 (Hox-1.6) function results in the reorganization of the murine hindbrain. *Development* **118**:1063-73.

**Carrasco, A. E., McGinnis, W., Gehring, W. J. and DeRobertis, E. M.** (1984). Cloning of an *X. laevis* gene expressed during early embryogenesis coding for a peptide region homologous to *Drosophila* homeotic genes. *Cell* **37**:409.

**Cohn, S., Simon, T., Roth, K., Birkenmeier, E., and Gordon, J.** (1992). Use of transgenic mice to map *cis*-acting elements in the Intestinal Fatty Acid Binding Protein Gene (*Fabpi*) that control its cell lineage-specific and regional patterns of expression along the duodenal-colonic and crypt-villus axes of the gut epithelium. *J. Cell Biol.* **119**: 27-44.

**Cui, Y., Brown, J. D., Moon, R. T. and Christian, J. L.** (1995). Xwnt-8b: a maternally expressed *Xenopus* Wnt gene with a potential role in establishing the dorsoventral axis. *Development* **121**:2177-2186.

**Chisaka, O., Musci, T. S. and Capecchi, M. R.** (1992). Developmental defects of the ear, cranial nerves, and hindbrain result from targeted disruption of the mouse homeobox gene Hox-1.6. *Nature* **355**:516-20.

**Chisaka, O. and Capecchi, M. R.** (1991). Regionally restricted developmental defects resulting from targeted disruption of the mouse homeobox gene hox-1.5. *Nature* **11**:458-459.

**Christian, J. L. and Moon, R. T.** (1992). Competence modifiers synergize with growth factors during mesoderm induction and patterning in *Xenopus*. *Cell* **71**:709-712.

**Dale, L., Matthews, G., Colman, A.** (1993). Secretion and mesoderm inducing activity of the TGF $\beta$ -related domain of *Xenopus* Vg1. *EMBO J.* **12**:4471-4480.

**Dale, L., Howes, G., Price, B. M. J. and Smith, J. C.** (1992). Bone morphogenetic protein 4: a ventralizing factor in early *Xenopus* development. *Development* **115**:573-585.

**Dale, L. and Slack, J. M. W.** (1987). Regional specificity within the mesoderm of early embryos of *Xenopus laevis*. *Development* **100**:279-295.

**De Castro Barbosa, J. J., Dockerty, M. B. and Waugh, J. M.** (1946). Pancreatic heterotopia. *Surg. Gyn. Obs.* **82**, 527-542.

**Dear, T. N., Colledge, W. H., Carlton, M.B.L., Lavenir, I., Larson, T., Smith, A. J. H., Warren, A. J., Evans, M. J., Sofroniew, M. V., and Rabbitts, T. H.** (1995). The *Hox11* gene is essential for cell survival during spleen development. *Development* **121**:2909-2915.

**Degnan, B. M., Degnan, S. M., Giusti, A. and Morse, D. E.** (1995). A HOX/HOM homeobox gene in sponges. *Gene* **155**:175-177.

**Deuchar, E. M.** (1975). *Cellular Interactions in Animal Development*. Chapman and Hall, London.

**Dick, M. H. and Buss, L. W.** (1994). A PCR-based survey of homeobox genes in *Ctenodrilus serratus* (Annelida: Polychaeta). *Molec. Phylogen. Evol.* **3**:146-158.

**Doll, U. and Niessing, J.** (1993). Continued expression of the chicken caudal homologue in endodermally derived organs. *Dev. Biol.* **156**:155-63.

**Duprey, P., Chowdhury, K., Dressler, G. R., Balling, R., Simon, D., Guenet, J. L. and Gruss, P.** (1988). A mouse gene homologous to the *Drosophila* gene *caudal* is expressed in epithelial cells from the embryonic intestine. *Genes & Dev.* **2**:1647-54.

**Fire, A., Harrison, S. W. and Dixon, D.** (1990). A modular set of lacZ fusion vectors for studying gene expression in *Caenorhabditis elegans*. *Gene* **93**, 189-198.

**Fitzpatrick, V. D., Percival-Smith, A., Ingles, C. J. and Krause, H. M.** (1992). Homeodomain-independent activity of the fushi-tarazu polypeptide in *Drosophila* embryos. *Nature* **356**: 610-612.

**Funayama, N., Fagotto, F., McCrea, P. and Gumbiner, B. M.** (1995). Embryonic axis induction by the armadillo repeat domain of  $\beta$ -catenin: evidence for intracellular signaling. *J. Cell Biol.* **128**:959-968.

**Gamer, L. W. and Wright, C. V. E.** (1995). Autonomous endoderm determination in *Xenopus*: regulation of expression of the pancreatic gene *XIHbox8*. *Dev. Biol.* **17**:240-251.

**Garcia-Fernandez, J. and Holland, P. W.** (1994). Archetypal organization of the amphioxus Hox gene cluster. *Nature* **370**:563-566.

**Gehring, W.** (1986). On the homeo box and its significance. *Bioessays* **5**:3-4.

**Gehring, W.** (1987). Homeoboxes in the study of development. *Science* **236**:1245-52.

**Gehring, W. J., Qian, Y. Q., Billeter, M., Furukubo-Tokunaga, K., Schier, A. F., Resendez-Perez, D., Affolter, M., Otting, G. and Wuthrich, K.** (1994). Homeodomain-DNA recognition. *Cell* **78**, 211-223.

**Gehring, W. J., Affolter, M. and Burglin, T.** (1994). Homeodomain proteins. *Ann. Rev. Bioch.* **63**:487-426.

**Gendron-Maguire, M., Mallo, M., Zhang, M. and Gridley, T.** (1993). HoxA-2 mutant mice exhibit homeotic transformation of skeletal elements derived from cranial neural crest. *Cell* **75**:1317-31.

**Gerhart, J., Danilchick, M., Doniach, T., Roberts, S., Rowning, B. and Stewart, R.** (1989). Cortical rotation of the *Xenopus* egg: consequences for the anteroposterior pattern of embryonic dorsal development. *Development* [Suppl.] **107**:37-51.

**German, M. S., Wang, J., Chadwick, R. B. and Rutter, W. J.** (1992). Synergistic activation of the insulin gene by a LIM-homeodomain protein and a basic helix-loop-helix protein: building a functional insulin mini-enhancer complex. *Genes & Dev.* **6**:2165-76.

**Golosow, N. and Grobstein, C.** (1962). Epitheliomesenchymal interaction in pancreatic morphogenesis. *Dev. Biol.* **4**:242-255.

**Gu, D. and Sarvetnick, N.** (1993). Epithelial cell proliferation and islet neogenesis in IFN- $\gamma$  transgenic mice. *Development* **118**:33-46.

**Gualdi, R., Bossard, P., Zheng, M., Hamada, Y., Coleman, J. R. and Zaret, K. S.** (1996). Hepatic specification of the gut endoderm *in vitro*: cell signaling and transcriptional control. *Genes & Dev.* **10**:1670-1682.

**Guazzi, S., Price, M., DeFelice, M., Demante, G., Mattei, M. G. and DiLauro, R.** (1990). Thyroid nuclear factor-1 (TTF-1) contains a homeodomain and displays a novel DNA binding specificity. *EMBO J.* **9**:3631-39.

**Gumbiner, B. M.** (1995). Signal transduction of beta-catenin. *Curr. Opin. Cell Biol.* **7**:634-640.

**Guz, Y., Montminy, M. R., Stein, R., Leonard, J., Gamer, L. W., Wright, C. V. and Teitelman, G.** (1995). Expression of murine STF-1, a putative insulin gene transcription factor, in beta cells of pancreas, duodenal epithelium, and pancreatic exocrine and endocrine progenitors during ontogeny. *Development* **121**: 11-18.

**Higuchi, Y., Herrera, P., Muniesa, P., Orci, L. and Vassalli, J. D.** (1992). Expression of a tumor necrosis factor in murine pancreatic B cells results in severe and permanent insulinitis without evolution towards diabetes. *J. Exp. Med.* **176**:1710-1731.

**Hill, R. E., Favor, J., Hogan, B. L., Ton, C. C., Saunders, G. F., Hanson, M., Prosser, J., Jordan, T., Hastie, N. D. and van Heyningen, V.** (1991). Mouse small eye results from mutations in a paired-like homeobox-containing gene. *Nature.* **354**:522-525.

**Hogan, B. L. M.** (1995). Upside-down ideas vindicated. *Nature* **376**:210-211.



**Hogan, B., Beddington, R., Costantini, F. And Lacy, E.** (1994). *Manipulating the Mouse Embryo: A Laboratory Manual*, 2nd ed. Cold Spring Harbor Laboratory Press; Cold Spring Harbor.

**Immerglück, K., Lawrence, P. A. and Bienz, M.** (1990). Induction across germ layers in *Drosophila* mediated by a genetic cascade. *Cell* **62**:261-268.

**James, R. and Kazenwadel, J.** (1991). Homeobox gene expression in the intestinal epithelium of adult mice. *J. Biol. Chem.* **266**:3246-51.

**Jetton, T. L., Liang, Y., Pettipher, C. C., Zimmerman, E. C., Cox, F. G., Horvath, K., Matschinsky, F. M. And Magnuson, M.** (1994). Analysis of upstream glucokinase promoter activity in transgenic mice and identification of glucokinase in rare neuroendocrine cells in the brain and gut. *J. Biol. Chem.* **269**: 3641-3654.

**Johnson, R. L., Riddle, R. D., Laufer, E. and Tabin, C.** (1994). Sonic hedgehog: a key mediator of anterior posterior patterning of the limb and dorso-ventral patterning of axial embryonic structures. *Bioch. Soc. Trans.* **22**:569-574.

**Jones, C. M., Lyons, K. M., Lapan, P. M., Wright, C. V. E. and Hogan, B. L. M.** (1992). DVR-4 (Bone Morphogenetic Protein-4) as a posterior-ventralizing factor in *Xenopus* mesoderm induction. *Development* **115**:639-647.

**Jonsson, J., Carlsson, L., Edlund, T. and Edlund, H.** (1994). Insulin-promoter-factor 1 is required for pancreas development in mice. *Nature* **371**:606-609.

**Karlsson, O., Thor, S., Norberg, T., Ohlsson, H. and Edlund, T.** (1990). Insulin gene enhancer binding protein Isl-1 is a member of a novel class of proteins containing both a homeodomain and a Cys-His domain. *Nature* **344**:879-82.

**Kaufman, T. C., Seeger, M. A. and Olsen, G.** (1990). Molecular and genetic organization of the Antennapedia gene complex of *Drosophila melanogaster*. In: *Advances in Genetics--Genetic Regulatory Hierarchies in Development*, vol. 27. M. Raff, ed., Academic Press, NY, pp. 309-362.

**Kimelman, D., Christian, J. L. and Moon, R. T.** (1992). Synergistic principles of development: overlapping patterning systems in *Xenopus* mesoderm induction. *Development* **116**:1-9.

**Krumlauf, R.** (1992). Evolution of the vertebrate Hox homeobox genes. *Bioessays* **14**:245-52.

**Krumlauf, R.** (1994). Hox genes in vertebrate development. *Cell* **2**:191-201.

**Krumlauf, R., Marshall, H., Studer, M., Norchev, S., Sham, M. H. and Lumsden, A.** (1993). Hox homeobox genes and regionalization of the nervous system. *J. Neurobiol.* **24**:1328-40.

**Lai, E., Prezioso, V. R., Tao, W. F., Chen, W. S. and Darnell, J. E., Jr.** (1991). Hepatocyte nuclear factor-3 alpha belongs to a gene family in mammals that is homologous to the *Drosophila* homeotic gene forkhead. *Genes & Dev.* **5**:416-27.

**Lararow, A.** (1952). Spontaneous recovery from alloxan diabetes in rats. *Diabetes* **1**:363-370.

**LeDouarin, N. M.** (1975). An experimental analysis of liver development. *Medical Biology.* **53**, 427-455.

**LeMoullic, H., Lallemand, Y. and Brulet, P.** (1990). Targeted replacement of the homeobox gene Hox-3.1 by the *Escherichia coli* lacZ in mouse chimeric embryos. *Proc. Natl. Acad. Sci. USA* **87**:4712-16.

**LeMoullic, H., Lallemand, Y. and Brulet, P.** (1992). Homeosis in the mouse induced by a null mutation in the Hox-3.1 gene. *Cell* **69**:251-64.

**Leonard, J., Peers, B., Johnson, T., Ferreri, K., Lee, S. and Montminy, M. R.** (1993). Characterization of somatostatin transactivating factor-1, a novel homeobox factor that stimulates somatostatin expression in pancreatic islet cells. *Mol. Endocrinol.* **7**, 1275-1283.

**Lewis, E. B.** (1978). A gene complex controlling segmentation in *Drosophila*. *Nature* **276**:565-70.

**Li, S., Crenshaw, E. B. 3rd., Rawson, E. J., Simmons, D. M., Swanson, L. W. and Rosenfeld, M. G.** (1990). Dwarf locus mutants lacking three pituitary cell types result from mutations in the POU-domain gene pit-1. *Nature* **347**:528-533.

**Lu, M., Miller, C. P., Habener, J. F.** (1996). Functional region of the homeodomain protein IDX-1 required for transactivation of the rat somatostatin gene. *Endocrinol.* **137**:2959-2967.

**Lufkin, T., Mark, M., Hart, C. R., Dolle, P., LeMeur, M. and Chambon, P.** (1992). Homeotic transformation of the occipital bones of the skull by ectopic expression of a homeobox gene. *Nature* **359**:835-41.

**Lufkin, T., Dierich, A., LeMeur, M., Mark, M. and Chambon, P.** (1991). Disruption of the hox-1.6 homeobox gene results in defects in a region corresponding to its rostral domain of expression. *Cell* **66**:1105-19.

**Mao, C. A., Wikramanayake, A. H., Gan, L., Chuang, C. K., Summers, R. G. and Klein, W. H.** (1996). Altering cell fates in sea urchin embryos by overexpressing SpOtx, an orthodenticle-related protein. *Development* **122**:1489-1498.

**McGinnis, W., Levine, M., Hafen, E., Kuroiwa, A. and Gehring, W. J.** (1984a). A conserved DNA sequence in homeotic genes of the *Drosophila* Antennapedia and Bithorax complexes. *Nature* **308**:428.

**McGinnis, W., Garber, R. L., Wirz, J., Kuroiwa, A. and Gehring, W. J.** (1984b) A homologous protein coding sequence in *Drosophila* homeotic genes and its conservation in other metazoans. *Cell* **37**:403-8.

**McGinnis, W.** (1994). A century of homeosis, a decade of homeoboxes. *Genetics* **3**:607-611.

**Melton, D.** (1987). Translocation of a localized maternal mRNA to the vegetal pole of *Xenopus* oocytes. *Nature* **328**:80-82.

**Melton, D.** (1991). Pattern Formation During Animal Development. *Science* **252**:234-241.

**Mendel, D. B., Hansen, L. P., Graves, M. K., Conley, P. B. and Crabtree, G. R.** (1991). HNF-1a and HNF-1b (vHNF-1) share dimerization and homeodomains, but not activation domains and form heterodimers *in vitro*. *Genes & Dev.* **5**:1042-56.

**Miller, C. P., McGehee, R. E. Jr. and Habener, J. F.** (1994). IDX-1: a new homeodomain transcription factor expressed in rat pancreatic islets and duodenum that transactivates the somatostatin gene. *EMBO J.* **13**:1145-1156.

**Mosquera, L., Forristall, C., Zhou, Y. and King, M. L.** (1993). A mRNA localized to the vegetal cortex of *Xenopus* oocytes encodes a protein with a nanos-like zinc finger domain. *Development* **117**:377-386.

**Muller, M. M., Carrasco, A. E. and DeRobertis, E. M.** (1984). A homeo-box-containing gene expressed during oogenesis in *Xenopus*. *Cell* **39**:157-62.

**Murphy, P. And Hill, R. E.** (1991). Expression of the mouse labial-like homeobox-containing genes, Hox 2.9 and Hox 1.6, during segmentation of the hindbrain. *Development* **111**:61-74.

**Nieuwkoop, P. D.** (1969). The formation of the mesoderm in urodele amphibians. I. Induction by the endoderm. *Wilhelm Roux Arch. Entwicklungsmech. Org.* **162**:341-373.

**Nieuwkoop, P. D.** (1973). The "organisation center" of the amphibian embryo: Its origin, spatial organisation and morphogenetic action. *Adv. Morphog.* **10**:1-39.

**Nieuwkoop, P. D.** (1977). Origin and establishment of embryonic polar axes in amphibian development. *Curr. Top. Dev. Biol.* **11**:115-132.

**Ohlsson, H., Karlsson, K. and Edlund, T.** (1993). IPF1, a homeodomain-containing transactivator of the insulin gene. *EMBO J.* **12**:4251-4259.

**Pang, K., Mukonoweshuro, C. and Wong, G. G.** (1994). Beta cells arise from glucose transporter type 2 (Glut2)-expressing epithelial cells of the developing rat pancreas. *Proc. Natl. Acad. Sci. USA* **91**:9559-9563.

**Peers, B., Sharma, S., Johnson, T., Kamps, M., Montminy, M.** (1995). The pancreatic islet factor STF-1 binds cooperatively with Pbx to a regulatory element in the somatostatin promoter: importance of the FPWMK motif and the homeodomain. *Molec. Cell Biol.* **15**:791-797.

**Peers, B., Leonard, J., Sharma, S., Teitelman, G. and Montminy, M. R.** (1994). Insulin expression in pancreatic islet cells relies on cooperative interactions between the helix loop helix factor E47 and the homeobox factor STF-1. *Mol. Endocrinol.* **8**:1798-1806.

**Peshavaria, M., Gamer, L., Henderson, E., Teitelman, G., Wright, C. V. and Stein, R.** (1994) XlHbox-8, an endodermal-specific *Xenopus* homeodomain protein, is closely related to a mammalian insulin gene transcription factor. *Molec. Endo.* **8**:806-816.

**Peshavaria, M., Towle, H. C., Robertson, R. P., Stein, R.** (1995). Reduction of insulin gene transcription in HIT T-15  $\beta$ -cells chronically exposed to supraphysiological glucose concentration is associated with the loss of STF-1 transcription factor expression. *Proc. Natl. Acad. Sci. USA* **92**:9127-9131.

**Poulsen, S. S., Nexø, E., Olsen, P. S., Hess, J. and Kirkegaard, P.** (1986). Immunohistochemical localization of epidermal growth factor in rat and man. *Histochemistry* **85**:389-394.

**Ramirez-Solez, R., Zheng, H., Whiting, J., Krumlauf, R. and Bradley, A.** (1993). Hoxb-4 (Hox-2.6) mutant mice show homeotic transformation of a cervical vertebra and defects in the closure of the sternal rudiments *Cell* **73**:279-94.

**Rijli, F. M., Mark, M., Lakkaraju, S., Dierich, A., Dolle, P. and Chambon, P.** (1993). A homeotic transformation is generated in the rostral branchial region of the head by disruption of Hoxa-2, which acts as a selector gene. *Cell* **75**:1333-49.

**Roberts, D. J., Johnson, R. L., Burke, A. C., Nelson, C. E., Morgan, B. A. and Tabin, C.** (1995). Sonic hedgehog is an endodermal signal inducing Bmp-4 and Hox genes during induction and regionalization of the chick hindgut. *Development* **121**:3163-3174.

**Roberts, C. W., Shutter, J. R. and Korsmeyer, S. J.** (1994). Hox11 controls the genesis of the spleen. *Nature* **368**:747-749.

**Roth, K. A., Rubin, D. C., Birkenmeier, E. H. and Gordon, J. I.** (1991). Expression of liver fatty acid-binding protein/human growth hormone fusion genes within the enterocyte and enteroendocrine cell populations of fetal transgenic mice. *J. Biol. Chem.* **266**:5949-5954.

**Salser, S. J. and Kenyon, C.** (1992). Activation of a *C. elegans* Antennapedia homologue in migrating cells controls their direction of migration. *Nature* **355**:255-258.

**Sambrook, J., Fritsch, E. F. and Maniatis, T.** (1989). Molecular Cloning: A laboratory manual. 2nd ed. Cold Spring Harbor Press, Plainview, NY.

**Scarpelli, D. G. And Rao, M. S.** (1981). Differentiation of regenerating pancreatic cells into hepatocyte like cells. Proc. Natl. Acad. Sci. USA **78**: 2577-2581.

**Schneider, S., Steinbeisser, H., Warga, R. M. and Hausen, P.** (1996). Beta-catenin translocation into nuclei demarcates the dorsalizing centers in frog and fish embryos. Mech. of Dev. **57**:191-198.

**Schneider-Maunoury, S., Topilko, P., Seitandou, T., Levi, G., Cohen-Tannoudji, M., Pournin, S., Babinet, C. and Charnay, P.** (1993). Disruption of Krox-20 results in alteration of rhombomeres 3 and 5 in the developing hindbrain. Cell **75**:1199-1214.

**Schummer, M., Scheurlen, I., Schaller, C. and Galliot, B.** (1992). HOM/HOX homeobox genes are present in hydra (*Chlorohydra viridisima*) and are differentially expressed during regeneration. EMBO J. **11**:1815-1823.

**Scott, M. P. and Weiner, A. J.** (1984). Structural relationships among genes that control development: sequence homology between the Antennapedia, Ultrabithorax, and fushi tarazu loci of *Drosophila*. Proc. Natl. Acad. Sci. USA **81**:4115.

**Scott, M. P., Tamkun, J. W. and Hartzell, G. W., 3rd.** (1989). The structure and function of the homeodomain. Biochim. Biophys. Acta. **989**:25-48.

**Sharma, S., Leonard, J., Lee, S., Chapman, H. D., Leiter, E. H. and Montminy M. R.** (1996). Pancreatic islet expression of the homeobox factor STF-1 relies on an E-box motif which binds USF. J. Biol. Chem. **271**:2294-2299.

**Shaw, J. W. And Latimer, E. O.** (1926). Regeneration of pancreatic tissue from the transplanted pancreatic duct in the dog. Am. J. Physiol. **76**:49-53.

**Sive, H. L.** (1993). The frog prince-ss: A molecular formula for dorsoventral patterning in *Xenopus*. Genes & Dev. **7**:1-12.

**Smith, L. J.** (1985). Embryonic axis orientation in the mouse and its correlation with blastocyst relationships to the uterus. II. Relationships from 4.5 to 9.5 days. J. Embryol. Exp. Morphol. **89**: 15-35.

**Smith, L. J., Dale, L. and Slack J. M. W.** (1985). Cell lineage labels and region-specific markers in the analysis of inductive interactions. J. Embryol. Exp. Morphol. **89**[Suppl.]:317-331.

**Smith, J. C.** (1993). Mesoderm-inducing factors in early vertebrate development. EMBO J. **12**: 4463-4470.

**Snow, M. H. L.** (1977). Gastrulation in the mouse: Growth and regionalization of

the epiblast. *J. Embryol. Exp. Morphol.* **42**:293-303.

**Sokol, S. and Melton, D. A.** (1991). Pre-existent pattern in *Xenopus* animal pole cells revealed by induction with activin. *Nature* **351**:409-411.

**Solcia, E., Capella, C., Buffa, R., Usellini, L., Fiocca, R. and Sessa, F.** (1987). Endocrine cells of the digestive system. In: *Physiology of the Gastrointestinal Tract*, 2nd ed. L. R. Johnson, ed. Raven Press, New York. pp 111-130.

**Spemann, H. and Mangold, H.** (1924). Induction of embryonic primordia by implantation of organizers from a different species. In: B. G. Willier and J. M. Oppenheimer (eds.), *Foundations of Experimental Embryology*. Hafner, New York, pp. 144-184.

**Tamura, S., Wang, X. H., Maeda, M. and Futai, M.** (1993). Gastric DNA binding proteins recognize upstream sequence motifs of parietal cell-specific genes. *Proc. Natl. Acad. Sci. USA* **90**:10876-80.

**Teitelman, G., Alpert, S., Polak, J. M., Martinez, A. and Hanahan, D.** (1993). Precursor cells of mouse endocrine pancreas coexpress insulin, glucagon and neuronal proteins tyrosine hydroxylase and neuropeptide Y, but not pancreatic polypeptide. *Development* **118**:1031-1039.

**Thomsen, G. H. and Melton, D. A.** (1993). Processed Vg1 protein is an axial mesoderm inducer in *Xenopus*. *Cell* **74**:433-441.

**Thorens, B., Cheng, Z., Brown, D. and Lodish, H.** (1990). Liver glucose transporter: a basolateral protein in hepatocytes and intestine and kidney cells. *Am. J. Physiol.* **259**:C279-C285.

**Torres, M. A., Yangsnyder, J. A., Purcell, S. M., Demarais, A. A., McGrew, L. L. and Moon, R. T.** (1996). Activities of the wnt-1 class of secreted signaling factors are antagonized by the wnt-5A class and by a dominant negative cadherin in early *Xenopus* development. *J. Cell Biol.* **133**:1123-1137.

**Walsh, J. H. and Dockray, G. J.** (1994). *Gut Peptides*. Raven Press, Inc. New York, NY

**Wang, B. B., Muller-Immergluck, M. M., Austin, J., Robinson, N. T., Chisholm, A. and Kenyon, C.** (1993). A homeotic gene cluster patterns the anteroposterior body axis of *C. elegans*. *Cell* **74**:29-42.

**Wessells, N. K. and Cohen, J. H.** (1967). Early pancreas organogenesis: morphogenesis, tissue interactions, and mass effects. *Dev. Biol.* **15**:237-270.

**Winnier, G., Blessing, M., Labosky, P. A. and Hogan, B. L. M.** (1995). Bone morphogenetic protein-4 is required for mesoderm formation and patterning in the mouse. *Genes & Dev.* **9**:2105-2116

**Wright, C. V. E., Schnegelsberg, P. and De Robertis, E. M.** (1988). XlHbox 8: a

novel *Xenopus* homeo protein restricted to a narrow band of endoderm. *Development* **105**:787-794.

**Wray, C. G., Jacobs, D. K., Kostriken, R., Vogler, A. P., Baker, R., DeSalle, R.** (1995). Homologues of the engrailed gene from five molluscan classes. *FEBS Letters* **365**:71-74.

**Yost, C., Torres, M., Miller, R. R., Huang, E., Kimelman, D. and Moon, R. T.** (1996). The axis-inducing activity, stability and subcellular distribution of  $\beta$ -catenin is regulated in *Xenopus* embryos by glycogen synthase kinase 3. *Genes & Dev.* **10**:1443-1454.

**Yukawa, K., Yasui, T., Yamamoto, A., Shiku, H., Kishimoto, T. and Kikutani, H.** (1993). Epoc-1: a POU domain gene expressed in murine epidermal basal cells and thymic stromal cells. *Gene* **133**:163-69.

**Zhong, W., Sladek, F. M. and Darnell, Jr., J. E.** (1993). The expression pattern of a *Drosophila* homolog to the mouse transcription factor HNF-4 suggests a determinative role in gut formation. *EMBO J.* **12**:535-44.